

MECHANISTIC STUDIES OF THE MEND-CATALYZED REACTION

A Thesis Submitted to the College of
Graduate Studies and Research
In Partial Fulfillment of the Requirements
For the Degree of Doctor of Philosophy
In the Department of Chemistry
University of Saskatchewan
Saskatoon

By

Maohai Fang

© Copyright Maohai Fang, October, 2010. All rights reserved.

PERMISSION TO USE

In presenting this thesis in partial fulfilment of the requirements for a Postgraduate degree from the University of Saskatchewan, I agree that the Libraries of this University may make it freely available for inspection. I further agree that permission for copying of this thesis in any manner, in whole or in part, for scholarly purposes may be granted by the professor or professors who supervised my thesis work or, in their absence, by the Head of the Department or the Dean of the College in which my thesis work was done. It is understood that any copying or publication or use of this thesis or parts thereof for financial gain shall not be allowed without my written permission. It is also understood that due recognition shall be given to me and to the University of Saskatchewan in any scholarly use which may be made of any material in my thesis.

Requests for permission to copy or to make other use of material in this thesis in whole or part should be addressed to:

Head of the Department of Chemistry
University of Saskatchewan
Saskatoon, Saskatchewan (S7N 5C9)

ABSTRACT

MenD, a thiamin diphosphate (ThDP)-dependent enzyme, catalyzes the reaction from isochorismate (ISC) to 2-succinyl-5-enolpyruvyl-6-hydroxy-3-cyclohexene-1-carboxylate (SEPHCHC), and thus is also called SEPHCHC synthase. This conversion is the first committed step in the classical menaquinone (Vitamin K₂) biosynthetic pathway, requiring 2-ketoglutarate (2-KG), ThDP and Mg²⁺. Since the biosynthesis of menaquinone is essential in some bacterial pathogens, for example *Mycobacterium tuberculosis*, MenD or the menaquinone pathway could be a target for drug development.

The method for the kinetic assay of the MenD-catalyzed reaction was evaluated by comparing UV spectrophotometric measurements and HPLC analysis. It was validated that the steady-state kinetics of the MenD-catalyzed reaction can be determined by monitoring UV absorbance of ISC at 278 nm and 300 nm.

Phosphonate analogues of 2-KG were synthesized and assayed as inhibitors of the MenD reaction. It was found that the phosphonate analogues of 2-KG are competitive inhibitors with varied affinity for MenD. Of the inhibitors, monomethyl succinyl phosphonate (MMSP) was the most effective, with a K_i of 700 nM. However, the potent MenD inhibitors show no effectiveness against mycobacterial growth.

An analogue of isochorismate, trans-(±)-5-carboxymethoxy-6-hydroxy-1,3-cyclohexadiene-1-carboxylate ((±)-CHCD), was synthesized. The (+)-CHCD was found to be an alternative substrate for the MenD-catalyzed reaction. When CHCD was utilized in the MenD reaction, 5-carboxymethoxy-2-(3-carboxy-propionyl)-6-hydroxy-cyclohex-2-enecarboxylate (CCHC) was isolated and characterized, which was believed to be the product of spontaneous isomerization of the SEPHCHC-like analogue. The kinetic study

of MenD reaction using (\pm)-CHCD, in association with the kinetics pattern probed by MMSP, demonstrated for the first time that the MenD-catalyzed reaction has a Ping Pong bi bi kinetic mechanism.

The analysis of sequence and structure of MenD from *E. coli* allowed the investigation of the active site residues and their catalytic functions by mutation of the individual residues. S32A, S32D, R33K, R33Q, E55D, R107K, Q118E, K292Q, R293K, S391A, R395A, R395K, R413K and I418L were prepared and assayed kinetically with respect to 2-KG, ISC, (\pm)-CHCD, ThDP and Mg^{2+} . The values of K_m^a and k_{cat}^a / K_m^a for the mutants, in comparison with that of wild type MenD, provide valuable insight into the catalytic mechanism of MenD.

ACKNOWLEDGMENTS

I would like to thank my supervisor Dr. David R. J. Palmer. While the year 2004 was the toughest time in my life, Dr. Palmer's offered me an important opportunity to continue studying chemistry in a different environment. I will never forget how much his patience and encouragement helped me over years. I greatly appreciate the freedom and independence in the Palmer lab that I enjoyed in learning science and getting used to a new culture. Without his kind help, I cannot imagine how I am able to go through the years facing pressures and frustrations.

The people I met in the Palmer lab, such as Yunhua Jia, Richard, Chris, Andrea, Karen Ho, Hongyan Zheng, and David Langill, helped make the lab a constructive, friendly and joyful place to work in. In addition, the people from the Sanders lab, such as Josiah, Karin, and Sarathy are very helpful and friendly. I would like to thank the people at SSSC such as Keith, Gabriele and Ken for the great help in instruments that is so important to my research work.

I would also like to thank the members of my advisory committee: Dr. David Sanders, Dr. Marek Majewski and Dr. J. R. Dimmock. I appreciate the time, instructions and advice they gave me. I also owe a great deal of appreciation to Dr. Ravindran for her warm help in the TA work.

I wish to thank my family for consistently tremendous love, support, understanding and encouragement. I appreciate greatly my fiancée Liuqing Yang for her love and motivation by which I can finally complete my study and thesis writing.

TABLE OF CONTENTS

PERMISSION TO USE.....	i
ABSTRACT.....	ii
ACKNOWLEDGMENTS	iv
TABLE OF CONTENTS.....	v
LIST OF TABLES.....	ix
LIST OF SCHEMES	ix
LIST OF FIGURES	x
LIST OF ABBREVIATIONS.....	xiii
1. INTRODUCTION	1
1.1 Menaquinone biosynthesis.....	1
1.2 The MenD-catalyzed reaction.....	4
1.3 Mechanism of the MenD-catalyzed reaction	5
1.3.1 Activation of enzyme-bound thiamin diphosphate (ThDP).....	6
1.3.2 Post-decarboxylation intermediate and carboligation.....	8
1.3.3 Cleavage of ThDP.....	9
1.4 The structural analysis of MenD.....	10
1.4.1 The overall structure of MenD.....	11
1.4.2 Cofactor binding of MenD.....	12
1.5 Analysis of active-site residues of MenD	13
1.5.1 I418 residue and V conformation of ThDP.....	14
1.5.2 E55 residue and tautomerization of ThDP.....	15
1.5.3 Thiazolium-proximal Q118 residue.....	16
1.5.4 S32 and S391 residues	17
1.5.5 Basic residues in the active site	17
1.6 Analogues of ThDP.....	18
1.7 Analogues of 2-ketoglutarate (2-KG) and isochorismate (ISC)	20
1.7.1 Succinyl phosphonate analogues of 2-KG.....	20
1.7.2 Analogues of isochorismate.....	24
1.8 Steady-state kinetics and inhibition studies of enzymes.....	26
1.9 Kinetic mechanism of bireactant biproduct (bi bi) reaction	32
1.10 Objectives of research.....	36
2. EXPERIMENTAL.....	38

2.1 Chemical synthesis.....	38
2.1.1 Succinic acid monobenzyl ester.....	39
2.1.2 Benzyl alkyl diester of succinyl phosphonate.....	40
2.1.3 Benzyl monoester succinyl phosphonate	41
2.1.4 Monoester succinyl phosphonate	43
2.1.5 Succinylphosphonate	44
2.1.6 Methyl monomethyl succinylphosphonate and ethyl monomethyl succinylphosphonate	45
2.1.7 Methyl acetylphosphonate and monomethyl butyrylphosphonate	47
2.1.8 β -Benzoylpropionic acid and 1-phenyl-1,4-butanediol	48
2.1.9 4-Oxo-4-phenylbutanal	49
2.1.10 Dimethyl 1-hydroxy-4-oxo-4-phenyl-butylphosphonate.....	50
2.1.11 Lithium monomethyl-(1-hydroxy-4-oxo-4-phenyl-butyl)-phosphonate.....	51
2.1.12 Benzyl 4-(dimethoxyphosphoryl)-4-hydroxybutanoate.....	52
2.1.13 Benzyl 4-acetoxy-4-(dimethoxyphosphoryl)butanoate	52
2.1.14 4-Acetoxy-4-(dimethoxyphosphoryl)butanoic acid.....	53
2.1.15 4-(Benzylamino)-1-(dimethoxyphosphoryl)-4-oxobutyl acetate.....	54
2.1.16 Dimethyl 4-(benzylamino)-1-hydroxy-4-oxobutylphosphonate.....	55
2.1.17 Lithium methyl 4-(benzylamino)-1-hydroxy-4-oxobutylphosphonate.....	56
2.1.18 Methyl 2- <i>tert</i> -butyldimethylsilyloxycyclohexa-3,5-diene-1-carboxylate.....	57
2.1.19 Methyl 2-(<i>tert</i> -butyldimethylsilyloxy)-7-oxabicyclo[4.1.0]hept-3-ene-3- carboxylate	58
2.1.20 Methyl 6-(<i>tert</i> -butyldimethylsilyloxy)-5-hydroxycyclohexa-1,3-diene- carboxylate	59
2.1.21 Methyl 6-(<i>tert</i> -butyldimethylsilyloxy)-5-(2-ethoxy-2-oxoethoxy)cyclohexa- 1,3-dienecarboxylate.....	60
2.1.22 Methyl 5-(2-ethoxy-2-oxoethoxy)-6-hydroxycyclohexa-1,3-diene carboxylate	61
2.1.23 5-(Carboxymethoxy)-6-hydroxycyclohexa-1,3-diene carboxylate (CHCD). 62	
2.1.24 5-Carboxymethoxy-6-hydroxy-cyclohexa-1,3-dienecarboxylic acid methyl ester (CHCDMe).....	64
2.1.25 Methyl 2-methoxy-3-(1-methoxy-1-oxopropan-2-yloxy)benzoate	64
2.1.26 3-(1-Carboxyethoxy)-2-methoxybenzoic acid.....	66
2.1.27 Methyl 2-hydroxy-3-(1-methoxy-1-oxopropan-2-yloxy)benzoate	67
2.1.28 3-(1-Carboxyethoxy)-2-hydroxybenzoic acid	68

2.1.29 Methyl 3-(2-methoxy-2-oxoethoxy)benzoate and methyl 3-(1-methoxy-1-oxopropan-2-yloxy)benzoate	68
2.1.30 3-(Carboxymethoxy)benzoic acid and 3-(1-carboxyethoxy)benzoic acid.....	70
2.2 Enzymology experimental	71
2.2.1 Mutagenesis	72
2.2.2 Gene overexpression and protein purification	74
2.2.3 Preparation of isochorismate (ISC).....	75
2.2.4 Isolation of (-)-5-(carboxylatomethoxy)-6-hydroxycyclohexa-1,3-diene carboxylate ((-)-CHCD).....	75
2.2.5 Isolation of 5-carboxymethoxy-2-(3-carboxy-propionyl)-6-hydroxy-cyclohex-2-enecarboxylate (CCHC)	77
2.2.6 Continuous assay of MenD- or mutant-catalyzed reactions using UV spectrophotometer.....	78
2.2.7 Determination of the concentrations of ISC and (\pm)-CHCD	79
2.2.8 HPLC analysis of the MenD reaction	80
2.2.9 Determination of K_m^a and V_{max}^a of the MenD reaction	81
2.2.10 Inhibition study of 2-KG phosphonate analogues with respect to 2-KG.....	82
2.2.11 Determination of the reversibility of the 2-KG phosphonate inhibition.....	83
2.2.12 Kinetic mechanism study of the MenD reaction using CHCD.....	83
3. RESULTS AND DISCUSSION.....	85
3.1 Chemical synthesis.....	85
3.1.1 Chemical synthesis of phosphonate analogues of 2-KG.....	85
3.1.2 Chemical synthesis of the analogues of ISC.....	89
3.2 Mutagenesis and protein expression	93
3.3 Preparation of isochorismate (ISC).....	94
3.4 Isochorismate analogues were tested for the MenD reaction	94
3.5 Characterization and analysis of CCHC	97
3.6 The continuous and HPLC assay of the MenD reaction using ISC.....	105
3.7 Determining concentration and ϵ_{300} of ISC and (\pm)-CHCD.....	109
3.8 Activity assays of MenD and mutants	112
3.9 Inhibition of the MenD-catalyzed reaction with phosphonate analogues of 2-KG	113
3.10 Reversibility of the inhibition by 2-KG phosphonate.....	119
3.11 Kinetic mechanism of the MenD reaction	121
3.12 Kinetic analysis of MenD and mutants.....	126

3.12.1 Residues interacting with ThDP	128
3.12.2 Residues interacting with 2-KG-ThDP adduct	131
3.12.3 Residues interacting with ISC.....	134
3.12.4 Residues interacting with 2-KG.....	137
3.13 Recent report on mutagenesis study of <i>B. subtilis</i> MenD.....	138
4. CONCLUSIONS	140
5. FUTURE WORK.....	143
6. APPENDIX.....	145
7. REFERENCES	151

LIST OF TABLES

Table 1.1: Inhibition patterns of dead-end competitive inhibitors for bi bi reaction ($A + B \rightarrow P + Q$).	35
Table 2.1: List of MenD mutagenic primers.....	72
Table 3.1: Inhibition constants of 2-KG phosphonate analogues for MenD reaction. ...	116
Table 3.2: Kinetic constants of the CHCD-utilizing MenD reaction.....	123
Table 3.3: Kinetic constants of wt-MenD.....	127
Table 3.4: Kinetic constants of I418L, E55D and S391A.. ..	128
Table 3.5: Kinetic constants of S32A, S32D and Q118E.....	131
Table 3.6: Kinetic constants of R33K, R33Q, R107K, R395A and R395K.....	135
Table 3.7: Kinetic constants of K292Q, R293K.....	136
Table 3.8: Kinetic constants of R413K.....	137

LIST OF SCHEMES

Scheme 3.1: Synthesis of phosphonate analogues of 2-KG.	86
Scheme 3.2: Synthesis of phosphonate analogue 15	88
Scheme 3.3: Synthesis of phosphonate analogues 21	89
Scheme 3.4: Synthesis of (\pm)-CHCD.	90
Scheme 3.5: Synthesis of (\pm)-CHCD methyl ester ((\pm)-CHCDMe).	91
Scheme 3.6: Synthesis of ISC analogues with benzene core.	92

LIST OF FIGURES

Figure 1.1: Structures of Vitamin K.	1
Figure 1.2: Classical menaquinone biosynthetic pathway.	2
Figure 1.3: Alternative menaquinone biosynthetic pathway.	3
Figure 1.4: The overall MenD-catalyzed reaction.	4
Figure 1.5: Proposed mechanism of MenD-catalyzed reaction.	5
Figure 1.6: Tautomerization of enzyme-bound ThDP.	7
Figure 1.7: Stetter reaction and mechanism.	8
Figure 1.8: Non-enzymatic analogous Michael reaction of acyl carbanion.	9
Figure 1.9: Regeneration of ThDP from carboligation product.	10
Figure 1.10: Diagram of EcMenD monomer (PDB: 2jla).	11
Figure 1.11: The stereo view of ThDP binding site (PDB: 2jla).	14
Figure 1.12: V-conformation of ThDP bound to MenD (PDB: 2jla).	15
Figure 1.13: Hunter's model for substrates binding to <i>EcMenD</i>	18
Figure 1.14: ThDP and some analogues.	19
Figure 1.15: The intermediates and analogues of 2-KG and 2-KG-ThDP adduct.	21
Figure 1.16: Some phosphonate analogues of 2-KG.	24
Figure 1.17: Isochorismate and analogues.	25
Figure 1.18: Aromatic analogues of isochorismate.	26
Figure 1.19: Equilibrium scheme of substrate, inhibitor and enzyme.	29
Figure 1.20: Inhibition patterns of lines in Lineweaver-Burk plots.	30
Figure 1.21: Dixon plot and Cornish-Bowden plot for diagnosing inhibition type.	31

Figure 1.22: Bi bi reaction mechanisms.	32
Figure 1.23 Double reciprocal plots for bi bi reactions.	34
Figure 3.1: SDS-PAGE gel of purified MenD mutants.	93
Figure 3.2: Comparison of HPLC and spectrophotometric analysis of the MenD reaction utilizing <i>trans</i> -(±)-CHCD.	96
Figure 3.3: HPLC chromatogram of MenD reaction mixture using CHCD as substrate.	97
Figure 3.4: The product from fraction at 37.5 min (refer to Figure 3.3).	98
Figure 3.5: HNMR spectroscopy of CCHC.	99
Figure 3.6: Jmod- ¹³ CNMR spectroscopy of CCHC.	100
Figure 3.7: H-H COSY spectroscopy of CCHC.	100
Figure 3.8: HMQC spectroscopy of CCHC.	101
Figure 3.9: Diels-Alder product of CHCD.	101
Figure 3.10: Proposed mechanism of CCHC formation.	102
Figure 3.11: HPLC analysis of MenD reaction using CHCD.	104
Figure 3.12: HPLC analysis of CCHC solution at pH 12-13.	104
Figure 3.13 (2 <i>S</i> ,3 <i>S</i>)-2,3-dihydroxy-dihydrobenzoate (2,3-CHD)-utilized MenD reaction.	105
Figure 3.14: The MenD-catalyzed reaction progress curve monitored at 278 nm by UV spectrophotometer.	106
Figure 3.15: HPLC analysis of the MenD reaction using ISC.	107
Figure 3.16: Comparison of UV and HPLC-observed progress curve of the MenD reaction using ISC.	107
Figure 3.17: Determination of the extinction coefficient of ISC at 300 nm.	111

Figure 3.18: Determination of the extinction coefficient of ISC at 300 nm.....	111
Figure 3.19: Saturation curves of the MenD-catalyzed reaction.	113
Figure 3.20: Graphic determination of MMSP inhibition of the MenD-catalyzed reaction.	114
Figure 3.21: Progress curves of MenD reaction for test of inhibition reversibility.....	119
Figure 3.22: Test for time-dependence of MMSP inhibition.....	120
Figure 3.23: Double reciprocal plots of the MenD-catalyzed reaction of CHCD..	122
Figure 3.24: Graphic determination of MMSP inhibition with respect to 2-KG in the MenD-catalyzed reaction of CHCD.....	124
Figure 3.25: Graphic determination of MMSP inhibition with respect to CHCD in the MenD-catalyzed reaction of CHCD.....	125
Figure 3.26: Proposed diagram of active site of MenD.....	138

LIST OF ABBREVIATIONS

<i>E. coli</i>	<i>Escherichia coli</i>
2,3-CHD	2,3-dihydroxy-2,3-dihydrobenzoate
2-KG	2-ketoglutarate
3,4-DHB	3,4-dihydroxy-benzoic acid
AHAS	acetoxyhydroxyacid synthase
AP	4'-aminopyrimidine of ThDP
APH+	4'-aminopyrimidinium of ThDP
<i>B. subtilis</i>	<i>Bacillus subtilis</i>
BAL	benzaldehyde lyase
BFDC	benzoylformate decarboxylase
BMEP	benzyl monoethyl succinylphosphonate
BMIP	benzyl monoisopropyl succinylphosphonate
BMMP	benzyl monomethyl succinylphosphonate
<i>C. jejuni</i>	<i>Campylobacter jejuni</i>
CCHC	5-carboxylmethoxyl-2-(3-carboxypropionyl)-6-hydroxy-cyclohex-2-enecarboxylate
CD	circular dichroism
CEAS	N ² -(2-carboxyethyl)arginine synthase
CESP	carboxy ethyl ester succinyl phosphonate
COSY	correlation spectroscopy
DBU	1,8-diazabicyclo[5.4.0]undec-7-ene
EcMenD	MenD from <i>Escherichia coli</i>
EMMP	ethyl monomethyl succinylphosphonate
EMSP	ethyl monoethyl succinyl phosphonate
GCL	glyoxylate carbonylase
<i>H. pylori</i>	<i>Helicobacter pylori</i>
HThDP	C ² α -hydroxyethylThDP
HMBC	heteronuclear multiple bond coherence
HMQC	heteronuclear multiple quantum coherence
IP	1',4'-iminopyrimidine of ThDP
IPTG	isopropyl- β -thiogalactopyranose
ISC	isochorismate
ITC	isothermal titration calorimetry
JMOD	J-modulated spin-echo experiment
KGDHC	2-ketoglutarate dehydrogenase complex
<i>L. plantarum</i>	<i>Lactobacillus plantarum</i>
LThDP	lactyl-ThDP
<i>M. tuberculosis</i>	<i>Mycobacterium tuberculosis</i>
MAP	methyl acetylphosphonate

MBP	methyl benzoylphosphonate
m-CPBA	meta-chloroperoxybenzoic acid
MESP	monoethyl succinyl phosphonate
MESP	monomethyl succinyl phosphonate
MISP	monoisopropyl succinylphosphonate
MMBP	monomethyl butyrylphosphonate
MMMP	methyl monomethyl succinylphosphonate
MMSP	monomethyl succinylphosphonate
MThDP	mandelyl-ThDP
NMR	nuclear magnetic resonance
PDC	pyruvate decarboxylase
PDH-E1	E1 subunit of pyruvate dehydrogenase
PLThDP	C2 α -phosphonolactylThDP
PMThDP	C2 α -phosphonolmandelylThDP
POX	pyruvate oxidase
<i>S. aureus</i>	<i>Staphylococcus aureus</i>
<i>S. cerevisiae</i>	<i>Saccharomyces cerevisiae</i>
SDS-PAGE	sodium dodecyl sulfate polyacrylamide gel electrophoresis
SEPHCHC	2-succinyl-5-enolpyruvyl-6-hydroxy-3-cyclohexene-1-carboxylate
SHCHC	(1R,6R)-2-succinyl-6-hydroxy-2,4-cyclohexadiene-1-carboxylate
SP	succinyl phosphonate
ThDP	thiamin diphosphate
TK	transketolase
TLC	thin layer chromatography
Tris	tris(hydroxymethyl)aminomethane
wt	wild type
YPD	yeast pyruvate decarboxylase

1. INTRODUCTION

1.1 Menaquinone biosynthesis

“Vitamin K” refers to a group of lipid-soluble compounds which have a 2-methyl-1,4-naphthoquinone core structure containing a polyisoprene side chain at position 3 (Figure 1.1). Vitamin K consists of a naturally occurring phyloquinone (vitamin K₁), menaquinone (vitamin K₂) and the synthetic menadione (vitamin K₃). Phyloquinone is found in cyanobacteria and plants, whereas menaquinone is principally present in bacteria. In mammals, menaquinone is normally produced by the intestinal bacteria and acquired from nutrients. Vitamin K is a critical participant in the functionalization of some proteins. For instance, vitamin K is the cofactor of γ -glutamyl carboxylase, which catalyzes the posttranslational conversion of glutamate residues in certain proteins to γ -carboxyglutamate. γ -Carboxyglutamate residues are good Ca²⁺ chelators with the essential involvement in various physiological processes such as blood coagulation and calcium metabolism¹.

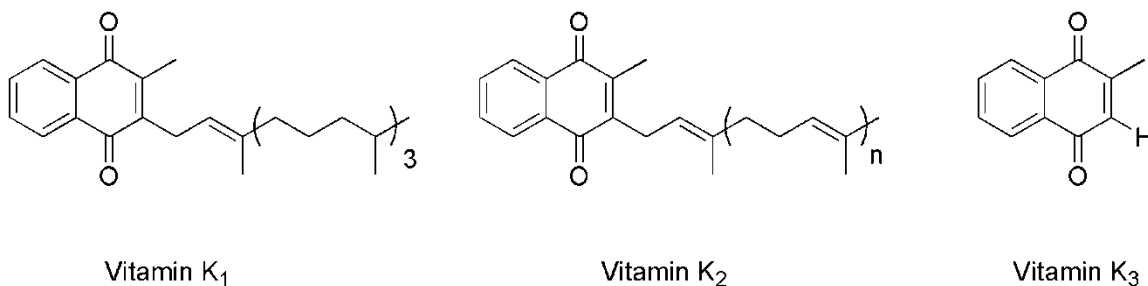


Figure 1.1: Structures of Vitamin K.

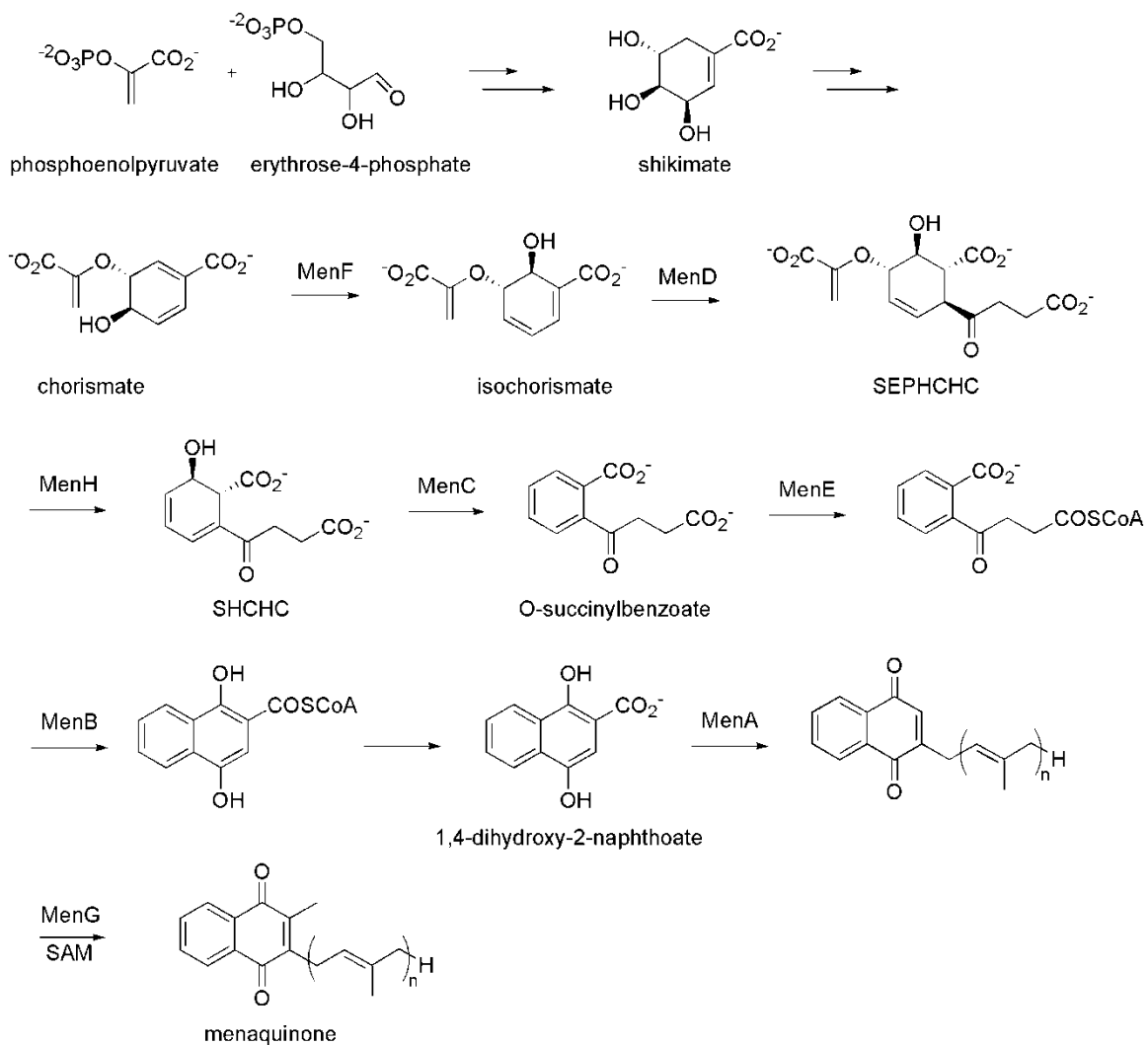


Figure 1.2: Classical menaquinone biosynthetic pathway.

After the extensive reviews on menaquinone biosynthesis by Bentley and Meganathan^{2,3}, the exploration of the biosynthetic pathway and the enzymatic catalysis of individual steps are still of great interest. Studies on menaquinone biosynthesis have been carried out mainly on the pathway in *E. coli*, as well as in *B. subtilis* and *M. tuberculosis*. The menaquinone biosynthesis pathway starts with chorismate (Figure 1.2), an intermediate from the shikimate pathway. Chorismate is first isomerized to isochorismate (ISC) by MenF. Then upon the catalysis of MenD, isochorismate reacts with 2-

ketoglutarate (2-KG) to form 2-succinyl-5-enolpyruvyl-6-hydroxy-3-cyclohexene-1-carboxylate (SEPHCHC). Over the steps catalyzed by a series of enzymes named from MenA to MenG, SEPHCHC is finally converted to menaquinone (vitamin K) through the intermediate 1,4-dihydroxy-2-naphthoate^{3,4,5,6}.

Recently, an alternative biosynthetic pathway of menaquinone was revealed in some microorganisms such as *H. pylori* and *C. jejuni*^{7,8,9}. Compared with the classical pathway of menaquinone mentioned above, the alternative pathway branches at chorismate and proceeds through the intermediate 1,4-dihydroxy-6-naphthoate, unlike the 1,4-dihydroxyl-2-naphthoate in classical pathway (Figure 1.2), to menaquinone (Figure 1.3).

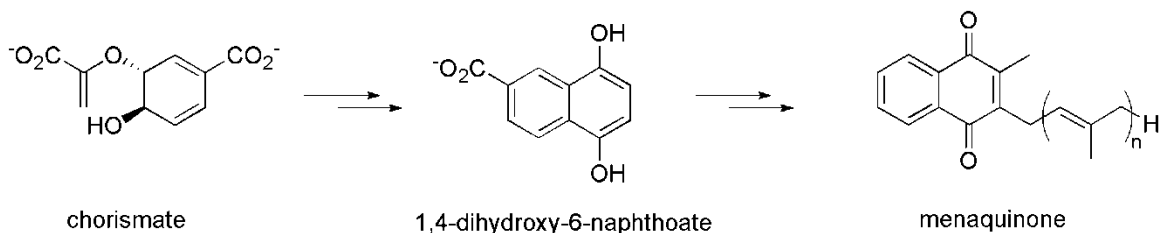


Figure 1.3: Alternative menaquinone biosynthetic pathway.

Although a new biosynthetic pathway for production of menaquinone was identified in some microorganisms, the search for a microorganism which has both the classical pathway and the alternative pathway was unsuccessful⁸. Therefore, those microorganisms which were known to have the classical pathway, such as *E. coli*, *B. subtilis* and *M. tuberculosis*, will solely rely on the classical pathway. Especially for the pathogenic organism *M. tuberculosis*, in light of the fact that the biosynthesis of menaquinone in the human body does not exist, the classical pathway is an attractive target for anti-tuberculosis drug development^{4,10}. Some compounds aimed at the inhibition of

menaquinone biosynthesis have been synthesized and tested against the enzymes in the pathway^{10,11,12}. For instance, an inhibitor of MenA showed significant growth inhibition against some drug-resistant Gram-positive bacteria¹⁰.

1.2 The MenD-catalyzed reaction

The conversion of isochorismate to 2-succinyl-5-enolpyruvyl-6-hydroxy-3-cyclohexadiene-1-carboxylate (SEPHCHC) in the classical menaquinone pathway is catalyzed by the enzyme MenD. This enzyme hence is also called 2-succinyl-5-enolpyruvyl-6-hydroxy-3-cyclohexene-1-carboxylate (SEPHCHC) synthase. The reaction catalyzed by MenD is the first committed step in the biosynthetic route. As shown in Figure 1.4, the MenD-catalyzed reaction, requiring thiamine diphosphate (ThDP) and metal ion Mg^{2+} as cofactors, converts isochorismate (ISC) and 2-ketoglutarate (2-KG) to SEPHCHC and CO_2 .

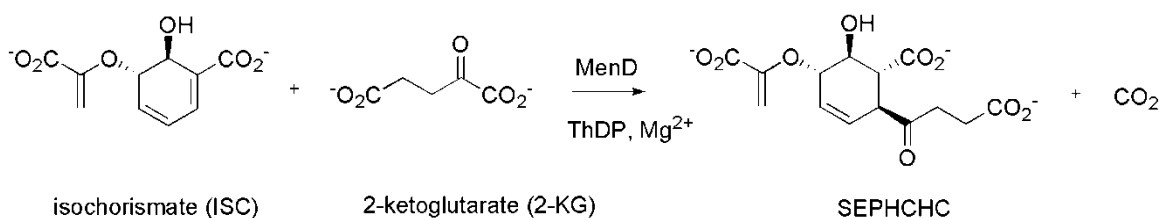


Figure 1.4: The overall MenD-catalyzed reaction.

MenD has been long annotated as SHCHC synthase^{13,14}, but recently Guo and his coworkers revealed that MenD actually catalyzes the production of SEPHCHC, which was previously proposed to be an intermediate precursor of SHCHC, but was isolated and characterized in terms of the structure and stereochemistry¹⁵. The conversion to SHCHC

from SEPHCHC was then attributed to the catalysis of the known enzyme MenH, although a spontaneous non-enzymatic 2,5-elimination to form SHCHC can occur readily under mild conditions (Fig. 1.5)^{5,6,15}.

1.3 Mechanism of the MenD-catalyzed reaction

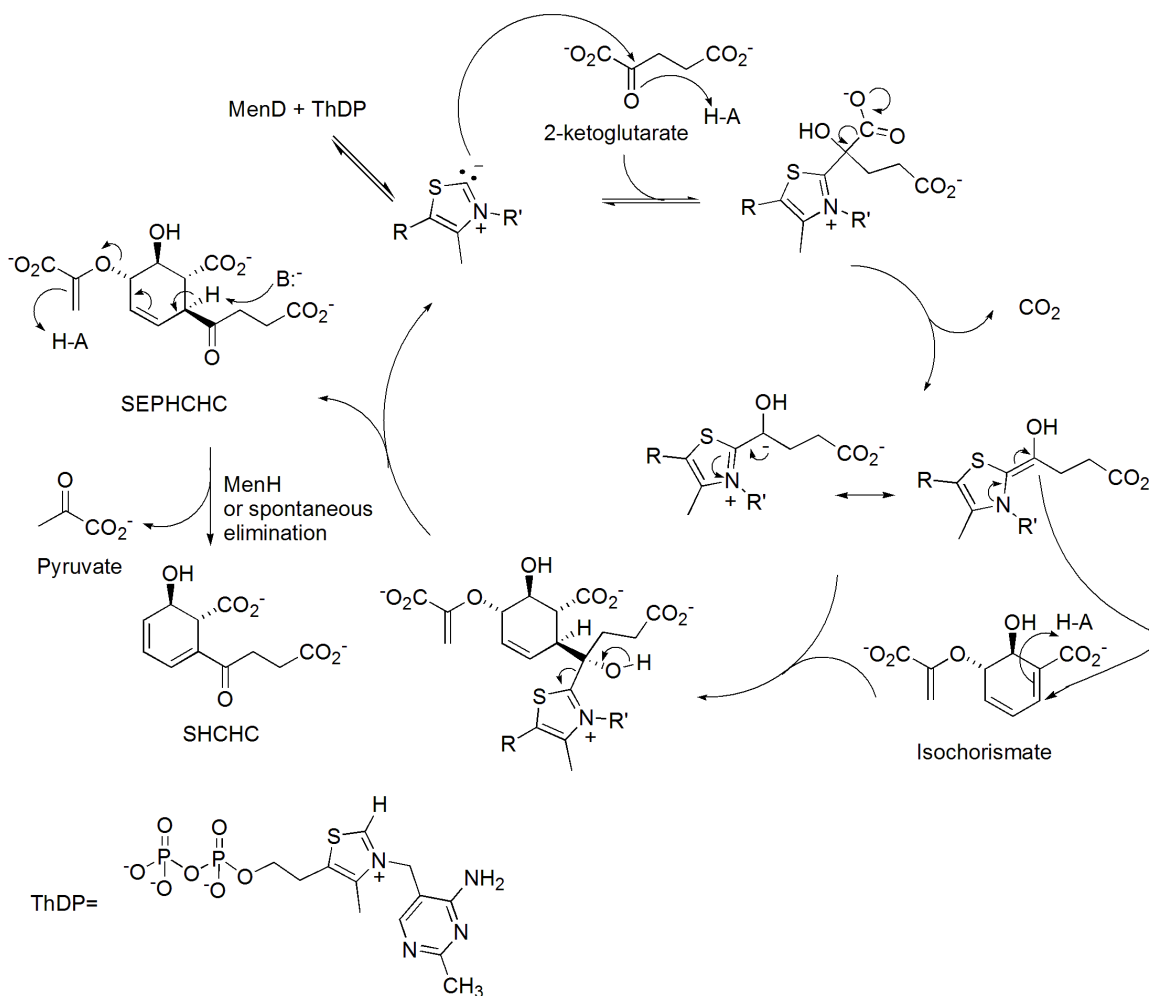


Figure 1.5: Proposed mechanism of MenD-catalyzed reaction.

Initially, MenD was postulated to undergo the ThDP-dependent 2-ketoglutarate decarboxylation with a mechanism identical to that in the 2-ketoglutarate decarboxylase

reaction^{16,17}. With the determination of the complete sequence of the gene *menD* and the characterization of the expressed enzyme, it was found that the enzyme actually has both activities of decarboxylation and subsequent addition to isochorismate. A mechanism for the MenD-catalyzed reaction was later proposed by Bentley and Meganathan on the basis of the ThDP-dependent decarboxylation in 2-ketoglutarate decarboxylase reaction and subsequent Michael addition to isochorismate (see Figure 1.5. Ref. 3 and references cited therein).

1.3.1 Activation of enzyme-bound thiamin diphosphate (ThDP)

MenD belongs to the pyruvate oxidase (POX) family of ThDP-dependent enzymes, including the E1 subunit of *E.coli* pyruvate dehydrogenase (PDH-E1), yeast pyruvate decarboxylase (YPD), POX, acetohydroxyacid synthase (AHAS), benzoylformate decarboxylase (BFDC), and others. In the proposed mechanism of the MenD reaction (Figure 1.5), the catalytic sequence is initiated by the binding and activation of ThDP in the same way as other ThDP-dependent enzymes¹⁸. In this widely accepted mechanism, published for over 50 years, the C2-H of the thiazolium ring is abstracted and the resulting nucleophilic carbene attacks electrophilic species such as the carbonyl of 2-ketoacid^{19,20}. The studies on the molecule ThDP and its role in enzymatic catalysis were extensively reviewed by Kluger and Tittmann²¹. More recently, a series of mini reviews about several different aspects of ThDP chemistry were published²². With the accumulation of the understanding on the chemistry of ThDP-dependent enzymes, especially the reports of many X-ray crystallographic structures for these types of enzymes, it was found that the activation of ThDP within the enzymatic environment is a

highly efficient and sophisticated process^{18,21}. The aminopyrimidine moiety of ThDP (AP) substantially contributes the C2-H abstraction by taking two preliminary actions: (1) adopting a V-conformation between the pyrimidine and thiazolium rings over the bridging methylene so as to achieve the proximity of the C2-H and the 4'-NH₂ (< 3.5 Å); (2) formation of the iminopyrimidine tautomer (IP) with the assistance from enzymes (Figure 1.6)²³. Actually, the tautomerization not only enables production of the nucleophile, but also participates in the protonation of the incipient adduct of ThDP and 2-ketoacid^{23,24,25}.

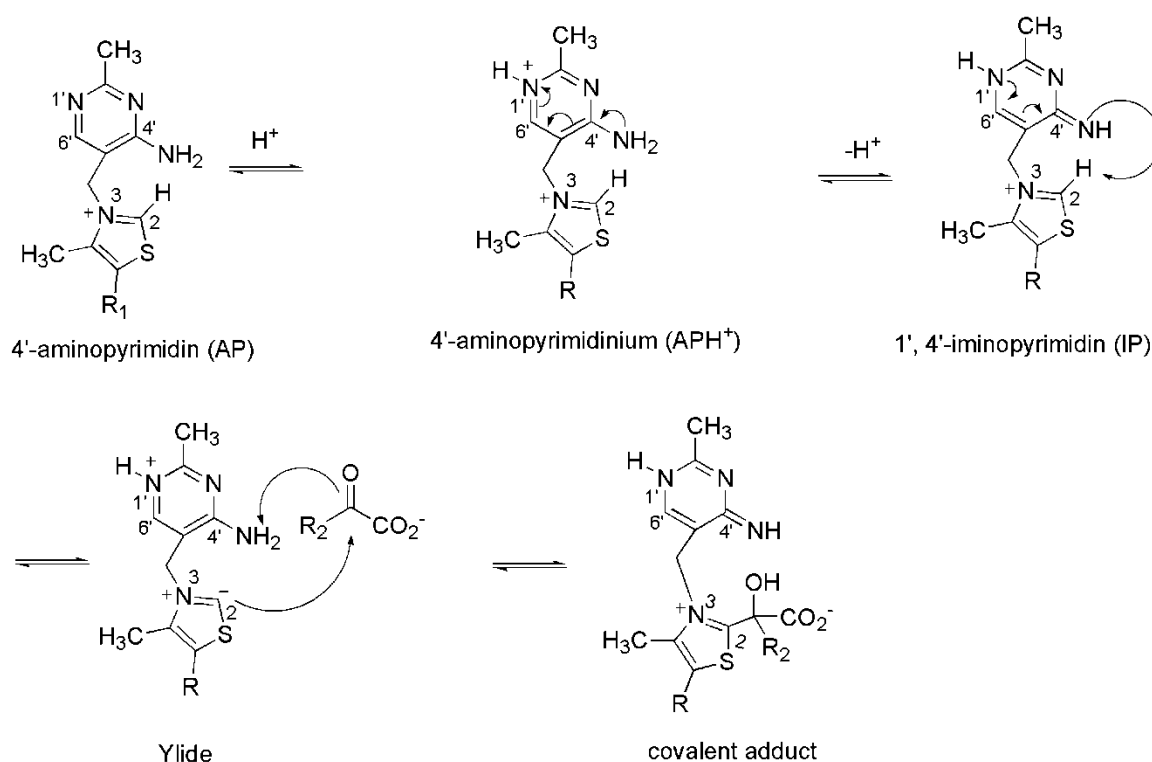


Figure 1.6: Tautomerization of enzyme-bound ThDP.

1.3.2 Post-decarboxylation intermediate and carboligation

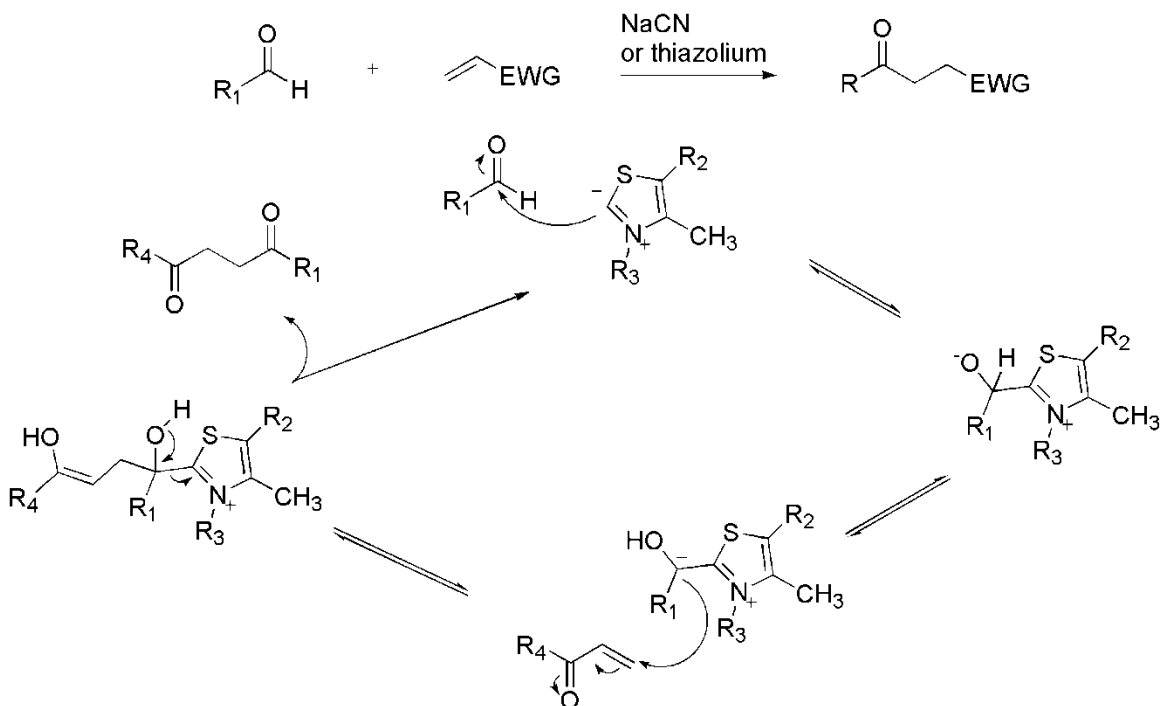


Figure 1.7: Stetter reaction and mechanism.

The highly conserved mechanism in ThDP-dependent enzymes utilizing 2-ketoacids involves formation of an “active aldehyde” by decarboxylation. The active species is now known as a conjugate pair of enamine and C2 α -carbanion (Figure 1.5). The delocalization of negative charge into the thiazolium ring reduces the energy of the resulting acyl carbanion in analogy to the non-enzymatic aldehyde-utilizing reactions catalyzed by cyanide or thiazolium, such as the Stetter reaction, in which the acyl carbanion undergoes 1,4-addition to a Michael acceptor (Figure 1.7)^{26,27}. Putatively, in the MenD reaction, the carboligation step was achieved by the reaction between the post-decarboxylation intermediate from 2-ketoacid and the Michael acceptor (here it is the α,β -unsaturated carboxylate moiety of isochorismate, Figure 1.5). Actually, this unusual

type of chemical reaction, with 2-ketoacid rather than aldehyde as the acyl anion donor, is not only present in enzymatic reactions. A closely analogous non-enzymatic reaction in aqueous solution was realized with thiamin catalysis (Figure 1.8)²⁸. This is an interesting example of the inspiration for organic chemists from enzyme-catalyzed reactions. This Stetter-like reaction catalyzed by MenD has not yet been reported for other ThDP-dependent enzymes.

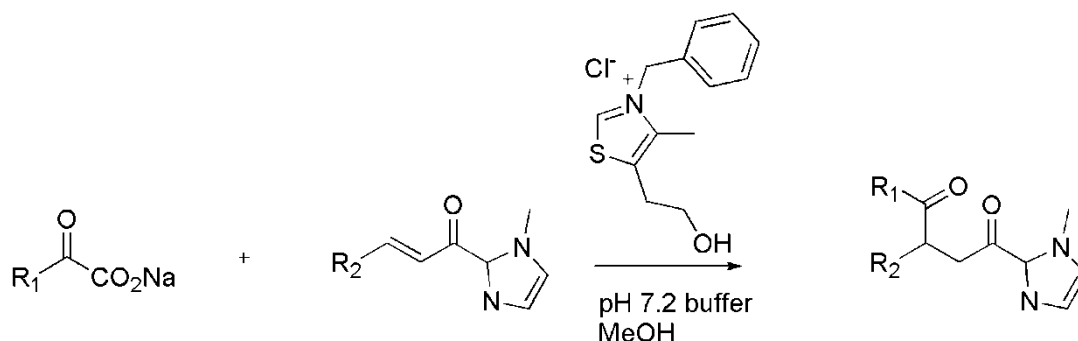


Figure 1.8: Non-enzymatic analogous Michael reaction of acyl carbanion²⁸.

1.3.3 Cleavage of ThDP

Tautomerization and ionization in ThDP seem to be the central mechanism in the ThDP-dependent enzyme reactions. Nemeria *et al.* concluded, from the data of several enzymes extensively studied, that the post-decarboxylation ThDP-bound intermediates with tetrahedral structure of C2 α atom exist in 1',4'-iminopyrimidinyl (IP) tautomeric forms, while the enamine intermediate may be in 4'-aminopyrimidinyl (AP or APH⁺) form because of the hybridization of C2 α atom²⁹. Furthermore, it was observed from many structural data that there are no residues identified as general acid-base catalysts to facilitate the proton transfer for the C2 α oxygen and the structures show close proximity

of the 4'-N and C2 α oxygen. This leads to a suggestion that ThDP itself, or more specifically, the 4'-N is responsible for the intramolecular proton shuttle as the only general acid-base in the entire catalytic cycle for ThDP enzymes³⁰. Accordingly, in the MenD-catalyzed reaction mechanism, it is plausible that the cleavage of ThDP after the carboligation step with isochorismate proceeds by transferring a proton from the IP to regenerate the AP form of ThDP (Figure 1.9)³¹.

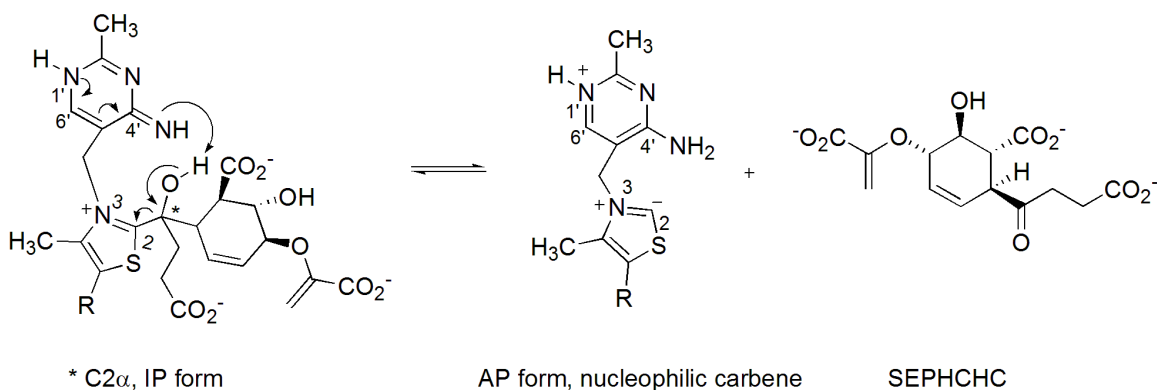


Figure 1.9: Regeneration of ThDP from carboligation product.

Although we can reasonably assume that the MenD reaction would share the mechanism for the pre-decarboxylation and some post-decarboxylation steps with other ThDP-dependent enzymes as noted above, we know little about how this fascinating enzyme works effectively. The elucidation of the catalytic details on the basis of the hypothetical mechanism above is a challenging task and will certainly add interesting and useful findings to the expanding database of ThDP-dependent enzyme reactions.

1.4 The structural analysis of MenD

1.4.1 The overall structure of MenD

Structurally, MenD belongs to the pyruvate oxidase (POX) family within the ThDP-dependent superfamily. The enzymes of this family all catalyze the decarboxylation of 2-ketoacids, therefore Duggleby named them as the “DC family”³². The first solved X-ray structure of ThDP-bound MenD from *E. coli* was reported by Hunter *et al* from Scotland in 2008³¹. Soon after, the structure of holo-MenD was published by Priyadarshi *et al* from Korea³³.

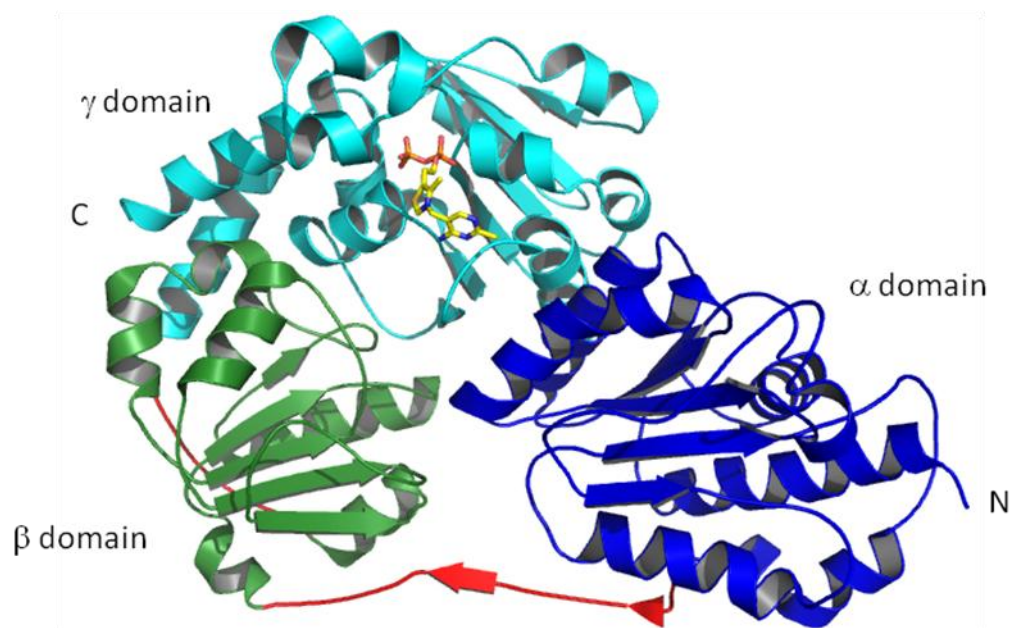


Figure 1.10: Diagram of EcMenD monomer (PDB: 2jla). α Domain in blue, β domain in green and γ domain in cyan, ThDP was shown in stick, and links between domains in red. Prepared using Pymol.

MenD from *E. coli* K12 (*EcMenD*) is composed of 556 amino acids and has a molecular mass of ~61.4 kDa. In practice, the overexpressed and purified *EcMenD* in our lab was shown in SDS-PAGE as a single band at around 64 kDa (with a fragment containing histidine-6 tag), reasonably consistent with the molecular mass of the

monomer. The gel filtration experiment demonstrated that the *EcMenD* exists mainly as a dimer with a predominant peak of 138 ± 4 kDa. Most other ThDP-dependent enzymes exist in dimeric or tetrameric forms^{14,31,34}.

Sequence alignments predict that the monomer of *EcMenD* consists of 3 domains with comparable sizes, typical of DC family enzymes³²: the α domain, residues 1-180; the β domain, residues 181-341; and the γ domain, residues 342-556. Furthermore, it was found that the central domain shows fewer conserved residues than the α and γ domain¹⁴. The solved X-ray structure provided clear evidence in agreement with the sequence alignment-derived prediction of domains, albeit there is some modification and correction (the α domain: residues 1-~200, the β domain: residues 210-335, and the γ domain: 340-556). In general, the solved structure of *EcMenD* fully conforms to the secondary and tertiary features summarized by Duggleby for DC family enzymes³²: (1) ThDP is bound at the interface of two subunits; (2) the N-terminal α domain, also called the Pyr domain, binds to the pyrimidine ring of ThDP, while the C-terminal γ domain, also called the PP domain, from the partner subunit binds to the diphosphate of ThDP; (3) the shorter β domain connects the α domain and the γ domain (Figure 1.10).

The apo-*EcMenD* X-ray crystal structure, along with the CD and ITC measurements, demonstrate a more flexible conformation than holo-enzyme and that the thermal as well as structural stability are enhanced by the binding of ThDP³³.

1.4.2 Cofactor binding of MenD

As noted above, MenD was identified structurally as a member of DC family, the largest of five families of ThDP-dependent enzymes. The analysis and comparison with other structurally characterized enzymes will be highly instructive to recognize how the ligands bind to MenD. First of all, it is not surprising for MenD to have a highly conserved ThDP-binding motif in Pyr domain, which was long revealed as GDGX₂₅₋₃₀NN motif before the appearance of X-ray structures³⁵. In *EcMenD*, this motif is present as Gly441-Asp442-X₂₅-Asn468-Asn469, where a polar pocket is formed to coordinate to divalent metal ion (Mg²⁺ or Mn²⁺ in MenD), along with the diphosphate moiety of ThDP. Secondly, the ThDP was oriented to adopt the conserved "V conformation" in the active site (Figure 1.11).

A structure of substrate-bound MenD has not been reported thus far, however Hunter *et al.* have built a model accommodating the putative post-decarboxylation intermediate of ThDP and 2-KG and the second substrate ISC³¹. It was predicted by the model that the carboxylate anions of the post-decarboxylation intermediate and ISC are balanced with basic residues such as arginines and lysines. The lack of the residues involved in removing the pyruvate side chain of ISC, as shown in the model, provides the structural evidence to support the assignment of MenD as SEPHCHC synthase. Although the model remains hypothetical, it is the foundation available at this time to guide mutagenesis of active-site residues.

1.5 Analysis of active-site residues of MenD

The crystal structures of MenD and comparison with other ThDP-dependent enzymes revealed certain active-site residues which are potentially implicated in substrate and

cofactor binding. As shown in Figure 1.11, residues such as S32, R33, E55, R107, Q118, K292, R293, S391, R395, R413 and I418, surround the catalytic center where ThDP is located. Conceivably, these residues, all bearing active side chain functional groups, may play catalytically important roles in MenD catalysis.

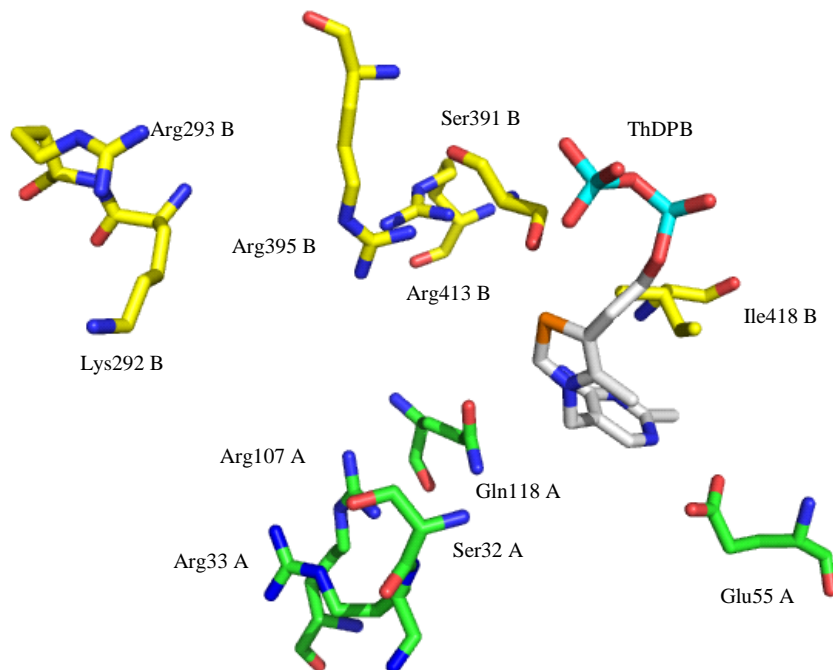


Figure 1.11: The stereo view of ThDP binding site (created from PDB file 2jla using Pymol). ThDP is bound at the interface of chain A and B. The ThDP is depicted as in chain B and surrounded by Ser32, Arg33, Glu55, Arg107, Gln118, Lys292, Arg293, Ser391, Arg395, Arg413 and Ile418. The residues and ThDP are colored as blue (N), red (O), orange (S), cyan (P). Carbons are colored differently as chain A (green), chain B (yellow) and ThDP (gray).

1.5.1 I418 residue and V conformation of ThDP

In ThDP-dependent enzymes, the large hydrophobic side chain of highly conserved isoleucine is important to help the V conformation of ThDP when bound to enzymes,

which is however not favored for ThDP in solution (Figure 1.12)¹⁸. In MenD, the highly conserved residue I418, as the I415 in PDC from *S. cerevisiae*³⁶, points between thiazolium and pyrimidine ring of ThDP with its hydrophobic side chain (Figure 1.11). The V conformation and the resulting close contact of C2 and 4'-NH₂ are essential to the activation of ThDP and the viability of the entire catalytic cycle, therefore the substitution of the residue I418 was expected to affect the reaction, maybe by the interference with the binding of ThDP. As a result, the mutation and kinetic measurement would demonstrate the effect and importance of this residue.

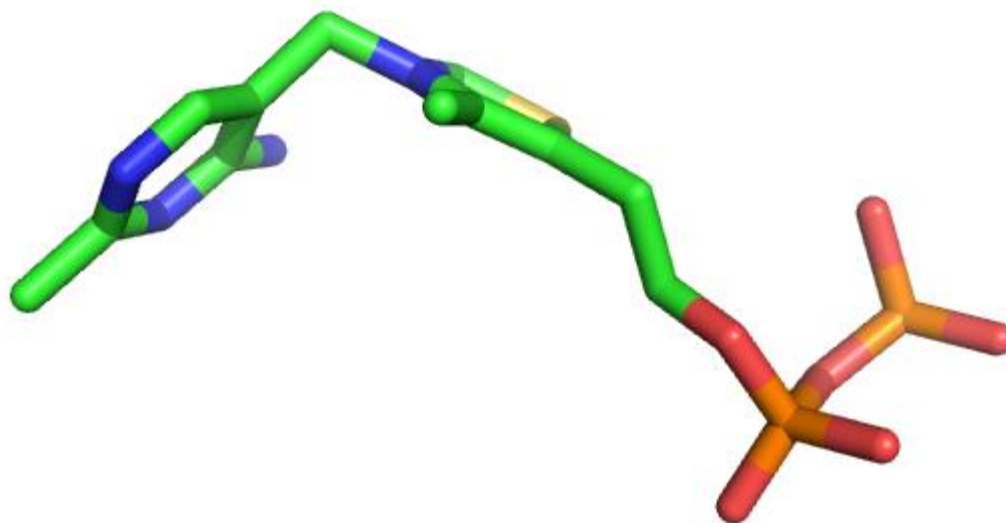


Figure 1.12: V-conformation of ThDP bound to MenD (PDB: 2jla).

1.5.2 E55 residue and tautomerization of ThDP

The glutamate-aided tautomerization of ThDP seems to be a universal mechanism for all the ThDP enzymes so far³⁷. The only exception was recently reported about the

enzyme glyoxylate carboligase (GCL)³⁸. In the MenD structure, as observed for many other ThDP enzymes, a highly conserved glutamate residue was found with the carboxylate side chain in hydrogen bond distance to N1' of the AP ring in ThDP (Figure 1.11). The protonation/deprotonation of N1' by glutamate presumably assists the tautomerization of AP (Figure 1.6 & Figure 1.9). As discussed earlier, it was recently recognized that the tautomerization and ionization of the AP plays a pivotal role in ThDP-dependent enzyme catalysis, and this glutamate residue is apparently critical in the process. The mutation of the glutamate to other residues, e.g. glutamine, invariably results in the reduction of catalytic activity for many ThDP-enzymes³⁷. In our lab, the abolished activity of E55Q mutants of *EcMenD* was reported¹⁴.

1.5.3 Thiazolium-proximal Q118 residue

In the MenD structure as shown in Figure 1.11, glutamine 118 is located close to the thiazolium C2. Similarly, benzaldehyde lyase (BAL)³⁹, AHAS, POX and N2-(2-carboxyethyl)arginine synthase (CEAS)⁴⁰ possess a similar thiazolium-proximal glutamine, whereas some other ThDP-dependent enzymes such as PDH-E1 and pyruvate decarboxylase (PDC) have histidine in the position. It was proposed that the polar glutamine residue serves to stabilize the enamine intermediate or transition state by electrostatic interaction rather than as a proton donor³⁰. Therefore, the replacement of glutamine with glutamate was speculated to disrupt the interaction because of the incompatibility of the carboxylate anion of Glu and the negative charge-bearing α -carbanion/enamine intermediate.

1.5.4 S32 and S391 residues

Alignment of the *EcMenD* sequence with benzoylformate decarboxylase (BFDC) demonstrated the S32 of MenD aligns with S26 of BFDC⁴¹. In the X-ray structure, S26 of BFD forms two hydrogen bonds with the carboxylate of the inhibitor (R)-mandelate, one by the hydroxyl of the side chain, the other one by the amidic nitrogen of the main chain. According to the kinetic study of mutant S26A, S26 was thought to be implicated in benzoylformate binding by interaction with the carboxylate anion and possibly also involved in other steps of the reaction pathway⁴². When BFDC was incubated with benzoylphosphonic acid, the enzyme was irreversibly inactivated. The X-ray structure clearly demonstrates that S26 is phosphorylated by accepting the phosphono group of benzoylphosphonic acid⁴³. In the X-ray structure of *EcMenD*, S32 is in a position pointing to the putative substrate binding pocket (Figure 1.11), suggesting the S32 residue may play a similar role in catalysis as the S26 residue in BFDC.

Serine 391 in *EcMenD* is in close contact with the diphosphate tail (2.8 Å) and the thiazolium sulfur (2.8 Å) of ThDP, suggesting the hydrogen bonds form between them. Therefore, serine 391 was speculated to mainly contribute to the binding and orientation of ThDP.

1.5.5 Basic residues in the active site

In Hunter's model simulating the substrate binding cavity, one striking feature is the presence of a series of basic residues (R33, R107, K292, R293, R395 and R413)

surrounding the substrates (Figure 1.11 and Figure 1.13)³¹. MenD's substrates, 2-KG and ISC, each bear two carboxylate anions, requiring a basic environment within MenD to accommodate these substrates. Among these 7 residues, K292 and R293 appear to be not close to the C2 of thiazolium, the presumed catalytic center. What roles these basic residues likely play in substrate binding and catalysis is of interest and kinetic assays of site-directed mutants will be informative to probe the active site of MenD.

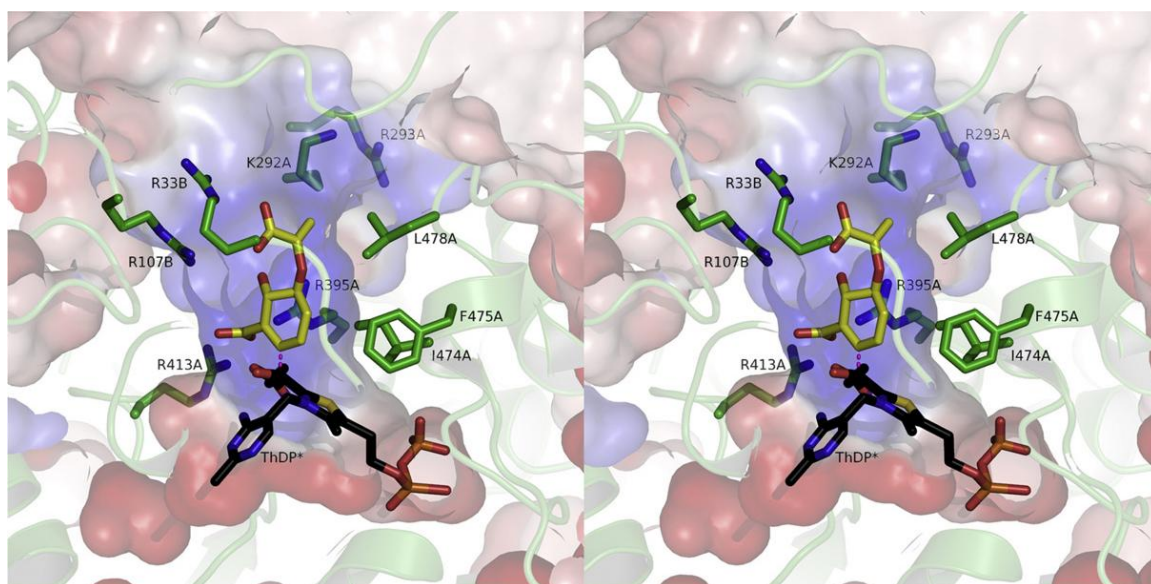


Figure 1.13: Hunter's model for substrates binding to *EcMenD*. The post-decarboxylation product of 2-KG-ThDP covalent adduct and ISC are shown⁴⁴.

1.6 Analogues of ThDP

In order to investigate binding and catalytic activity of ThDP, many ThDP analogues have been synthesized⁴⁵. Because these analogues usually lack the functional ability of ThDP but still possess high affinity with ThDP-dependent enzymes, many of them are able to incapacitate ThDP-dependent reaction efficiently. Therefore in kinetic and

structural studies they are powerful mechanistic tools to probe substrate binding and snapshots of the elementary catalytic steps along the reaction sequences.

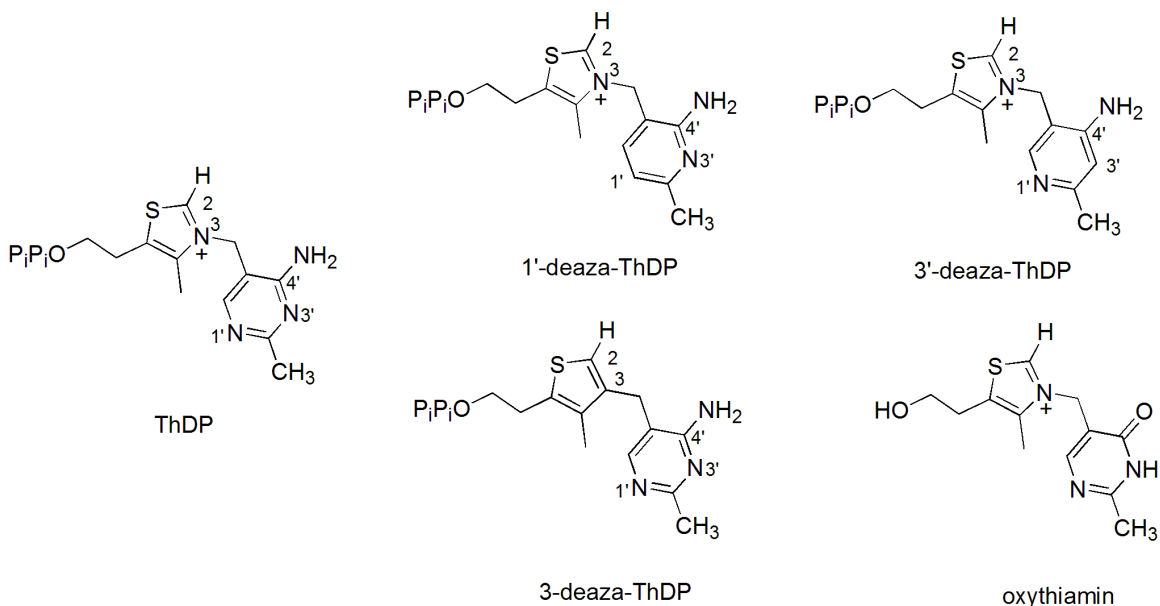


Figure 1.14: ThDP and some analogues.

Analogues of ThDP comprise the modifications to aminopyrimidine (AP) and thiazolium ring (Figure 1.14). For example, the 1'-deaza-ThDP and 3'-deaza-ThDP were used to test the role of N1' and N3' on AP ring on several enzymes. The results suggested that the N3' was not crucial for function. However, the replacement of N1' with carbon abolished the activity of catalysis, supporting the now widely accepted glutamate-aided tautomerization mechanism⁴⁶. 3-Deaza-ThDP, synthesized by Hawksley *et al*⁴⁷, is representative of the thiazolium-modified analogues. It demonstrated much tighter binding affinity to several ThDP-dependent enzymes including PDC and 2-KG dehydrogenase than ThDP and the binding is faster and irreversible⁴⁸. The absence of positive charge in the ring makes 3-deaza-ThDP a good mimic of the neutral carbene

intermediate (Figure 1.5), probably accounting for the tighter binding in enzymes⁴⁵. 3-Deaza-ThDP has been applied mainly by Leeper's group to obtain the co-crystallization of ThDP-dependent enzymes bound with substrates to provide the information of the active sites and catalysis⁴⁹. Recently, a report about inhibition studies of oxythiamin and derivatives against MenD from *S. aureus* appeared⁵⁰.

1.7 Analogues of 2-ketoglutarate (2-KG) and isochorismate (ISC)

1.7.1 Succinyl phosphonate analogues of 2-KG

Since methyl acetylphosphonate (MAP), the first phosphonate analogue of pyruvate, was synthesized and used as inhibitor against pyruvate dehydrogenase (PDH-E1)⁵¹, phosphonate analogues of 2-ketoacids continue to be perhaps the most powerful mechanistic probe rather than as inhibitors in the studies of ThDP-dependent enzymes which utilize 2-ketoacids as substrates (Figure 1.15)^{52,53}. The phosphonate moiety bearing one negative charge is an isoelectric mimic of the 1-carboxylate of 2-ketoacid, therefore phosphonate analogues of 2-ketoacids are able to bind to the enzymes and even form the covalent adducts with ThDP by following the enzymatic mechanism. Covalent adducts with phosphonate analogues are presumably inactive to subsequent steps because the 2-ketophosphonate cannot undergo the decarboxylation-like dephosphorylation reaction to yield carbanion/enamine, which is the central intermediate for these types of reactions. As a result, the phosphonate analogues generally behave as dead-end inhibitors with respect to the ThDP-dependent enzymes utilizing decarboxylation step in catalysis. C2 α -

phosphonolactylThDP (PLThDP) and C2 α -phosphonomandelylThDP (PMThDP) were also chemically synthesized to simulate lactyl-ThDP (LThDP) and mandelyl-ThDP (MThDP), which are the tetrahedral intermediates formed by condensation of pyruvate or benzoylformate with ThDP in enzymes⁵⁴.

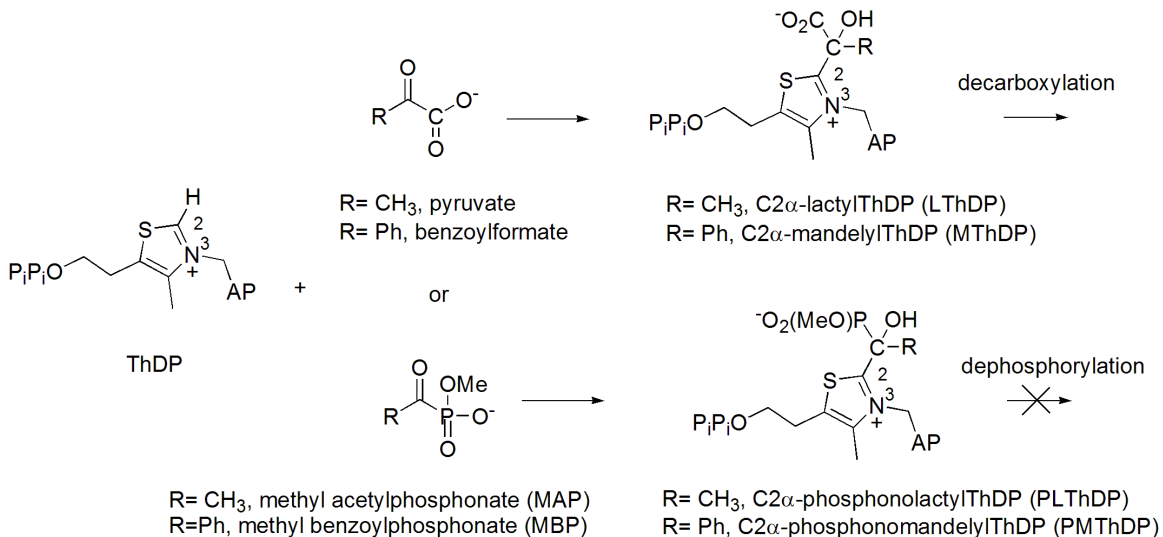


Figure 1.15: The intermediates and analogues of 2-KG and 2-KG-ThDP adduct.

The phosphonate analogues of 2-ketoacids (pyruvate or benzoylformate) and their pre-decarboxylation intermediates (PLThDP or PMThDP) have been widely used in kinetic and structural studies of ThDP-utilizing enzymes such as pyruvate decarboxylase (PDC), pyruvate dehydrogenase E1 subunit (PDH-E1), pyruvate oxidase (POX), benzaldehyde lyase (BAL) or benzoylformate decarboxylase (BFDC).

It was observed spectroscopically that the PLThDP exists in the form of the 1',4'-iminopyrimidine (IP) tautomer when bound in the active sites of yeast PDC and *E. coli* PDH-E1, as does the tetrahedral intermediate C2 α -hydroxyethylThDP (HETThDP), suggesting that all the tetrahedral ThDP-bound covalent complex would prefer IP

tautomer^{24,29}. At almost the same time, the structures of PLThDP-bound *E. coli* PDH-E1⁵⁵ and *L. plantarum* POX⁵⁶ were solved and published. Several common structural features can be summarized from the two cases, and may be applicable for other ThDP-dependent enzymes: (1) similar to the carboxylate of LThDP, the phosphonate moiety of PLThDP is perpendicular to its thiazolium ring in enzymes; (2) the C2-C α bond of PLThDP, slightly distorted from the aromatic plane of thiazolium, may facilitate the subsequent decarboxylation; (3) the hydroxyl of C α is in close contact with the 4'-N of pyrimidine, strongly supporting the existence of 1',4'-iminopyrimidine form and putative proton transfer between them; (4) the methoxy moiety of the phosphonate points towards the exit of the active site with no steric clash. That is to say, PLThDP is not only a good structural mimic of LThDP, but also a good functional analog in the catalytic steps prior to decarboxylation.

Unlike the benzoylphosphonic acid that irreversibly inactivates BFDC by phosphorylation of the S26 residue⁴³, methyl benzoylphosphonate (MBP) is a mechanism-based, competitive and reversible inhibitor of BFDC. MBP forms stable PMThDP with ThDP in BFDC in analogy to the covalent tetrahedral intermediate, as evidenced by circular dichroism, mass spectrometry and X-ray analysis^{52,53}. Compared with the PLThDP in POX and PDH-E1, PMThDP shows almost the same structural features in the active site of BFDC. Benzaldehyde lyase (BAL) catalyzes the reversible conversion of (R)-benzoin to benzaldehyde. Interestingly, BAL was found to be able to catalyze the decarboxylation of benzoylformate and phenylpyruvic acid too⁵⁷. This BFDC-like activity was thus used to incorporate MBP into the active site of BAL³⁹. MBP was found to be a time- and concentration-dependent inactivator of BAL and indeed form

the pre-decarboxylation intermediate PMThDP in BAL as revealed in the X-ray structure. The PMThDP-bound structure in BAL allows the interpretation of the binding mode in BAL: Ala28, His29, Gln113, and Thr73 likely form the network of hydrogen bonds with PMThDP. The comparison of the binding mode of PMThDP in BAL and BFDC suggested low active-site residues conservation⁵².

In studies of multienzyme 2-ketoglutarate dehydrogenase complex (KGDHC), several 2-KG phosphonate analogues were synthesized (Figure 1.16)^{58,59,60}. Because KGDHC catalyzes the ThDP-dependent decarboxylation of 2-KG, the 2-KG phosphonate analogue should form the pre-decarboxylation intermediate that cannot yield the critical carbanion/enamine conjugate. The inhibition studies with these phosphonates were carried out using KGDHC (isolated and in intact cells). The results indicated that the succinyl phosphonate (SP), monoethyl succinyl phosphonate (MESP) and carboxy ethyl ester succinyl phosphonate (CESP) are inhibitory to isolated brain KGDHC, whereas ethyl monoethyl succinyl phosphonate (EMSP) is ineffective. In cell system containing KGDHC, it was found that EMSP needs hydrolysis of the ester to obtain the inhibitory ability as SP and its monoethyl esters (MESP and CESP). Also, SP and its monoethyl esters were not effective inhibitors of other enzymes utilizing 2-KG or 2-ketoacids such as some aminotransferases and pyruvate dehydrogenase (PDH-E1), probably because those aminotransferases tested are not ThDP-dependent and PDH-E1 does not recognize 2-KG as alternative substrate. In short, the SP and its derivatives demonstrated the inhibition against KGDHC *in vitro* and *in vivo* with specificity for KGDHC and preference over SP diethyl esters (EMSP). The results are apparently encouraging for the

further investigation of 2-KG-specific ThDP enzymes using 2-KG phosphonate analogues.

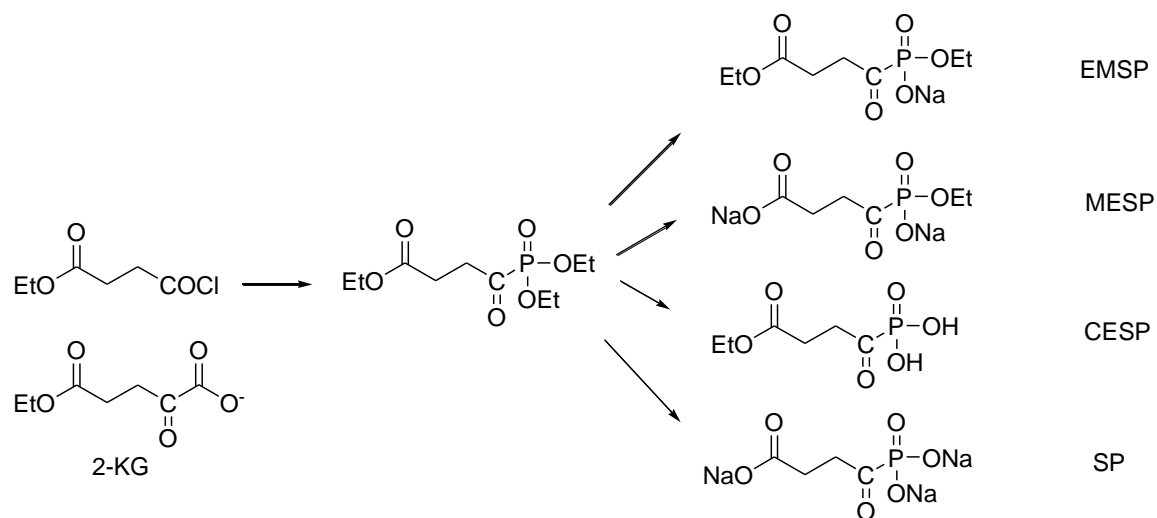


Figure 1.16: Some phosphonate analogues of 2-KG.

1.7.2 Analogues of isochorismate

Isochorismate (ISC) is known as an unstable intermediate compound in biosynthetic pathways⁶¹, such as in enterobactin biosynthesis. ISC can be prepared enzymatically from chorismate, although chemical synthesis of the racemic mixture was reported⁶². The absolute configuration of naturally occurring isochorismate was determined to be *trans*-(+)-5*S*,6*S*-5-[(1-carboxyethenyl)oxy]-6-hydroxy-1,3-cyclohexadiene-1-carboxylic acid⁶³. In studies of chorismate or isochorismate-utilizing enzymes, such as isochorismate synthase (IS) and isochorismatase, many analogues of isochorismate were prepared and used to investigate the catalysis⁶⁴.

Among the analogues of isochorismate, the molecules with the core of the 1,3-cyclohexadiene-1-carboxylate or benzoate are of greater interest due to the resemblance of the planar 1,3-cyclohexadiene conformation of isochorismate. Among 5,6-dihydrobenzoate, (2S,3S)-2-amino-3-hydroxy-2,3-dihydrobenzoate and (2S,3S)-2,3-dihydroxy-2,3-dihydrobenzoate (Figure 1.17), only (2S,3S)-2,3-dihydroxy-2,3-dihydrobenzoate was accepted by MenD to undertake 1,4-addition reaction as isochorismate⁶⁵. (2S,3S)-2,3-dihydroxy-2,3-dihydrobenzoic acid is the product from hydrolytic cleavage of isochorismate catalyzed by isochorismatase, therefore possessing the relative and absolute configuration of isochorismate. In that study, results suggested that the MenD-catalyzed 1,4-addition is limited to 1,3-cyclohexadiene-1-carboxylate scaffold, and is tolerant of even lacking the enolpyruvyl side chain.

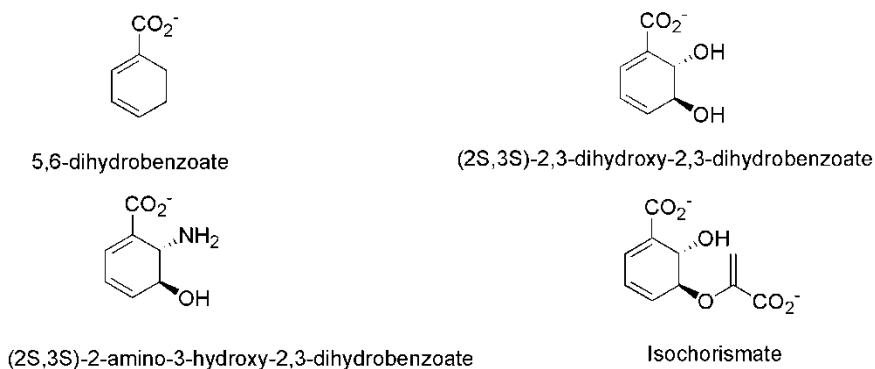


Figure 1.17: Isochorismate and analogues.

In studies of salicylate synthase and isochorismatase, aromatic analogues of isochorismate were designed and found them to be potent inhibitors of the enzymes (Figure 1.18)^{64,66}.

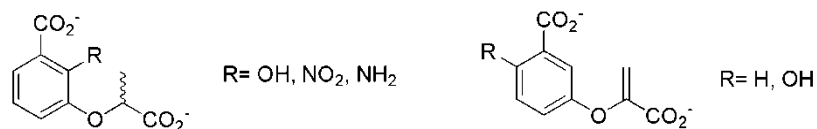


Figure 1.18: Aromatic analogues of isochorismate.

In the MenD reaction, isochorismate is actually playing a pivotal role since it provides the structural core for the product SEPHCHC and presumably isochorismate gets involved in all mechanistic steps after decarboxylation in the catalytic mechanism (Figure 1.5). Substrate analogues bearing a cyclohexadiene or benzoate moieties might get involved in or inhibit the MenD reaction, adding to the toolbox of the mechanistic probes which are useful for elucidation of the MenD reaction mechanism.

1.8 Steady-state kinetics and inhibition studies of enzymes

Although X-ray crystallography and NMR structural analysis of proteins in solution became powerful recently and demonstrates advantages in some aspects, kinetic analysis of enzyme-catalyzed reaction represents the most common method of elucidating enzyme mechanism. In an enzyme-catalyzed reaction, a progress curve (i.e. depletion of substrate or accumulation of product over time) usually has an early linear phase, ranging from seconds to several hundred seconds typically. Initial rate refers to the reaction rate at this linear phase when a steady state or quasi-equilibrium is reached. During the steady state, the concentrations of various enzymatic intermediates are in equilibrium and essentially constant. In classic textbooks of enzyme kinetics, for the simplest one substrate-one product reaction, the well-known Henri-Michaelis-Menten equation is introduced based on rapid equilibrium or steady-state approaches as equation 1.1:

$$v = \frac{V_m [S]}{K_m + [S]} \quad (1.1)$$

where $[S]$ is concentration of substrate, V_m is the maximal rate at very high (or "saturating") concentrations of substrate, and K_m , referred to as Michaelis constant in the literature, is the substrate concentration when initial rate is half the V_m .

Derivation of equation 1.1 gives some linear forms of the Henri-Michaelis-Menten equation which are especially useful under certain circumstances, for example the Lineweaver-Burk equation (also called double reciprocal equation, equation 1.2) and Hanes-Woolf equation (equation 1.3):

$$\frac{1}{v} = \left(\frac{K_m}{V_m} \frac{1}{[S]} \right) + \frac{1}{V_m} \quad (1.2)$$

$$\frac{[S]}{v} = [S] \left(\frac{1}{V_m} \right) + \frac{K_m}{V_m} \quad (1.3)$$

Among enzyme-catalyzed reactions, multisubstrate and multiproduct reactions are actually more common in biochemistry. In kinetic analysis of a multisubstrate system, if other substrate concentrations stay unchanged or are at the saturating level, the reaction can be treated as a one-substrate reaction with respect to the substrate with the concentration varied. Thus the principle, and the terms V_m and K_m , as discussed above are still applicable in the case of a more complex enzyme reaction.

Inhibitors are small molecules able to reduce enzyme activity by interfering with turnover in different ways. The study of enzyme inhibition is always one of the most important topics in enzymology, and in the pharmaceutical industry. Inhibitors can interact with enzymes reversibly or irreversibly. According to different binding modes (Figure 1.19), reversible inhibitors are generally categorized as competitive, noncompetitive, uncompetitive and mixed (thorough discussion was presented in the book by Segel⁶⁷):

1) Reversible competitive inhibitors can bind to the active sites of enzymes and thus block the binding of substrate in competitive manner;

2) Noncompetitive inhibitors bind with equal affinity to both the free enzyme and the enzyme-substrate complex at a site distinct from substrate binding site;

3) Uncompetitive inhibitors bind only to the enzyme-substrate complex at a site distinct from the substrate binding site, but not to free enzyme;

4) Mixed inhibitors are less commonly encountered compared with the three types of inhibition above. Similar to noncompetitive inhibition, mixed inhibitors bind to both free enzyme and the enzyme-substrate complex at a site distinct from substrate binding site, but with different affinity. Thus noncompetitive inhibitor can be considered as a special case of mixed inhibitor.

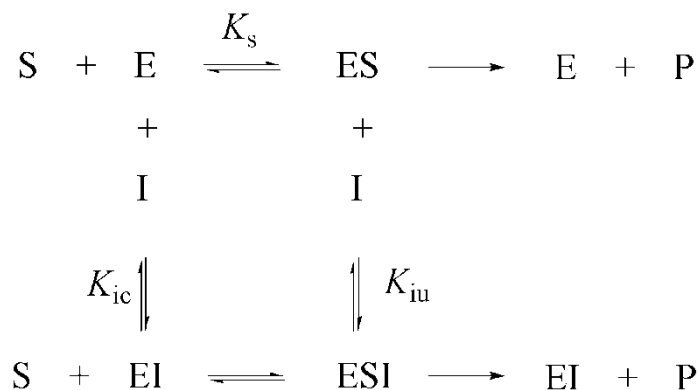


Figure 1.19: Equilibrium scheme of substrate, inhibitor and enzyme. K_s is the dissociation constant of substrate (S) and enzyme (E); K_{ic} is the dissociation constant of competitive inhibitor (I) and enzyme (E); K_{iu} is the dissociation constant of uncompetitive inhibitor (I) and enzyme-substrate complex (ES).

The type of inhibition can be determined graphically by a number of methods. A Lineweaver-Burk plot is a commonly encountered means of diagnosing inhibition type. At several fixed inhibitor concentrations, the double-reciprocal plot of $1/v$ versus $1/[S]$ usually yields overlaying straight lines in a pattern that is characteristic of the inhibition type. As shown in Figure 1.20, for competitive inhibitors, the straight lines intersect at their y intercepts (A); for noncompetitive inhibitors, lines intersect at x intercepts (B); for uncompetitive inhibitors, plot appears as a series of parallel lines (C) and mixed inhibitors, lines intersect above or below x axis dependent on the binding affinity to free enzyme and enzyme complex(D).

Alternatively, a combination of Dixon plot⁶⁸ ($1/v$ versus $[I]$ at several fixed $[S]$) and Cornish-Bowden plot^{69,70,71} ($[S]/v$ versus $[I]$ at several fixed $[S]$) can conveniently give the inhibition constant K_i (dissociation constant for enzyme-inhibitor (EI) complex) and inhibition type. As shown in Figure 1.21, for a competitive inhibitor, a Dixon plot gives directly the value of K_{ic} , while a Cornish-Bowden plot appears as parallel lines (A); for a mixed inhibitor (noncompetitive inhibitor is a special case of mixed inhibitor), although a

Dixon plot appears the same as for a competitive inhibitor, a Cornish-Bowden plot shows intersecting lines. In addition, the two plots give value of K_{ic} and K_{iu} respectively (B); for uncompetitive inhibitor, a Dixon plot shows parallel lines and a Cornish-Bowden plot appears as intersecting lines. In short, a combination of Dixon and Cornish-Bowden plots provide a straightforward method to graphically determine inhibition type and inhibition constants, therefore this approach also has wide application in the kinetic study of enzyme inhibition.

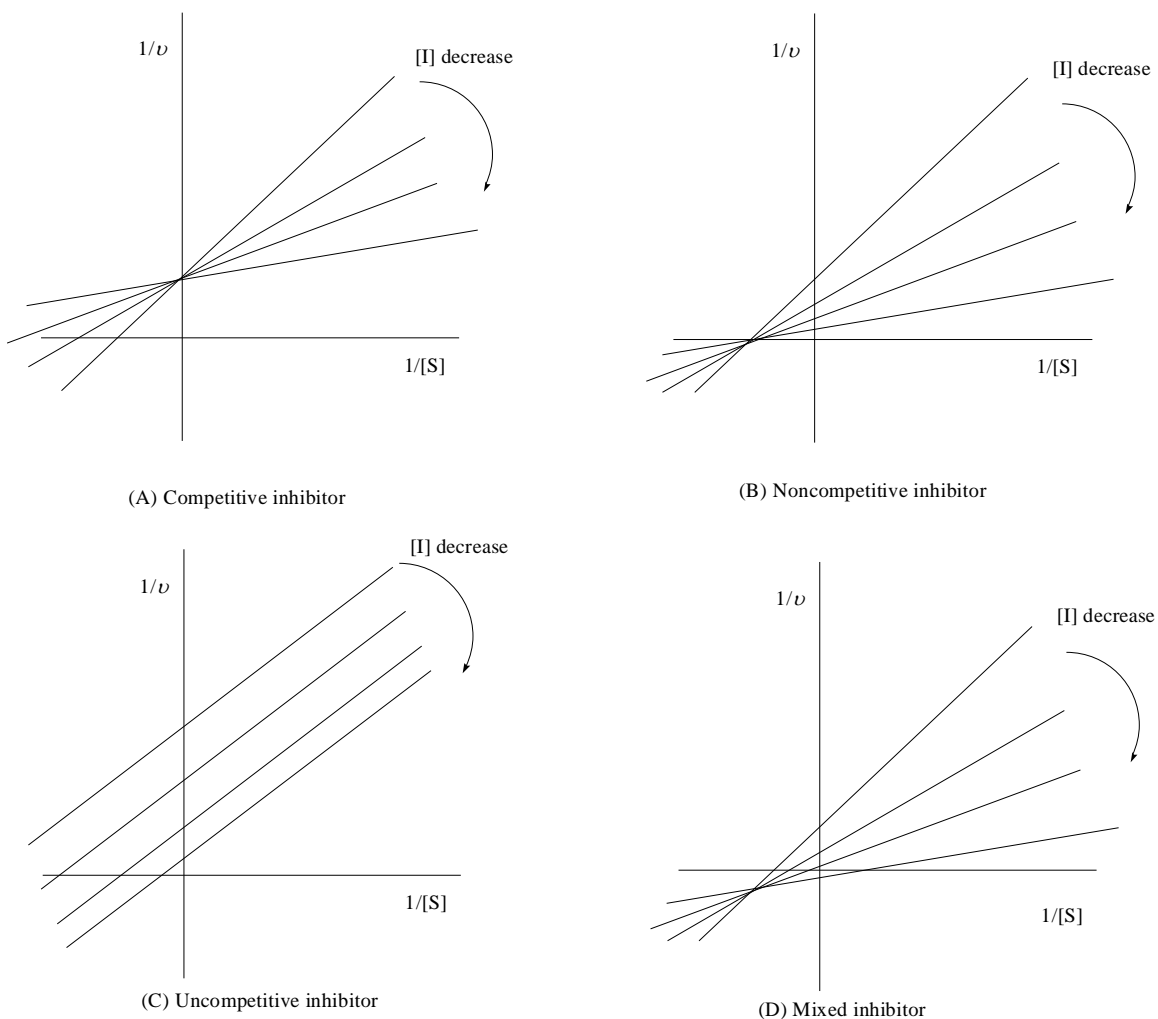


Figure 1.20: Inhibition patterns of lines in Lineweaver-Burk plots. (A) Competitive inhibitor; (B) noncompetitive inhibitor; (C) uncompetitive inhibitor; (D) mixed inhibitor.

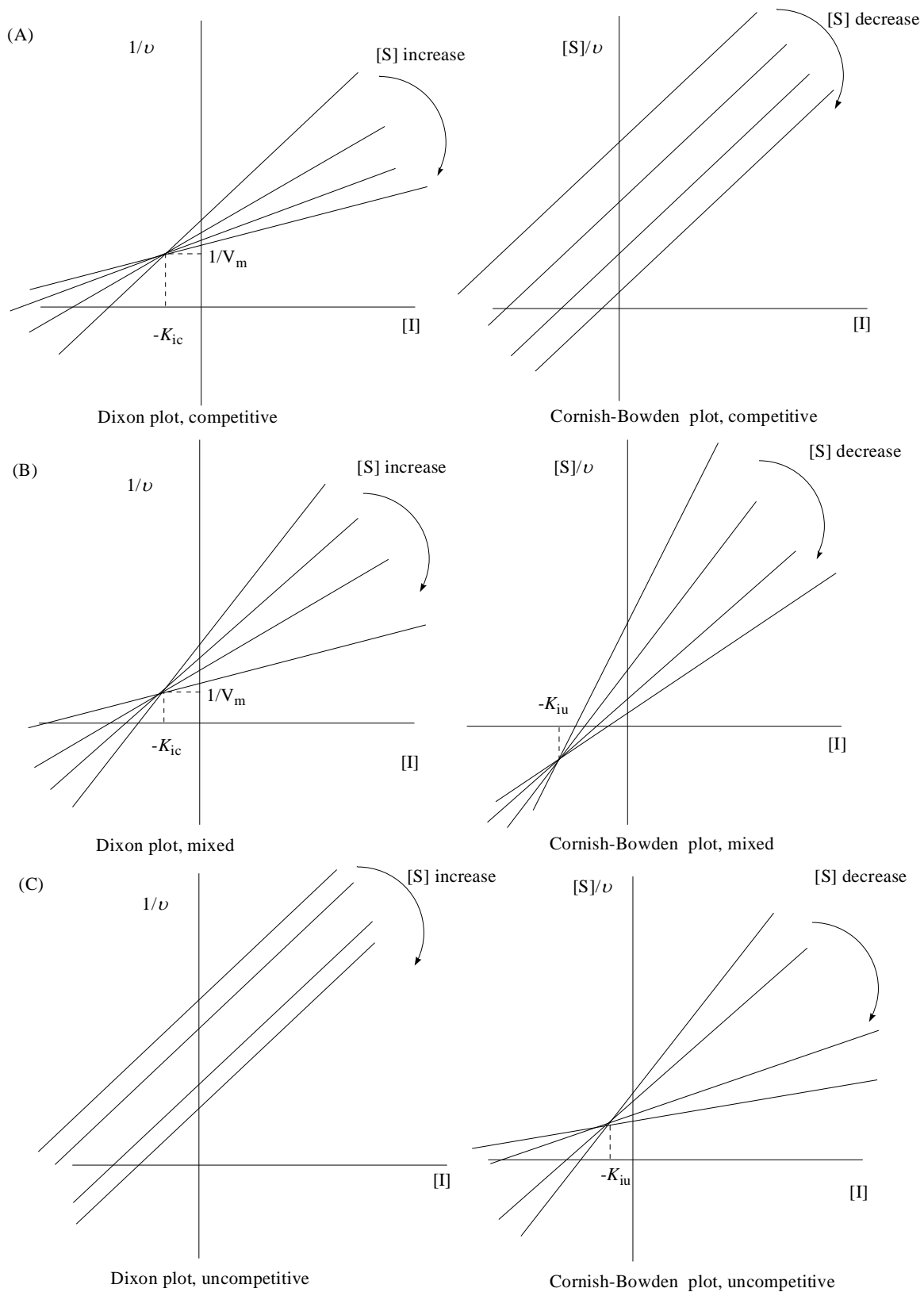


Figure 1.21: Dixon plot and Cornish-Bowden plot for diagnosing inhibition type.

1.9 Kinetic mechanism of bireactant biproduct (bi bi) reaction

A general nomenclature is utilized to depict the number of substrates and products in an enzyme-catalyzed reaction. For example, a reaction utilizing two substrates and producing two products is referred to as bi bi reaction; bi uni reaction means two substrates react, producing a single product.

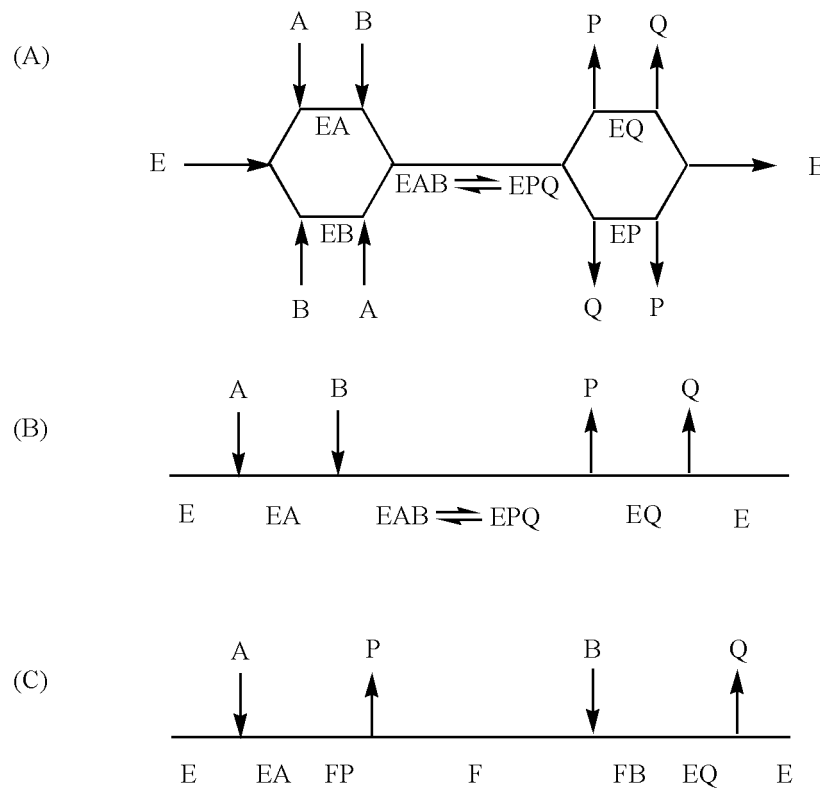


Figure 1.22: Bi bi reaction mechanisms. (A) Random ordered; (B) compulsory ordered; (C) ping-pong mechanism.

In the study of multisubstrate and multiproduct enzymatic reactions, the order in which substrates bind to the enzyme and products are released from the enzyme complex is of interest in that it is the reflection of reaction mechanism catalyzed by enzymes. In

the case of bi bi reaction ($A + B \rightarrow P + Q$), there are basically two types of mechanism: ternary-complex and ping-pong.

1) In a ternary-complex mechanism, two substrates bind to the enzyme in random order (random ordered bi bi reaction, Figure 1.22A) or in compulsory order (compulsory ordered bi bi reaction, Figure 1.22B). As illustrated in Figure 1.22, regardless of which substrate binds first, the ternary complex EAB is formed and turned over to product P and Q. The double reciprocal plots (Fig. Figure 1.23, $1/v$ versus $[A]$ at several fixed $[B]$, vice versa) for both ternary-complex mechanisms appear as intersecting set of lines, therefore one cannot distinguish random and compulsory ordered mechanisms by this method;

2) Ping-pong bi bi reaction is also called double displacement reaction. As illustrated in Figure 1.22C, product P is released before second substrate B binds to the enzyme (i.e. substrate B cannot bind to free enzyme). According to the steady-state approach, the initial rate equation for a ping-pong bi bi reaction can be obtained (equation 1.4).

$$v = \frac{V_m[A][B]}{K_m^B[A] + K_m^A[B] + [A][B]} \quad (1.4)$$

where K_m^A and K_m^B are the Michaelis constants for substrate A and B respectively. The double reciprocal plot for ping-pong bi bi reaction yields a set of parallel lines when one substrate concentration is varied at several constant concentrations of the other substrate (Figure 1.23B), distinct from the pattern of intersecting lines for ternary-complex bi bi reaction.

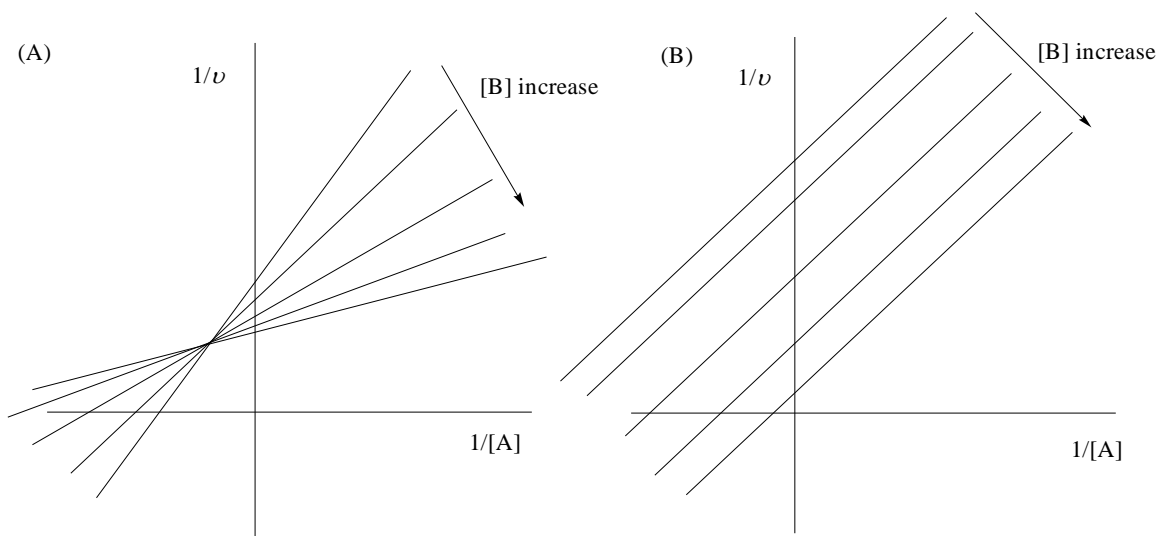


Figure 1.23 Double reciprocal plots for bi bi reactions. (A) Ternary-complex mechanism; (B) ping-pong mechanism.

As mentioned above, a double reciprocal plot cannot distinguish two different mechanisms involving ternary-complex. However, if there is product inhibition or dead-end competitive inhibition of one substrate in the bi bi enzymatic reaction, specific inhibition patterns for different mechanisms can be observed from kinetic analysis when one substrate concentration is varied and the other substrate is fixed at non-saturating concentration (\sim apparent K_m). The relationships in the case of inhibition patterns in the case of bi bi reaction were derived and summarized elsewhere (e.g. by Segel⁶⁷) as Table 1.1. According to Table 1.1, a dead-end competitive inhibitor can be used to not only distinguish compulsory and random ternary-complex mechanisms, but also determine the substrate binding order in a compulsory ordered reaction. Furthermore, a ping-pong mechanism has a specific inhibition pattern which allows the differentiation from ternary-complex mechanism, supplementary to the aforementioned double reciprocal plot method.

Table 1.1: Inhibition patterns of dead-end competitive inhibitors for bi bi reaction ($A + B \rightarrow P + Q$)⁷².

Reaction mechanism	Competitive inhibitor for substrate	Inhibition pattern	
		For varied [A]	For varied [B]
Random ordered	A B	Competitive Noncompetitive	Noncompetitive Competitive
Compulsory ordered (A binds first)	A B	Competitive Uncompetitive	Noncompetitive Competitive
Compulsory ordered (B binds first)	A B	Competitive Noncompetitive	Uncompetitive Competitive
Ping-pong (Double displacement)	A B	Competitive Uncompetitive	Uncompetitive Competitive

1.10 Objectives of research

When this project was started, MenD was still described as a SHCHC synthase as the first committed enzyme in the classical biosynthesis of vitamin K2 (menaquinone)¹⁴. However, subsequent studies showed that MenD actually catalyzes the formation of SEPHCHC^{5,6,15} and the X-ray structures of apo- and holo-MenD from *E. coli* also appeared in the literature^{31,33}. These reports represent a revolutionary advance in the enzymological research of MenD. However, the mechanism of the MenD-catalyzed reaction remains hypothetical; the systematic kinetics and structure-function relationships have not been explored.

In order to elucidate the enzymatic mechanism of MenD and confirm the suggestion that MenD is an SEPHCHC synthase, and on the basis of speculation as shown in Figure 1.5, some mechanistic probes were designed as structural analogues of the substrates and used to investigate the kinetics of the MenD reaction. Furthermore, point mutations of relevant residues in active site could be conducted on the basis of the published X-ray structure and sequence alignments with homologous enzymes. The kinetic studies of a series of MenD mutants in comparison with wild type enzyme could reveal the roles of specific residues and will lead to improving our understanding of the structure-function relationships within this enzyme.

In summary, the specific objectives of this work were as follows:

- 1) Validation of the method for kinetic assay of the MenD-catalyzed reaction using spectrophotometric measurement and HPLC analysis;
- 2) Determination of the steady-state kinetics of the MenD-catalyzed reaction;

- 3) Synthesis of succinyl phosphonate analogues of 2-KG and determination of inhibition constants;
- 4) Synthesis of ISC analogues and investigation of the MenD-catalyzed reaction using the analogues;
- 5) Investigation of the kinetic mechanism of the MenD-catalyzed reaction using the analogues of 2-KG and ISC;
- 6) Point mutation of the active site residues of MenD and determination of the kinetics of the MenD mutants.

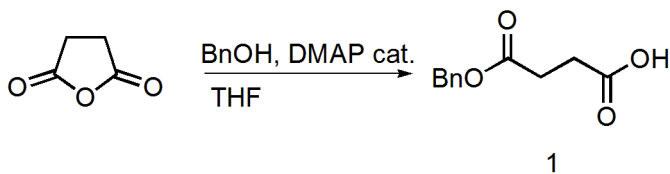
2. EXPERIMENTAL

2.1 Chemical synthesis

Experiments that required anhydrous conditions were performed under an inert atmosphere of either dry argon or nitrogen gas. Glassware was dried overnight in an oven set at 120 °C and assembled under a stream of inert gas. All reagents were obtained from commercial suppliers (Sigma-Aldrich, Alfa-Aesar, VWR and TCI) and used without further purification unless indicated otherwise. Dichloromethane and acetonitrile were freshly distilled from calcium hydride. Thin layer chromatography (TLC) was performed on precoated silica gel plates (Merck Kieselgel 60F₂₅₄, 0.25 mm thickness) and visualized with phosphomolybdic acid-cerium sulfate reagent (solution prepared as: conc. H₂SO₄ (9 ml), phosphomolybdic acid (10 g), Ce(SO₄)₂ (2.5 g) and water (added up to 250 ml)), iodine vapors, ninhydrin (1.5 % w/v solution in *tert*-butanol) or ultraviolet light at 254 nm. Flash chromatography was performed using Merck silica gel 60 (230-400 mesh). All NMR spectra for ¹HNMR, ¹³CNMR, COSY, HMBC, HMQC, and JMOD were acquired using a Bruker 500 MHz spectrometer with samples dissolved in the appropriate deuterated solvents. Chemical shifts for ¹HNMR and ¹³CNMR were reported in ppm downfield from tetramethylsilane and determined by the residual solvent proton signal; chemical shifts of ³¹PNMR were reported in ppm downfield from 85% phosphoric acid as standard. Mass spectrometry was performed on a mass spectrometer API Qstar

XL pulsar hybrid LC/MS/MS system with Agilent 1100 series HPLC or an integrated syringe pump. Melting points were measured on a Gallencamp melting point apparatus and are not corrected. The NMR and high-resolution mass spectrometry were determined in the Saskatchewan Structural Sciences Centre (<http://www.usask.ca/sssc/>). Specific rotations ($[\alpha]_D$) are the average of 5 determinations for one solution at ambient temperature using a 1 ml, 10 cm cell; the units are $\text{deg dm}^{-1}\text{cm}^3\text{g}^{-1}$, the concentrations (c) are reported in g/100 ml, and the values are rounded to reflect the accuracy of the measured concentrations (the major source of error).

2.1.1 Succinic acid monobenzyl ester

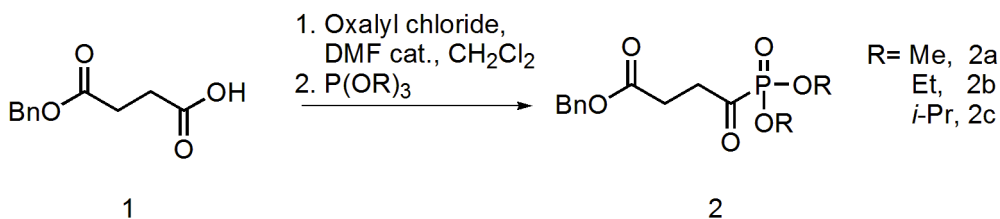


This compound was prepared as described in the literature⁷³. Succinic anhydride (6.0 g, 60 mmol), benzyl alcohol (5.4 g, 50 mmol) and DMAP (0.3 g, 2.5 mmol) were refluxed in anhydrous THF (30 ml) under argon overnight. White powder was recrystallized from ethyl acetate and hexane (9.1 g, yield: 87%). The ¹H NMR and ¹³C NMR spectra are consistent with that of the literature.

¹H NMR (CDCl₃): δ 2.71 (m, 4H), 5.16 (s, 2H), 7.36 (m, 5H);

¹³C NMR (CDCl₃): δ 28.9, 28.9, 66.7, 128.2, 128.3, 128.6, 135.7, 171.8, 171.2.

2.1.2 Benzyl alkyl diester of succinyl phosphonate



At 0 °C, succinic acid monobenzyl ester (6.25 g, 30.0 mmol) was suspended in 25 ml dry CH₂Cl₂ containing 1 drop of DMF. Oxalyl chloride (16.5 ml, 2.0 M in DCM, 33.0 mmol) was added dropwise under argon atmosphere. After stirring at ambient temperature for 1 hour, the reaction mixture became a clear solution. After 30 minutes, the volatiles were rotary evaporated (40 °C) to yield a brown oily residue (6.80 g, ca. 100%). This residue was used without further purification. To 3.50 g (15.4 mmol) of the residue was added trimethyl phosphite (1.82 ml, 15.4 mmol) slowly at 0 °C; bubbles evolved immediately. After stirring at ambient temperature for 2 hours, the mixture was concentrated in vacuo to give brown oil (**2a**, 4.63 g, ca. 100%). The product was used next without further purification.

¹H NMR (CDCl₃, 500MHz): δ 2.69 (t, *J* = 6.0 Hz, 2 H) 3.15 (td, *J* = 6.5 Hz, 2.0 Hz, 2 H), 3.84 (d, *J* = 10.5 Hz, 3H), 3.86 (d, *J* = 10.5 Hz, 3H), 5.11 (s, 2 H), 7.33 (m, 5 H);

³¹P NMR (CDCl₃, 200 MHz): δ -1.0;

HRMS (ESI⁺): calcd for C₁₃H₁₈O₆P 301.0835, found 301.0840 ([M+H]⁺); calcd for C₁₃H₁₇O₆NaP 323.0654, found 323.0656 ([M+Na]⁺).

Benzyl diethyl ester of succinyl phosphonate (**2b**) was prepared as **2a** in ca. 100% yield.

2b: ^1H NMR (CDCl_3 , 500 MHz): δ 1.36 (m, 6 H), 2.68 (t, $J = 6.5$ Hz, 2 H), 3.17 (td, $J = 6.5$ Hz, 2.3 Hz, 2 H), 4.21 (m, 4 H), 5.11 (s, 2 H), 7.34 (m, 5 H);

^{31}P NMR (CDCl_3 , 200 MHz): δ -1.5;

HRMS (ESI^+): calcd for $\text{C}_{15}\text{H}_{22}\text{O}_6\text{P}$ 329.1148, found 329.1141 ($[\text{M}+\text{H}]^+$).

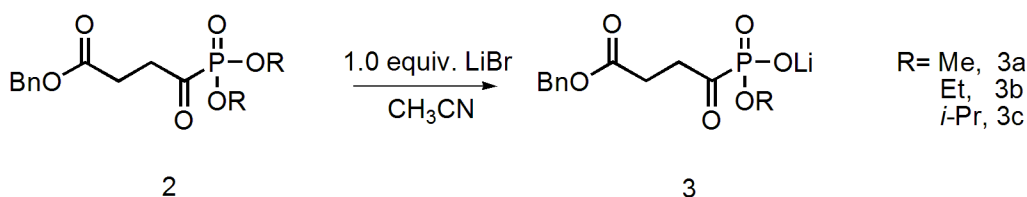
Benzyl diisopropyl ester of succinyl phosphonate (**2c**) were prepared as **2a** in ca. 100% yield

2c: ^1H NMR (CDCl_3 , 500 MHz): δ 1.36 (m, 12 H), 2.67 (t, $J = 6.5$ Hz, 2 H), 3.18 (td, $J = 6.5$ Hz, 2.5 Hz, 2 H), 4.77(m, 2 H), 5.13 (s, 2 H), 7.34 (m, 5 H);

^{31}P NMR (CDCl_3 , 200MHz): δ -4.5;

HRMS (ESI^+): calcd for $\text{C}_{17}\text{H}_{26}\text{O}_6\text{P}$ 357.1461, found 357.1469 ($[\text{M}+\text{H}]^+$).

2.1.3 Benzyl monoester succinyl phosphonate



The preparation followed the literature method with slight modification⁷⁴. Triester **2a** (2.60 g, 8.66 mmol) was dissolved in dry acetonitrile (11 ml), and then the solution was stirred with anhydrous LiBr (0.75 g, 8.66 mmol). The resulting yellow solution was heated to 70 °C (oil bath) under argon atmosphere. A white precipitate formed within 10

minutes and was vacuum filtered after 20 hours, then washed with dry acetonitrile and anhydrous diethyl ether. White powder was obtained (benzyl monomethyl succinyl phosphonate, **BMMP**, **3a**, 2.10 g, 83%).

^1H NMR (D_2O , 500 MHz): δ 2.69 (t, $J = 6.0$ Hz, 2 H), 3.16 (td, $J = 6.0$ Hz, 2.0 Hz, 2 H), 3.55 (d, $J = 10.5$ Hz, 3 H), 5.16 (s, 2 H), 7.43 (m, 5 H);

^{13}C NMR (D_2O , 125 MHz): δ 27.4 (d, $J_{\text{c-p}} = 4.5$ Hz), 38.5 (d, $J_{\text{c-p}} = 49.0$ Hz), 53.3 (d, $J_{\text{c-p}} = 6.0$ Hz), 67.5, 128.6, 129.0, 129.2, 129.5, 135.9, 175.1, 219.2 (d, $J_{\text{c-p}} = 165.5$ Hz);

^{31}P NMR (D_2O , 200 MHz): δ -0.5;

HRMS(ESI): calcd for $\text{C}_{12}\text{H}_{14}\text{O}_6\text{P}$ 285.0533, found 285.0531 ($[\text{M-Li}]^-$); (ESI $^+$): calcd for $\text{C}_{12}\text{H}_{14}\text{LiO}_6\text{PK}$ 331.0319, found 331.0327 ($[\text{M+K}]^+$).

Benzyl monoethyl succinyl phosphonate (**BMEP**, **3b**) was prepared as **3a** from **2b**.

3b (yield: 70%): ^1H NMR (D_2O , 500 MHz): δ 1.21 (t, $J = 7.1$ Hz, 3 H), 2.67 (t, $J = 6.2$ Hz, 2 H), 3.17 (td, $J = 6.0$ Hz, 2.0 Hz, 2 H), 3.87 (m, 2 H), 5.16 (s, 2 H), 7.43 (m, 5 H);

^{13}C NMR (D_2O , 125 MHz): δ 16.3 (d, $J_{\text{c-p}} = 5.5$ Hz), 27.5 (d, $J_{\text{c-p}} = 4.5$ Hz), 38.4 (d, $J_{\text{c-p}} = 49.0$ Hz), 63.0 (d, $J_{\text{c-p}} = 6.0$ Hz), 67.5, 128.6, 129.0, 129.2, 135.9, 175.2, 219.6 (d, $J_{\text{c-p}} = 166.0$ Hz);

^{31}P NMR (D_2O , 200 MHz): δ -1.5;

HRMS(ESI): calcd for $\text{C}_{13}\text{H}_{16}\text{O}_6\text{P}$ 299.0690, found 299.0688($[\text{M-Li}]^-$).

Benzyl monoisopropyl succinyl phosphonate (**BMIP**, **3c**) was prepared as **3a** from **2c**.

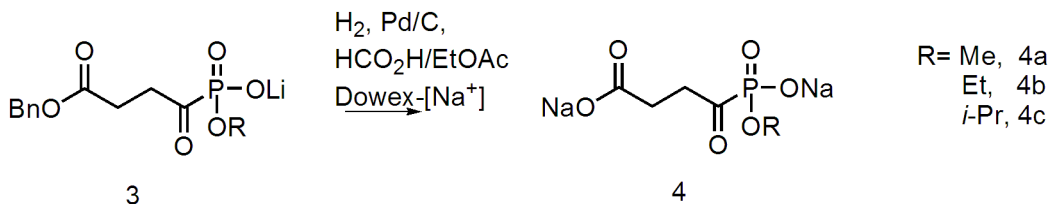
3c (yield: 62%): ^1H NMR (CDCl_3 , 500 MHz): δ 1.21 (d, $J = 6.0$ Hz, 6 H), 2.67 (t, $J = 6.5$ Hz, 2 H), 3.18 (d, $J = 6.5$ Hz, 2 H), 4.39 (m, 1 H), 5.16 (s, 2 H), 7.43 (m, 5 H);

^{13}C NMR (CDCl_3 , 125 MHz): δ 23.7, 23.8, 27.5 (d, $J_{\text{c-p}} = 4.5$ Hz), 38.4 (d, $J_{\text{c-p}} = 49.0$ Hz), 67.5, 71.5 (d, $J_{\text{c-p}} = 6.0$ Hz), 128.6, 128.6, 128.9, 129.2, 136.0, 175.2, 219.9 (d, $J_{\text{c-p}} = 167.5$ Hz);

^{31}P NMR (CDCl_3 , 200 MHz): δ -3.0.

HRMS(ESI^+): calcd for $\text{C}_{14}\text{H}_{19}\text{LiO}_6\text{P}$ 321.1073, found 321.1082 ($[\text{M}+\text{H}]^+$).

2.1.4 Monoester succinyl phosphonate



Compound **3a** (0.50g, 1.7 mmol) was dissolved in a mixture of EtOAc (10 ml) and formic acid (3 ml) and was hydrogenated with 10% Pd/C (50 mg) using a balloon technique. After 16 h, the reaction mixture was vacuum filtered through celite and the filter cake was washed with EtOAc and water. The filtrate was evaporated to give pale yellow oil (0.41 g). This material was dissolved in water (1-2 ml) and passed through a column of Dowex 50W-X8 (Na^+) by eluting with deionized water. The desired fractions were pooled and evaporated (40 $^\circ\text{C}$) *in vacuo* to give pale yellow oily residue. The residue was triturated in acetone and dried *in vacuo*. Pale yellow powder was obtained (monomethyl succinyl phosphonate, **MMSP**, **4a**, 0.35 g, 85%).

^1H NMR (D_2O , 500 MHz): δ 2.44 (t, J = 6.5 Hz, 2H), 3.08 (t, J = 6.5 Hz, 2H), 3.63 (d, J = 10.5 Hz, 3H);

^{31}P NMR (D_2O , 200 MHz): δ 0.0;

HRMS(ESI^+): calcd for $\text{C}_5\text{H}_8\text{O}_6\text{Na}_2\text{P}$ 240.9848, found 240.9853($[\text{M}+\text{H}]^+$)

Monoethyl succinyl phosphonate (**MESP**, **4b**) was prepared as **4a** from **4b**.

4b (yield: 60%): ^1H NMR (D_2O , 500 MHz): δ 1.26 (t, J = 7.0 Hz, 3 H), 2.66 (t, J = 6.1 Hz, 2 H), 3.17 (td, J = 6.2 Hz, 1.7 Hz, 2 H), 4.0 (m, 2 H);

^{31}P NMR (D_2O , 200 MHz): δ -1.5;

HRMS(ESI^+): calcd for $\text{C}_6\text{H}_{10}\text{O}_6\text{Na}_2\text{P}$ 255.0010, found 255.0010($[\text{M}+\text{H}]^+$)

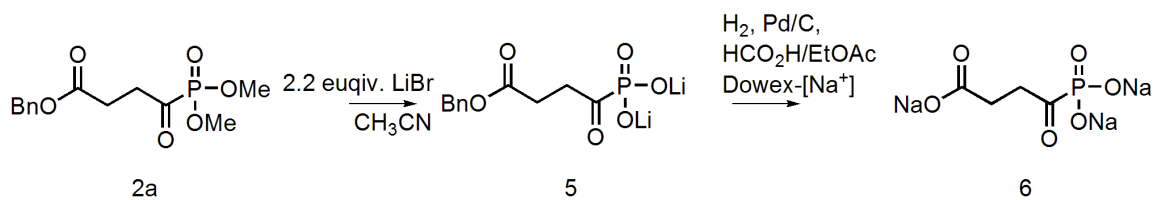
Monoisopropyl succinyl phosphonate (**MISP**, **4c**) were prepared as **4a** from **4c**.

4c (yield: 87%): ^1H NMR (D_2O , 500 MHz): δ 1.26 (d, J = 7.0 Hz, 6 H), 2.40 (t, J = 6.0 Hz, 2 H), 3.09 (t, J = 6.0 Hz, 2 H), 4.46 (q, J = 7.0 Hz, 1 H);

^{31}P NMR (D_2O , 200 MHz): δ -2.47;

HRMS(ESI^+): calcd for $\text{C}_7\text{H}_{12}\text{O}_6\text{Na}_2\text{P}$ 269.0161, found 269.0163 ($[\text{M}+\text{H}]^+$); calcd for $\text{C}_7\text{H}_{13}\text{O}_6\text{NaP}$ 247.0341, found 247.0321($[\text{M}-\text{Na}+2\text{H}]^+$).

2.1.5 Succinylphosphonate



Compound **2a** (4.63 g, 15.4 mmol) and LiBr (2.94 g, 33.9 mmol) were dissolved in dry acetonitrile (30 ml), and the reaction mixture was heated to reflux under argon for 72 hours. The precipitate was filtered and washed with dry acetonitrile and anhydrous ether. White powder was yielded (**5**, 4.16 g, 95%). Compound **6** (succinylphosphonate, **SP**) was then prepared from **5** as **4a-c**.

5 (yield: 95%): $^1\text{H NMR}$ (D_2O , 500 MHz): δ 2.61 (t, $J = 6.3$ Hz, 2 H), 3.16 (td, $J = 5.9$ Hz, 1.2 Hz, 2 H), 5.17 (s, 2 H), 7.43 (m, 5 H);

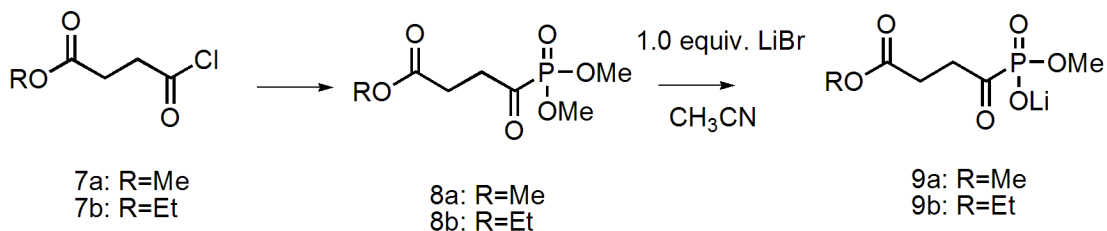
$^{13}\text{C NMR}$ (D_2O , 125 MHz): δ 27.8 (d, $J_{\text{c-p}} = 3.6$ Hz), 38.1 (d, $J_{\text{c-p}} = 44.0$ Hz), 67.4, 128.7, 128.9, 129.2, 136.1, 176.0, 226.4 (d, $J_{\text{c-p}} = 158.4$ Hz);

$^{31}\text{P NMR}$ (D_2O , 200 MHz): δ -0.59.

6 (yield: 85%): $^1\text{H NMR}$ (D_2O , 500 MHz): δ 2.35 (t, $J = 7.1$ Hz, 2 H), 3.01 (td, $J = 7.2$, 1.1 Hz);

HRMS(ESI): Calcd for $\text{C}_4\text{H}_6\text{O}_6\text{P}$ 180.9907, found 180.9911($[\text{M}-3\text{Na}+2\text{H}]^-$).

2.1.6 Methyl monomethyl succinylphosphonate and ethyl monomethyl succinylphosphonate



Methyl monomethyl succinylphosphonate (**MMMP, 9a**) was prepared from **7a**⁷⁵ and trimethyl phosphite via **8a** as **3a-c**.

9a (yield:): ¹H NMR (D₂O, 500 MHz): δ 2.66 (t, *J* = 6.0 Hz, 2 H), 3.14 (t, *J* = 6.0 Hz, 2 H), 3.60 (d, *J* = 10.5 Hz, 3 H), 3.68 (s, 3 H);

¹³C NMR (D₂O, 125 MHz): δ 27.1 (d, *J*_{c-p} = 4.0 Hz), 38.4 (d, *J*_{c-p} = 49.0 Hz), 52.7, 53.3 (d, *J*_{c-p} = 6.0 Hz), 176.0, 219.4 (d, *J*_{c-p} = 165.7 Hz)

³¹P NMR (D₂O, 200 MHz): δ -0.45;

HRMS(ESI): Calcd for C₆H₁₀O₆P 209.0221, found 209.0215 ([M-Li]).

Ethyl monomethyl succinylphosphonate (**EMMP, 9b**) was prepared as **9a**.

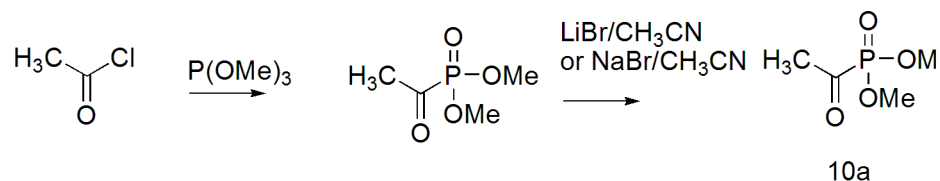
9b (yield:): ¹H NMR (D₂O, 500 MHz): δ 1.23 (t, *J* = 7.0 Hz, 3 H), 2.64 (t, *J* = 6.0 Hz, 2 H), 3.15 (t, *J* = 6.0 Hz, 2 H), 3.61 (d, *J* = 10.5 Hz, 3 H), 4.14 (q, *J* = 7.0 Hz, 2 H);

¹³C NMR (D₂O, 125 MHz): δ 13.6, 27.5 (d, *J*_{c-p} = 4.5 Hz), 38.5 (d, *J*_{c-p} = 36 Hz), 53.3 (d, *J*_{c-p} = 6.0 Hz), 62.3, 175.6, 219.4 (d, *J*_{c-p} = 165.7 Hz);

³¹P NMR (D₂O, 200 MHz): δ -0.47.

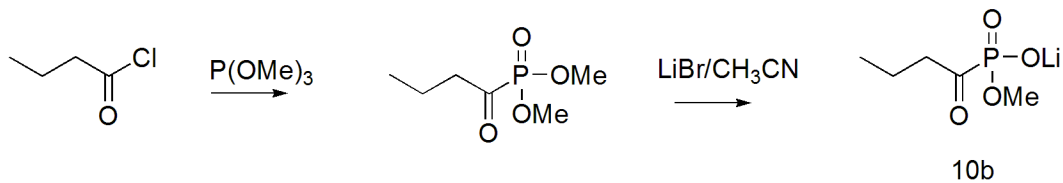
HRMS(ESI): Calcd for C₇H₁₂O₆P 223.0377, found 223.0367 ([M-Li]).

2.1.7 Methyl acetylphosphonate and monomethyl butyrylphosphonate



Methyl acetylphosphonate (**MAP, 10a**) was prepared from acetyl chloride as described in the literature⁷⁴.

10a: ¹H NMR (D₂O, 500 MHz): δ 2.43 (d, *J* = 5.0 Hz, 3 H), 3.62 (d, *J* = 10.5 Hz, 3 H).



Monomethyl butyrylphosphonate (**MMBP, 10b**) was prepared from butyryl chloride as described in literature⁷⁴.

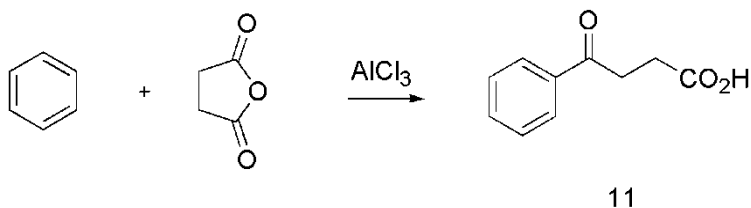
10b: ¹H NMR (D₂O, 500 MHz): δ 0.89 (t, *J* = 7.5 Hz, 3 H), 1.60 (m, 2 H), 2.80 (d, *J* = 7.5 Hz, 2 H), 3.62 (d, *J* = 10.0 Hz, 3 H);

¹³C NMR (D₂O, 125 MHz): δ 13.2, 16.4 (d, *J*_{c-p} = 3.0 Hz), 45.4 (d, *J*_{c-p} = 45.5 Hz), 53.2 (d, *J*_{c-p} = 6.0 Hz), 222.6 (d, *J*_{c-p} = 160.3 Hz);

³¹P NMR (D₂O, 200 MHz): δ 0.16;

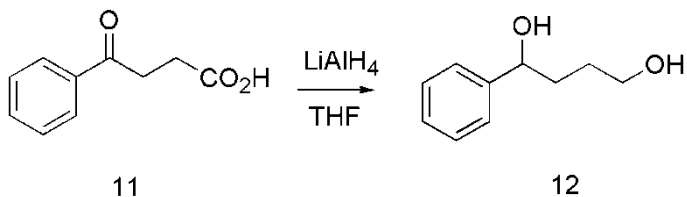
HRMS (ESI): Calcd for C₅H₁₀O₄P 165.0322, found 165.0362 ([M-Li]⁻).

2.1.8 β -Benzoylpropionic acid and 1-phenyl-1,4-butanediol



β -Benzoylpropionic acid (compound **11**) was prepared as described in the literature^{76,77}. The mixture of succinic anhydride (6.8 g, 68 mmol) and anhydrous AlCl₃ (20.0 g, 0.15 mol) in dry benzene (30 ml) was heated up to reflux for 30 min. After cooled to room temperature, the reaction mixture was poured in a mixture of conc. HCl (10 ml) and ice (100 g). White precipitate was formed with stirring and collected by filtration. The product cake was washed with cold water and petroleum ether. After dried under high vacuum, white powder was obtained (11.5 g, Yield: 95%). The ¹H NMR spectrum is consistent with that of the literature.

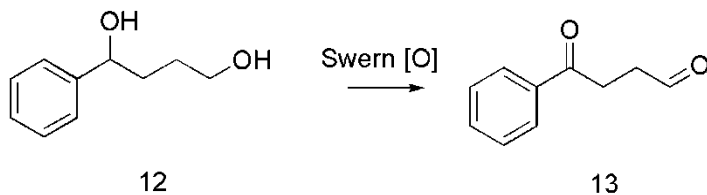
¹H NMR (CDCl₃): 2.82 (t, 2H, *J* = 6.51 Hz, CH₂CO₂H), 3.32 (t, 2H, *J* = 6.51 Hz, COCH₂), 7.47 (t, 2H, *J* = 7.66 Hz, Ph-*H*), 7.59 (t, 1H, *J* = 7.22 Hz, Ph-*H*), 7.99 (d, 2H, *J* = 7.88 Hz, Ph-*H*).



1-Phenyl-1,4-butanediol (**12**) was prepared as described in literature with a modified work-up and purification⁷⁸. The resulting white powder (crude product) was washed with CHCl_3 on a filter and the collected filtrate was evaporated to give yellow oily residue. The residue was purified with dry-column flash chromatography (30-100% ethyl acetate/hexane) to give **12** as a colorless liquid (yield: 85%, *lit.* 93%).

^1H NMR (CDCl_3): δ 1.66 (m, 2H, CH_2), 1.84 (m, 2H, CH_2), 2.76 (br, 2H, 2OH), 3.65 (m, 2H, CH_2OH), 4.70 (td, $J = 6.28, 2.16$ Hz, 1H, CHOH), 7.24-7.35 (m, 5H, Ph-H).

2.1.9 4-Oxo-4-phenylbutanal



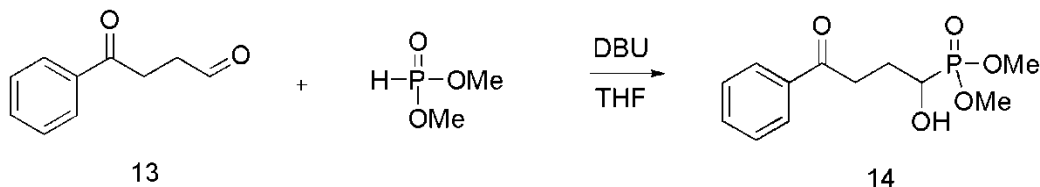
The compound **13** was prepared with a modified literature method (change temperature control)⁷⁹. At -78 °C under argon, to a solution of oxalyl chloride (56 ml, 112 mmol, 2M in dichloromethane) and dry dichloromethane (150 ml) was slowly added anhydrous DMSO (13.6 ml). After stirring for 10 min, a solution of 1-phenyl-1,4-butanediol (4.0 g, 24 mmol) in 60 ml dichloromethane was added over 20 min. The mixture was kept at -78 °C for 40 min and then Et_3N (80 ml) was added slowly. After stirring at -78 °C for 20 min, the reaction mixture was warmed up to room temperature

and then passed through a silica gel pad (ca. 5 cm high). Dichloromethane was used to wash the pad. The collected brown solution was evaporated to give yellow residue. The residue was purified by flash column with 15% EtOAc in hexane to give **13** (3.73g, yield: 96%, *lit.* 80%) as a yellow-brown liquid ($R_f = 0.29$, 40% EtOAc in hexane).

^1H NMR (CDCl_3): δ 2.93 (t, $J = 6.31$ Hz, 2H, CH_2), 3.33 (t, $J = 6.32$ Hz, 2H, CH_2), 7.47 (m, 2H, Ph- H), 7.57 (m, 1H, Ph- H), 7.98 (m, 2H, Ph- H), 9.90 (s, 1H, CHO);

^{13}C NMR(CDCl_3): δ 31.0, 37.7, 128.4, 130.0, 133.4, 136.5, 197.9, 200.7..

2.1.10 Dimethyl 1-hydroxy-4-oxo-4-phenyl-butylphosphonate



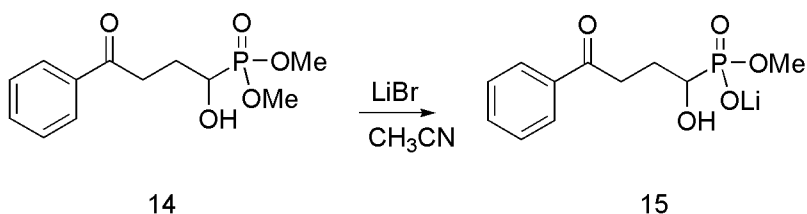
The compound **14** was prepared according to the literature method⁸⁰. The crude product (green oily residue) was purified by flash column with 100% EtOAc to afford **14** as a white solid (yield: 74%, mp. 88-90 °C).

^1H NMR (CDCl_3): δ 2.14 (m, 1H of CH_2CHOH), 2.27 (m, 1H of CH_2CHOH), 3.28 (m, 2H, CH_2CO), 3.81 (2d, 6H, $J_{\text{HP}} = 10.32$ Hz, 2P-O CH_3), 4.04 (m, 1H, CHO H), 7.45 (m, 2H, Ph- H), 7.56 (m, 1H, Ph- H), 7.97 (m, 2H, Ph- H);

^{31}P NMR (CDCl_3): δ 26.80;

^{13}C NMR (CDCl_3): δ 25.9 (d, $^3J_{\text{CP}} = 2.0$ Hz, CH_2CO), 34.7 (d, $^2J_{\text{CP}} = 13.5$ Hz, $\text{CH}_2\text{CH}(\text{OH})\text{P}$), 53.5 (d & d, $^2J_{\text{CP}} = 6.3, 7.1$ Hz, 2P-OCH_3), 67.1 (d, $J_{\text{CP}} = 162.3$ Hz, CHOH), 128.1, 128.6, 133.2, 136.9, 200.2.

2.1.11 Lithium monomethyl-(1-hydroxy-4-oxo-4-phenyl-butyl)-phosphonate



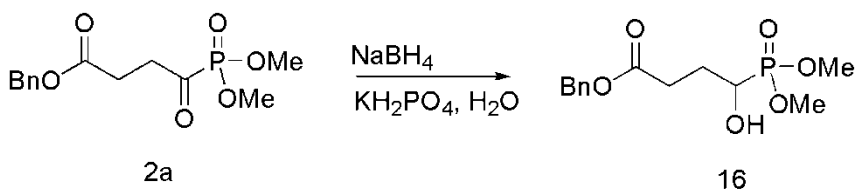
A solution of dimethyl 1-hydroxy-4-oxo-4-phenyl-butylphosphonate (**14**, 0.14 g, 0.50 mmol) and lithium bromide (43 mg, 0.50 mmol) in acetonitrile (4 ml) was heated to 70 °C (oil bath) under argon overnight. The white precipitate was collected by vacuum filtration and washed with acetonitrile and diethyl ether to give **5** (0.10 g, yield: 76%) as a white powder.

^1H NMR (D_2O): δ 1.99 (m, 1H of CH_2CHOH), 2.17 (m, 1H of CH_2CHOH), 3.31 (m, 1H of COCH_2), 3.25 (m, 1H of COCH_2), 3.61 (d, 3H, $J = 9.9$ Hz, P-OCH_3), 3.84 (m, 1H, CHOH), 7.55 (m, 2H, Ph-H), 7.68 (m, 1H, Ph-H), 8.00 (m, 2H, Ph-H);

^{31}P NMR (D_2O): δ 22.29;

^{13}C NMR (D_2O): δ 27.1 (d, $^3J_{\text{CP}} = 3.3$ Hz, CH_2CO), 35.7 (d, $^2J_{\text{CP}} = 12.7$ Hz, $\text{CH}_2\text{CH}(\text{OH})\text{P}$), 52.5 (d, $^2J_{\text{CP}} = 6.2$ Hz, P-OCH_3), 67.6 (d, $J_{\text{CP}} = 158.5$ Hz, CHOH), 128.7, 129.3, 134.42, 136.9, 205.8.

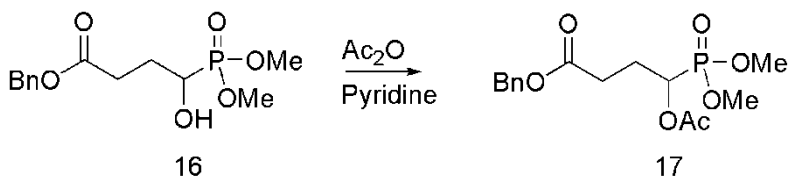
2.1.12 Benzyl 4-(dimethoxyphosphoryl)-4-hydroxybutanoate



The compound **16** was prepared from **2a** according to the literature⁸¹. Crude product (yellow oil) was purified by flash column with 70-100% EtOAc in hexane to give **2** (yield: 69%) as a colorless liquid ($R_f = 0.1$, 70% EtOAc in hexane).

¹H NMR (CDCl₃): δ 2.10 & 2.01 (2m, 2H, CH₂CH₂CH), 2.62 (m, 2H, COCH₂), 3.77 & 3.76 (d & d, $J_{HP} = 10.2$ Hz, 6H, 2POCH₃), 3.97 (m, 1H, CHOH), 5.11 (d, $J = 1.75$ Hz, 2H, PhCH₂), 7.24 (m, 5H, Ph-H).

2.1.13 Benzyl 4-acetoxy-4-(dimethoxyphosphoryl)butanoate



At 0 °C, to a solution of compound **16** (3.12 g, 10.4 mmol) in pyridine (10 ml) was added acetic anhydride (2.0 ml, 21.2 mmol, ca. 2 equiv.) under argon atmosphere. The reaction mixture was stirred at room temperature overnight. Pyridine was removed by coevaporation with toluene and the brown oily residue was taken with EtOAc (50 ml),

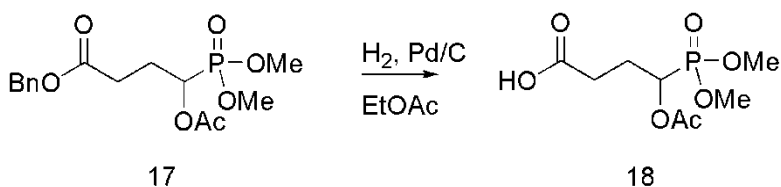
washed with 1N HCl (15 ml x 3), water (10 ml) and brine (10 ml) and dried over Na₂SO₄. After concentration *in vacuo*, benzyl 4-acetoxy-4-(dimethoxyphosphoryl) butanoate (**17**) was given as a pale yellow liquid (3.38 g, yield: 94%). The product was used for next step without further purification.

¹H NMR (CDCl₃): δ 2.10 (s, 3H, CH₃CO), 2.15 (m, 1H, one H of CH₂CHOH), 2.26 (m, 1H, one H of CH₂CHOH), 2.47 (m, 2H, COCH₂), 3.78 (2d, *J*_{HP} = 10.5, 11.0 Hz, 6H, 2P-OCH₃), 5.11 (s, 2H, PhCH₂), 5.33 (m, 1H, CHOAc), 7.34 (m, 5H, Ph-H);

³¹P NMR (D₂O): δ 22.53;

¹³C NMR (D₂O): δ 20.7, 24.9, 30.4 (d, ²*J*_{CP} = 12.0 Hz, CH₂CH), 53.5, 66.7, 66.6 (d, *J*_{CP} = 169.1 Hz, CH-P), 128.4, 128.7, 135.9, 169.8, 172.2.

2.1.14 4-Acetoxy-4-(dimethoxyphosphoryl)butanoic acid



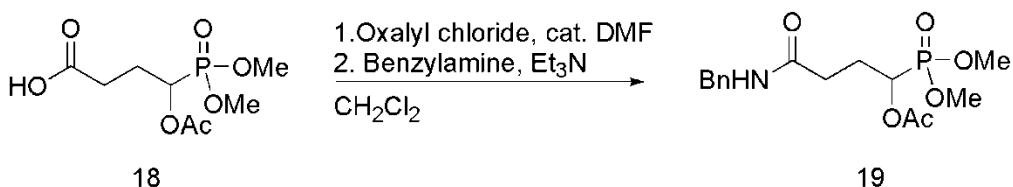
Compound **17** (3.0 g, 8.7 mmol) in EtOAc (25 ml) was hydrogenated with 10% Pd/C (0.5 g) using a balloon technique. After overnight, the reaction mixture was vacuum filtered through celite. The filtrate was evaporated *in vacuo* to give 4-acetoxy-4-(dimethoxyphosphoryl)butanoic acid (**18**) as a colorless liquid (2.20 g, yield: ca. 100%). The product was used for next step without further purification.

^1H NMR (CDCl_3): δ 2.11 (br, 4H, CH_3CO and one H of CH_2CHOAc), 2.22 (m, 1H, one H of CH_2CHOAc), 2.43 (m, 2H, COCH_2), 3.78 (m, 6H, 3P-O CH_3), 5.33 (m, 1H, CHOAc);

^{31}P NMR (D_2O): δ 22.66;

^{13}C NMR (D_2O): δ 20.6, 24.7, 30.0 (d, $^2J_{\text{CP}} = 12.1$ Hz, CH_2CH), 53.6, 53.7, 66.5 (d, $J_{\text{CP}} = 169.2$ Hz, CH-P), 169.8, 176.7.

2.1.15 4-(Benzylamino)-1-(dimethoxyphosphoryl)-4-oxobutyl acetate

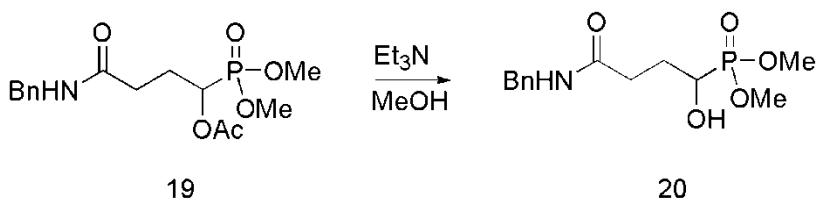


At 0 °C, to a solution of compound **18** (1.08 g, 4.25 mmol) in dry dichloromethane (5 ml) was added 1 drop of DMF under argon protection. Oxalyl chloride (2.33 ml, 2.0 M in dichloromethane) was added slowly. The reaction mixture was allowed to stir at room temperature and volatiles were evaporated after 1.5 hours. The resultant residue was taken with dichloromethane (30 ml) and cooled to 0 °C, to which Et_3N (0.65 ml, 4.67 mmol) and benzylamine (0.51 ml, 4.67 mmol) were added slowly. The mixture stirred at room temperature overnight and then concentrated *in vacuo*. The residue was partitioned in HCl (1N, 15 ml) and EtOAc (50 ml). The organic layer was separated and washed twice with HCl (1N, 15 ml), then sat. NaHCO_3 (15 ml) and brine (10 ml), and dried over

Na₂SO₄. The solvent was removed *in vacuo* to give the crude product (0.64 g) as a pale yellow liquid. The crude product was purified by flash column with 5% MeOH in dichloromethane to give compound **19** (0.48 g, yield: 33%) as a colorless liquid (R_f = 0.35, MeOH in dichloromethane, visualized with I₂). ¹H NMR showed that the product was still with some impurity and the product was used for next step without further purification.

¹H NMR (CDCl₃): δ 2.05 (s, 3H, CH₃CO), 2.21 & 2.12 (2m, 2H, CH₂CHOH), 2.62 & 2.45 (2m, 2H, COCH₂), 3.70 (m, 6H, 2 P-OCH₃), 4.40 (t, J = 2.6 Hz, 2H, PhCH₂), 5.26 (m, 1H, CHOAc), 6.52 (br, 1H, CONH), 7.25 (m, 5H, Ph-H).

2.1.16 Dimethyl 4-(benzylamino)-1-hydroxy-4-oxobutylphosphonate



A mixture of compound **19** (0.47 g, 1.37 mmol) and Et₃N (0.29 ml, 2.08 mmol) in MeOH (30 ml) was stirred at room temperature. The reaction was monitored by TLC (R_f = 0.24, 10% MeOH in dichloromethane, visualized with I₂). After 16 hours, the reaction mixture was partitioned in EtOAc and HCl solution. The organic layer was separated and the aqueous layer was extracted with EtOAc (x 3). The combined organic layer was dried over Na₂SO₄ and evaporated *in vacuo* to give a pale yellow liquid (0.34 g), which was

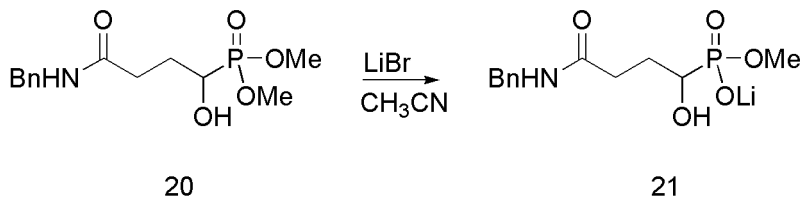
eluted with 5% MeOH in dichloromethane to give compound **6** (0.15 g, yield: 36%) as a colorless liquid.

^1H NMR (CDCl_3): δ 2.15 & 2.07 (2m, 2H, CH_2CH), 2.60 & 2.52 (2m, 2H, COCH_2), 3.81 (2d, $J_{\text{HP}} = 10.3, 10.3$ Hz, 6H, 2P-O CH_3), 4.01 (m, 1H, CHOH), 4.44 (t, $J = 2.6$ Hz, 2H, PhCH_2), 6.29 (br, 1H, CONH), 7.33 (m, 5H, Ph-H);

^{31}P NMR (D_2O): δ 26.55;

^{13}C NMR (D_2O): δ 27.4, 33.3 (d, $^2J_{\text{CP}} = 13.5$ Hz, CH_2CH), 44.2, 53.7 (2d, $^2J_{\text{CP}} = 6.3, 7.1$ Hz, 2P-O CH_3), 67.8 (d, $J_{\text{CP}} = 163.5$ Hz, CH-P), 128.0, 128.2, 129.1, 138.4, 173.4.

2.1.17 Lithium methyl 4-(benzylamino)-1-hydroxy-4-oxobutylphosphonate



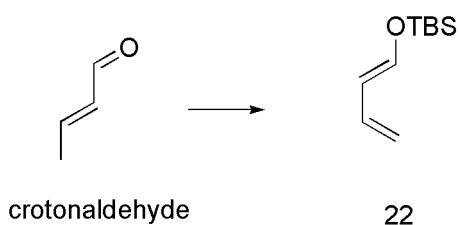
A solution of compound **20** (0.15 g, 0.50 mmol) and lithium bromide (43 mg, 0.50 mmol) in acetonitrile (4 ml) was heated to 70 °C (oil bath) under argon overnight. The precipitate was collected by vacuum filtration and washed with acetonitrile and diethyl ether to give **21** (0.10 g, yield: 68%, m.p. 223-225 °C) as a pale yellow powder.

^1H NMR (CDCl_3): δ 2.10 & 1.93 (2m, 2H, CH_2CH), 2.55 & 2.47 (2m, 2H, 2 COCH_2), 3.62 (d, $J_{\text{HP}} = 10.0$ Hz, 3H, P-OCH_3), 3.77 (m, 1H, CHOH), 4.42 (s, 2H, PhCH_2), 7.44 (m, 5H, Ph-H);

^{31}P NMR (D_2O): δ 22.05;

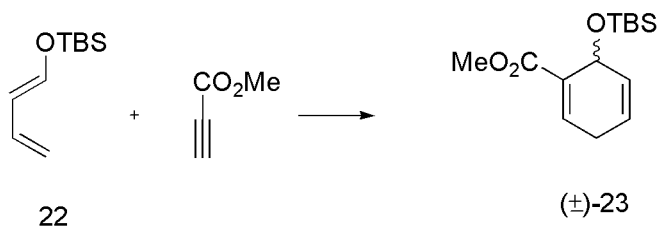
^{13}C NMR (D_2O): δ 28.4, 33.1 (d, $^2J_{\text{CP}} = 13.1$ Hz, $\text{CH}_2\text{CH}(\text{OH})\text{P}$), 43.5, 52.5 (d, $^2J_{\text{CP}} = 6.3$ Hz, 2 P-OCH_3), 68.5 (d, $J_{\text{CP}} = 158.3$ Hz, CH-P), 127.8, 127.9, 129.3, 138.6, 176.5.

2.1.18 Methyl 2-*tert*-butyldimethylsilyloxycyclohexa-3,5-diene-1-carboxylate



1-[(*tert*-Butyl-dimethylsilyl)oxy]1,3-butadiene (**22**) was prepared as oily residue from crotonaldehyde according to the literature method (yield: 72%, *lit.* 84%)⁸². The HNMR spectrum is consistent with that of the literature.

^1H NMR (CDCl_3): δ 0.16 (s, 6H), 0.92 (s, 9H), 4.81 (t, 1H, $J = 10.0$ Hz), 4.98 (t, 1H, $J = 17.0$ Hz), 5.73 (t, 1H, $J = 11.5$ Hz), 6.22 (dt, 1H, $J = 17.0, 10.5$ Hz), 6.57 (d, 1H, $J = 12.0$ Hz).

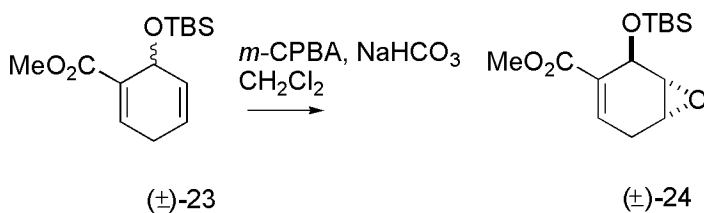


Methyl 2-*tert*-butyldimethylsilyloxycyclohexa-3,5-diene-1-carboxylate (compound **23**) was prepared from **22** and methyl propiolate according to literature method (yield: 60%, *lit.* 71%, $R_f = 0.26$ in 5% EtOAc/hexane)⁸³. The HNMR and CNMR spectra are consistent with that of the literature.

¹H NMR (CDCl₃): δ 0.94 (s, 3H), 0.12 (s, 3H), 0.86 (s, 9H), 2.84 (m, 2H), 3.76 (s, 3H), 5.07 (m, 1H), 5.87 (appar. d, 2H, $J = 1.5$ Hz), 7.01 (t, 1H, $J = 3.0$ Hz);

¹³C NMR (CDCl₃): δ -4.3, -4.0, 18.2, 26.0, 27.5, 51.6, 61.7, 124.9, 128.3, 131.8, 137.8, 167.4.

2.1.19 Methyl 2-(*tert*-butyldimethylsilyloxy)-7-oxabicyclo[4.1.0]hept-3-ene-3-carboxylate



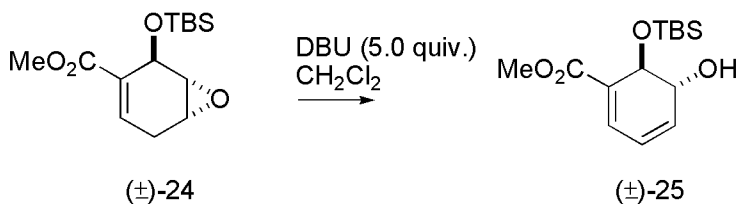
Methyl 2-(*tert*-butyldimethylsilyloxy)-7-oxabicyclo[4.1.0]hept-3-ene-3-carboxylate (compound **24**) was prepared with modified literature method⁸³. A solution of *m*-CPBA (ca. 65%, 20.0 g, 75.3 mmol) in CH₂Cl₂ (150 ml) was washed with brine in 500 ml

separatory funnel. The organic layer was separated and dried over anhydrous MgSO₄. The MgSO₄ was filtered off to obtain dry *m*-CPBA solution in CH₂Cl₂. Diene **23** (10.13 g, 37.7 mmol), NaHCO₃ (9.50 g, 113.1 mmol) and CH₂Cl₂ (250 ml) were mixed and heated to reflux in a 1L three-necked round-bottom flask equipped with a condenser and a dropping funnel under nitrogen gas protection. The dried *m*-CPBA solution in CH₂Cl₂ was added to the mixture through the dropping funnel over 30 min. The resulting mixture was then heated to reflux for additional 4 hours, then cooled to room temperature and stirred overnight. The reaction mixture was filtered through celite and the filtrate was washed with sat. Na₂S₂O₅ solution (140 ml x 3), sat. NaHCO₃ solution (100 ml x 2), H₂O (100 ml) and brine (100 ml), dried over Na₂SO₄, and then evaporated *in vacuo* to give oily residue. The residue was purified by flash chromatography using 5-10% EtOAc/hexane to give product as a colorless liquid (7.60 g, yield: 71%, R_f = 0.18 in 15% EtOAc/Hexane).

¹H NMR (CDCl₃): δ 0.09 (s, 3H), 0.18 (s, 3H), 0.87 (s, 9H), 2.73 (m, 2H), 3.25 (m, 1H), 3.32 (m, 1H), 3.73 (s, 3H), 5.03 (s, 1H), 6.74 (m, 1H).

¹³C NMR (CDCl₃): δ -4.5, -4.5, 18.2, 25.9, 26.0, 49.4, 51.7, 54.4, 63.0, 129.4, 135.6, 166.7.

2.1.20 Methyl 6-(*tert*-butyldimethylsilyloxy)-5-hydroxycyclohexa-1,3-diene-carboxylate



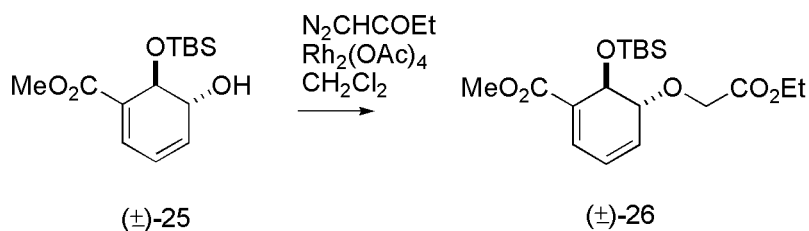
Epoxide **24** (1.95 g, 6.86 mmol) and 1,8-diazabicyclo[5.4.0]undec-7-ene (5.21 g, 34.22 mmol) were dissolved in CH_2Cl_2 (60 ml) and stirred under argon at room temperature overnight. The solvent was removed *in vacuo* and the residue was taken with EtOAc (50 ml). Then the resulting solution was washed with sat. NaHCO_3 solution (15 ml x 3) and brine (15 ml), dried over Na_2SO_4 and evaporated *in vacuo* to give a brown oily residue. The residue was purified with a flash chromatography using 25% EtOAc/hexane to give methyl 6-(*tert*-butyldimethylsilyloxy)-5-hydroxycyclohexa-1,3-diene-carboxylate (**25**) as a colorless liquid (1.65g, yield: 85%, $R_f = 0.17$ in 25% EtOAc/hexane).

^1H NMR (CDCl_3): δ 0.1 (s, 3H), 0.2 (s, 3H), 0.82 (s, 9H), 1.44 (d, 1H, $J = 7.5$ Hz, OH), 4.13 (m, 1H), 4.68 (s, 1H), 6.26 (dd, 1H, $J = 9.0, 5.5$ Hz), 6.32 (dd, 1H, $J = 9.0, 5.5$ Hz), 7.11 (d, 1H, $J = 5.5$ Hz).

^{13}C NMR (CDCl_3): δ -4.8, 4.5, 18.1, 25.7, 51.7, 67.7, 69.3, 124.5, 129.6, 132.5, 132.5, 167.1;

HRMS (CI^+): calcd for $\text{C}_{14}\text{H}_{25}\text{O}_4\text{Si}$ 285.1522, found 285.1528 ($[\text{M}+1]^+$)

2.1.21 Methyl 6-(*tert*-butyldimethylsilyloxy)-5-(2-ethoxy-2-oxoethoxy)cyclohexa-1,3-dienecarboxylate



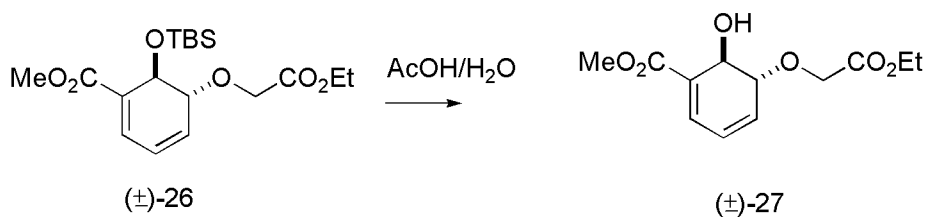
To a solution of diene alcohol **25** (1.14 g, 4.01 mmol) in dry CH_2Cl_2 (2 ml) was added rhodium (II) acetate dimer (8.8 mg, 1 mol %). A solution of ethyl diazoacetate (containing 15% CH_2Cl_2 , 0.27 g, 2.01 mmol) in CH_2Cl_2 (1 ml) was added under argon at room temperature over 1 hour. After stirring for additional 1 hour, the reaction mixture was concentrated *in vacuo* and purified with flash chromatography using 10-50% EtOAc/hexane to give the unreacted diene alcohol **25** (0.60 g) and methyl 6-(*tert*-butyldimethylsilyloxy)-5-(2-ethoxy-2-oxoethoxy)cyclohexa-1,3-dienecarboxylate (**26**) as a colorless liquid (0.50 g, yield: 71% based on consumed starting material, $R_f = 0.32$ in 25% EtOAc/hexane).

^1H NMR (CDCl_3): δ 0.06 (s, 3H), 0.16 (s, 3H), 0.80 (s, 9H), 1.27 (t, 3H, $J = 7.0$ Hz), 3.76 (s, 3H), 4.06 (m, 3H, CHOCH_2), 4.20 (q, 2H, $J = 7.0$ Hz), 4.75 (s, 1H), 6.26 (dd, 1H, $J = 9.5, 5.0$ Hz), 6.35 (dd, 1H, $J = 9.5, 5.5$ Hz), 7.10 (d, 1H, $J = 5.5$ Hz);

^{13}C NMR (CDCl_3): δ -4.7, -4.4, 14.3, 18.1, 25.0, 51.8, 61.1, 65.1, 65.4, 76.4, 126.3, 129.3, 130.1, 132.8, 170.0, 170.4;

HRMS (EI^+): calcd for $\text{C}_{18}\text{H}_{30}\text{O}_6\text{Si}$ 370.1812, found 370.1820 ($[\text{M}]^+$).

2.1.22 Methyl 5-(2-ethoxy-2-oxoethoxy)-6-hydroxycyclohexa-1,3-diene carboxylate



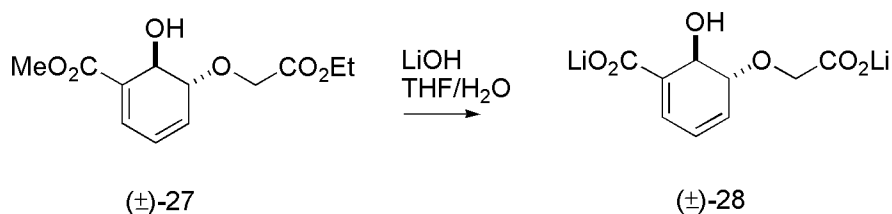
Compound **26** (0.43 g, 1.11 mmol) was mixed with AcOH (9 ml) and H₂O (6 ml), and the mixture was stirred at room temperature overnight. The reaction mixture was evaporated to dryness *in vacuo* to give a pale yellow oily residue. The residue was purified with a flash chromatography using 40% EtOAc/hexane to give product methyl 5-(2-ethoxy-2-oxoethoxy)-6-hydroxycyclohexa-1,3-diene carboxylate (**27**) as a colorless liquid (0.25 g, yield: 84%, $R_f = 0.18$ in 40% EtOAc/hexane).

¹H NMR (CDCl₃): δ 1.28 (t, 3H, $J = 7.0$ Hz), 3.43 (s, 1H), 3.80 (s, 3H), 4.21 (q, 2H, $J = 7.0$ Hz), 4.28 (s, 2H), 4.34 (ddd, 1H, $J = 6.5, 3.0, 1.5$ Hz), 4.88 (d, 1H, $J = 6.5$ Hz), 6.16 (ddd, 1H, $J = 9.5, 5.5, 1.5$ Hz), 6.30 (dd, 1H, $J = 9.0, 3.0$ Hz), 7.01 (d, 1H, $J = 5.5$ Hz); .

¹³C NMR (CDCl₃): δ 14.3, 52.2, 61.1, 67.0, 69.5, 79.6, 123.9, 129.6, 132.8, 133.0, 167.5, 170.7..

HRMS (EI⁺): calcd for C₁₂H₁₆O₆ 256.0947, found 256.0942 ([M]⁺).

2.1.23 5-(Carboxymethoxy)-6-hydroxycyclohexa-1,3-diene carboxylate (CHCD)



1.) Acid form of CHCD

At 0 °C, to the mixture of di-ester **27** (0.64 g, 3.9 mmol) in THF/H₂O (24 ml/6 ml) was added LiOH.H₂O (982 mg, 23.4 mmol). The mixture was stirred at room temperature for 24 hours. Volatiles were removed *in vacuo* below 30 °C, and the residue was diluted to 2.0 ml with deionized water and passed through Dowex 50WX8-100 [H⁺] column. Fractions with pH < 3 (or monitored by the UV absorbance at 280 nm) were lyophilized and checked by ¹H NMR. The pure product ((±)-**CHCD**, **28**) was pale brown powder.

¹H NMR (D₂O): δ 4.19 (dd, 1H, *J* = 5.0, 1.5 Hz), 4.70 (s, 1H), 4.24 (s, 2H), 6.37 (dd, 1H, *J* = 9.5, 5.0 Hz), 6.46 (dd, 1H, *J* = 10.5, 5.5 Hz), 7.24 (d, 1H, *J* = 5.5 Hz)..

2.) Lithium salt of CHCD

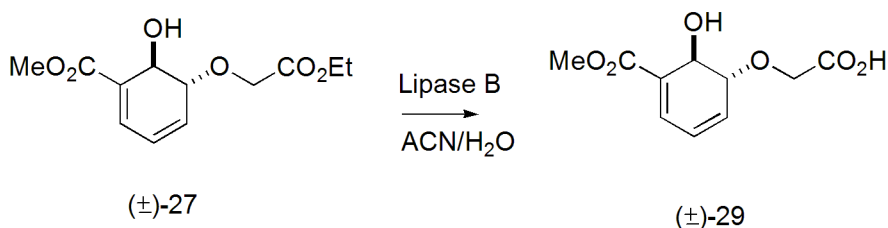
The preparation is the same as the acid form, but the crude product was loaded to the Dowex 1X8-100 [Cl⁻] column. After washed with deionized water, the column was eluted with LiCl solution (0~1.0 M). Fractions were monitored by the UV absorbance at 280 nm. Appropriate fractions were lyophilized and checked by ¹H NMR. The lyophilized residues with good purity were triturated for several times with a mixture of acetone and methanol (v/v 10:1). White powder was collected by vacuum filtration and dried under oil pump.

¹H NMR (D₂O): δ 3.95 (s, 2H), 4.11 (m, 1H), 4.70 (d, 1H, *J* = 3.0 Hz), 6.19 (dd, 1H, *J* = 9.5, 5.0 Hz), 6.32 (dd, 1H, *J* = 10.5, 5.5 Hz), 6.82 (d, 1H, *J* = 5.5 Hz);.

^{13}C NMR (D_2O): δ 65.9, 66.9, 76.6, 126.5, 127.5, 130.0, 134.0, 174.4, 177.9;

HRMS(ESI $^-$): calcd for $\text{C}_9\text{H}_8\text{LiO}_6$ 219.0486, found 219.0490 ($[\text{M-Li}]^-$).

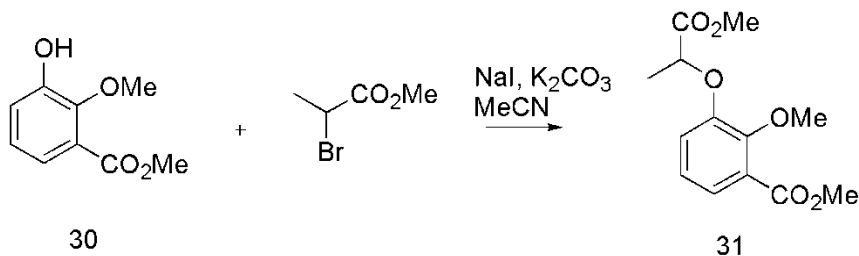
2.1.24 5-Carboxymethoxy-6-hydroxy-cyclohexa-1,3-dienecarboxylic acid methyl ester (CHCDMe)



At room temperature, diester **27** was mixed with acetonitrile (2 ml) and H_2O (2 ml). To the mixture was added Novozyme 435 (104 mg, *Candida antarctica* Lipase B immobilized on acrylic resin, Sigma). The mixture was stirred for 2.5 hours at room temperature and filtered through a cotton plug in glass pipette, washed with a mixture of acetonitrile and H_2O (v/v 1:1). The collected filtrate was rotary evaporated and lyophilized to yield pale yellow residue ((\pm) -CHCDMe, **29**).

^1H NMR (D_2O): δ 3.68 (s, 3H), 4.07 (s, 1H, $J = 5.0$ Hz), 4.61 (s, 1H), 4.09 (s, 2H), 6.26 (dd, 1H, $J = 9.5, 5.0$ Hz), 6.34 (dd, 1H, $J = 9.5, 6.0$ Hz), 7.13 (d, 1H, $J = 6.0$ Hz).

2.1.25 Methyl 2-methoxy-3-(1-methoxy-1-oxopropan-2-yloxy)benzoate



Methyl 3-hydroxy-2-methoxybenzoate (**30**) was prepared starting from 2,3-dihydroxybenzoic acid according to the literature method⁸⁴.

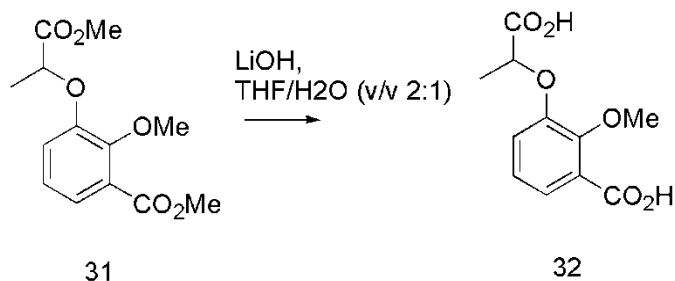
¹H NMR (CDCl₃): δ 3.91 (s, 3H), 3.92 (s, 3H), 6.02 (s, 1H, OH), 7.04 (appar. t, 1H, *J* = 8 Hz), 7.14 (dd, 1H, *J* = 8, 1.5 Hz), 7.38 (dd, 1H, *J* = 8, 1.5 Hz).

The mixture of compound **30** (0.73 g, 4.0 mmol), NaI (0.12 g, 20 mol %), anhydrous K₂CO₃ (1.10 g, 2.0 equiv.) methyl 2-bromopropionate (0.58 ml, 1.3 equiv.) and MeCN (40 ml) was refluxed under argon overnight. The reaction was monitored with TLC (5% MeOH in CH₂Cl₂). After removal of solvent *in vacuo*, the residue was taken with CH₂Cl₂ (20 ml) and H₂O (10 ml). The aqueous layer was separated and extracted with CH₂Cl₂ (10 ml x 2). The organic layers were combined and dried over MgSO₄. After removal of solvent, the residue was purified with a flash chromatography using 2% MeOH/CH₂Cl₂ to give methyl 2-methoxy-3-(1-methoxy-1-oxopropan-2-yloxy)benzoate (**31**) as a colorless liquid (0.83 g, yield: 77%).

¹H NMR (CDCl₃): δ 1.64 (d, 3H, *J* = 7.0 Hz), 3.73 (s, 3H), 3.89 (s, 3H), 3.94 (s, 3H), 4.79 (q, 1H, *J* = 7.0 Hz), 7.01 (m, 2H), 7.37 (dd, 1H, *J* = 7.0, 2.5 Hz);

^{13}C NMR (CDCl_3): δ 18.6, 52.1, 52.2, 61.6, 74.1, 119.8, 123.7, 124.0, 126.6, 150.3, 151.5, 166.5, 172.2. ,.

2.1.26 3-(1-Carboxyethoxy)-2-methoxybenzoic acid



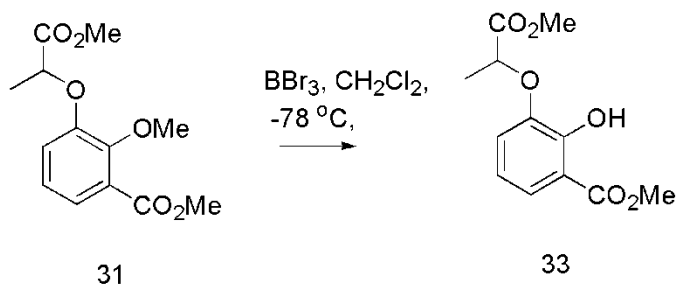
Compound **31** (0.33 g, 1.23 mmol) was mixed with LiOH.H₂O (0.21 g, 5.01 mmol, 4.0 equiv.) in a mixture of THF (4 ml) and H₂O (2 ml), and stirred at room temperature overnight. THF was removed *in vacuo* and to the solution was added H₂O (*ca.* 5 ml). The resulting aqueous solution was then washed with EtOAc (7 ml) and acidified to pH = 1-2 with aq. HCl (5 M), then extracted with EtOAc (15 ml x 2). The combined organic phase was washed with brine (10 ml) and dried over MgSO₄, and evaporated *in vacuo* to give 3-(1-carboxyethoxy)-2-methoxybenzoic acid (**32**) as pale yellow liquid. After recrystallization from EtOAc/hexane (v/v 1:1), a white solid was obtained (0.25 g, yield: 83%, m.p. 135-137 °C).

^1H NMR (CDCl_3): δ 1.75 (d, 3H, J = 7.0 Hz), 4.14 (s, 3H), 4.89 (q, 1H, J = 7.0 Hz), 7.09 (dd, 1H, J = 8.0, 1.5 Hz), 7.16 (appar. t, 1H, J = 8.0 Hz), 7.76 (dd, 1H, J = 8.0, 1.5 Hz);

^{13}C NMR (CDCl_3): δ 18.6, 62.7, 73.4, 120.0, 123.1, 125.0, 125.7, 149.3, 150.2, 166.1,

175.7.

2.1.27 Methyl 2-hydroxy-3-(1-methoxy-1-oxopropan-2-yloxy)benzoate

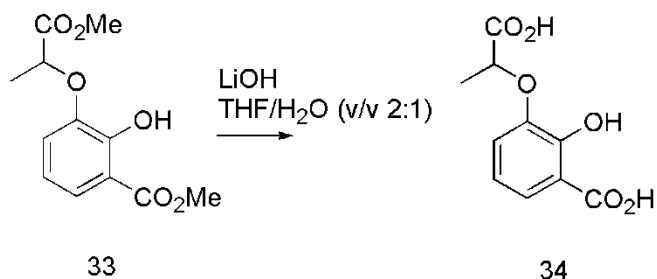


To a solution of compound **31** (0.39 g, 1.45 mmol) in dry CH_2Cl_2 (15 ml) at $-78\text{ }^\circ\text{C}$ was added BBr_3 (1.0 M solution in CH_2Cl_2 , 2.90 ml, 2.90 mmol) under argon. The reaction mixture was stirred for 40 min at $-78\text{ }^\circ\text{C}$ and H_2O (2.0 ml) was added slowly, then warmed up to room temperature, H_2O (10 ml) was added. The aqueous phase was separated and extracted with CH_2Cl_2 (15 ml x 3). The combined organic phase was dried over Na_2SO_4 and evaporated to give colorless oily residue. The residue was purified by flash chromatography using 0.5% MeOH/ CH_2Cl_2 to give methyl 2-hydroxy-3-(1-methoxy-1-oxopropan-2-yloxy)benzoate **as oily residue (33)** (0.26 g, yield: 70%).

^1H NMR (CDCl_3): δ 1.66 (d, 3H, $J = 7.0$ Hz), 3.74 (s, 3H), 3.94 (s, 3H), 4.84 (q, 1H, $J = 7.0$ Hz), 6.77 (appar. t, 1H, $J = 8.0$ Hz), 7.09 (dd, 1H, $J = 8.0, 1.0$ Hz), 7.51 (dd, 1H, $J = 8.0, 1.5$ Hz), 10.99 (s, 1H); .

^{13}C NMR (CDCl_3): δ 18.7, 52.3, 52.5, 74.7, 113.6, 118.6, 123.1, 123.6, 146.4, 153.4, 170.8, 172.6.

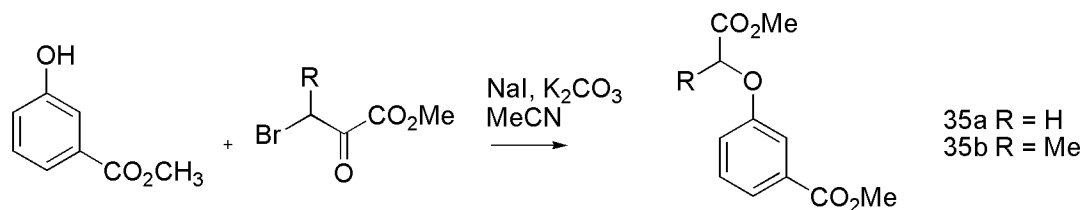
2.1.28 3-(1-Carboxyethoxy)-2-hydroxybenzoic acid



Compound **33** (0.13 g, 0.51 mmol) was mixed with LiOH.H₂O (86 mg, 2.05 mmol, 4.0 equiv.) in a mixture of THF (3 ml) and H₂O (1.5 ml), and stirred at room temperature for 2 days. THF was removed *in vacuo* and to the solution was added H₂O (*ca.* 5 ml). The resulting aqueous solution was then washed with EtOAc (5 ml x 3) and acidified to pH = 1-2 with aq. HCl (5 M), then extracted with EtOAc (15 ml x 2). Combined organic phase was washed with brine (10 ml) and dried over MgSO₄, evaporated *in vacuo* to give white solid. The white solid was recrystallized from CHCl₃ to yield 3-(1-carboxyethoxy)-2-hydroxybenzoic acid (**34**) as white powder (65 mg, yield: 56%, m.p. 158-160 °C).

¹H NMR (CDCl₃/CD₃OD (1 drop)): δ 1.65 (d, 3H, *J* = 7.0 Hz), 4.76 (q, 1H, *J* = 7.0 Hz), 6.79 (appar. t, *J* = 8.0 Hz), 7.09 (dd, 1H, *J* = 8.0, 1.5 Hz), 7.56 (dd, 1H, *J* = 8.0, 1.5 Hz). (Consistent with the literature⁶⁶)

2.1.29 Methyl 3-(2-methoxy-2-oxoethoxy)benzoate and methyl 3-(1-methoxy-1-oxopropan-2-yloxy)benzoate

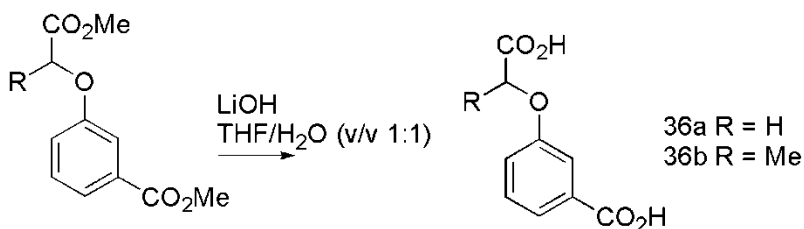


The mixture of methyl 3-hydroxybenzoate (0.60 g, 4.0 mmol), NaI (0.12 g, 20mol%), anhydrous K_2CO_3 (1.10 g, 2.0 equiv.), methyl bromoacetate or methyl 2-bromopropionate (5.2 mmol, 1.3 equiv.) and MeCN (40 ml) was refluxed under argon overnight. The reaction was monitored with TLC (2% MeOH/ CH_2Cl_2). After removal of the solvent *in vacuo*, the residue was taken with EtOAc (30 ml) and H_2O (15 ml). The organic layer was separated and extracted with brine (10 ml x 2). The organic layer was dried over $MgSO_4$ and evaporated *in vacuo* to dryness. After removal of solvent, the residue was eluted with 2% MeOH in CH_2Cl_2 to give methyl 3-(2-methoxy-2-oxoethoxy)benzoate (**35a**) and methyl 3-(1-methoxy-1-oxopropan-2-yloxy)benzoate (**35b**) (1H NMR indicated the only impurity was excess methyl bromoacetate or methyl 2-bromopropionate, yield: *ca.*100%) as pale yellow liquid. The products were used for next step without further purification.

35a 1H NMR ($CDCl_3$): δ 3.81 (s, 3H), 3.91 (s, 3H), 4.69 (s, 2H), 7.14 (ddd, 1H, $J = 8.0, 2.5, 0.5$ Hz), 7.36 (appar. t, 1H, $J = 8.0$ Hz), 7.54 (dd, 1H, $J = 2.5, 1.5$ Hz), 7.69 (d, 1H, $J = 7.5$ Hz);

35b 1H NMR ($CDCl_3$): δ 1.64 (d, 3H, $J = 7.0$ Hz), 3.76 (s, 3H), 3.90 (s, 3H), 4.84 (q, 1H, $J = 7.0$ Hz), 7.09 (dd, 1H, $J = 8.0, 2.5$ Hz), 7.34 (appar. t, 1H, $J = 8.0$ Hz), 7.53 (dd, 1H, $J = 2.5, 1.5$ Hz), 7.69 (d, 1H, $J = 7.5$ Hz).

2.1.30 3-(Carboxymethoxy)benzoic acid and 3-(1-carboxyethoxy)benzoic acid



Compound **35a** or **35b** (ca. 4.0 mmol) was mixed with LiOH.H₂O (0.67 g, 16.0 mmol, 4.0 equiv.) in a mixture of THF (5 ml) and H₂O (5 ml), and stirred at room temperature overnight. THF was removed *in vacuo* and to the solution was diluted with H₂O (ca. 10 ml). The resulting aqueous solution was then washed with CH₂Cl₂ (15 ml) and acidified to pH = 1-2 with aq. HCl (5 M), then extracted with EtOAc (15 ml x 2). Combined organic phase was washed with brine (10 ml) and dried over MgSO₄, evaporated *in vacuo* to give crude product (**36a** 0.87 g, pale yellow solid; **36b** 0.70 g, pale yellow solid). After recrystallization from EtOAc/hexane, white solid was obtained (**36a** 0.72 g, yield: 82%, m.p. 213-215 °C; **36b** 0.60 g, yield: 76%, m.p. 184-186 °C).

36a ¹H NMR (CD₃OD): δ 4.72 (s, 2H), 7.18 (dd, 1H, *J* = 8.0, 2.0 Hz), 7.39 (appar. t, 1H, *J* = 8.0 Hz), 7.55 (s, 1H), 7.63 (d, 1H, *J* = 7.5Hz),

¹³C NMR (CDCl₃): δ 65.9, 116.3, 120.7, 123.8, 130.6, 133.3, 159.5, 169.4, 172.4..

36b ¹H NMR (CD₃OD): δ 1.61 (d, 3H, , *J* = 7.0 Hz), 4.86 (q, 1H, dd, 1H, *J* = 7.0 Hz), 7.13 (dd, 1H, *J* = 8.0, 2.5 Hz), 7.37 (appar. t, 1H, *J* = 8.0 Hz), 7.51 (s, 1H), 7.62 (d, 1H, *J*

= 7.5 Hz);.

¹³C NMR (CDCl₃): δ 17.4, 72.1, 115.3, 119.7, 122.3, 129.2, 131.9, 157.8, 168.0, 174.1..

2.2 Enzymology experimental

Chemicals including buffers, 2-ketoglutarate (2-KG), ThDP, ampicillin, IPTG etc. were purchased from Sigma-Aldrich, VWR, EMD and were Molecular Biology Grade or were of the highest grade available. Centrifugation was performed using a Beckman J2-HS refrigerated centrifuge with a F500 or JA-25.50 rotor or Beckman Coulter microfuge 18 and 22R centrifuge. UV-visible spectrophotometry was performed using DU-640 spectrophotometer with a circulating bath-controlled temperature block. Bradford assay kit was obtained from Bio-Rad. The centrifugal filter used was Nanosep centrifugal device with 30 kDa cut-off from Pall Life Science. The cultures were lysed using Virosonic 600 ultrasonic cell disrupter. The purification of His-tagged proteins were routinely performed on BIOCAD 700E Perfusion Chromatography Workstation of Applied Biosystems using a Hitrap Chelating HP column from GE Health (1.0 ml) or a NTA Superflow Cartridge (1.0 ml) from QIAGEN. DNA primers were purchased from Alpha DNA. The *pfu* DNA polymerase and the QuickChange mutagenesis kit were obtained from Stratagene. PCR amplification were performed using PXE 0.2 Thermal Cycler of Thermo Electron Corporation. The isolation of isochorismate or CHCD was performed with the AKTAhplc in a refrigerated chamber using Lichropep RP-18 column from Merck. HPLC analysis or isolation was carried out on Agilent 1100 series with diode array multi-wavelength detector and G1313A autosampler using Zorbax SB-C18

(4.6 × 250 mm) analytical column or Zorbax SB-C18 (9.4 × 250 mm) semi-preparative column. DNA sequencings were performed at the DNA Technologies Unit, National Research Council (NRC), Plant Biology Institute (PBI), Saskatoon, SK, Canada. The competent cells of *E. coli* XL1-Blue and BL21-Gold were prepared following Macova's protocol⁴¹.

2.2.1 Mutagenesis

The plasmid containing the wild type *menD* gene was obtained from Dan Toogood⁸⁵. Mutageneses for *R107K*, *K292Q*, *R293K* and *R413K* were performed using the QuickChange kit from Stratagene according to the manufacturer's manual. The primers for site-directed mutagenesis (ordered from Alpha DNA, QC, Canada) are shown as below (Table 2.1).

Table 2.1: List of MenD mutagenic primers. The underlined sequences indicate the codon for new amino acids. *R107K* (change 5'-C₃₁₉GC-3' to 5'-AAG-3'); *K292Q* (change 5'-A₈₇₄AA-3' to 5'-CAA-3'); *R293K* (change 5'-C₈₇₇GG-3' to 5'-AAG-3'); *R413K* (change 5'-C₁₂₃₇GT-3' to 5'-AAG-3').

Mutants	Sequence of primers
<i>R107K</i>	5' to 3' C TTA ACC GCC GAT <u>AAG</u> CCG CCG GAG CTA ATT GAC TGC (Forward) 5' to 3' GCA GTC AAT TAG CTC CGG CGG <u>CTT</u> ATC GGC GGT TAA G (Reverse)
<i>K292Q</i>	5' to 3' C CTG ACG GGG <u>CAA</u> CGG CTC CTG CAA TG (Forward) 5' to 3' CA TTG CAG GAG CCG <u>TTG</u> CCC CGT CAG G (Reverse)
<i>R293K</i>	5' to 3' C CTG ACG GGG AAA <u>AAG</u> CTC CTG CAA TGG CAG G (Forward) 5' to 3' C CTG CCA TTG CAG GAG <u>CTT</u> TTT CCC CGT CAG G (Reverse)
<i>R413K</i>	5' to 3' CG GTG TAC AGC AAC <u>AAG</u> GGG GCC AGC GGT ATC G (Forward) 5' to 3' C GAT ACC GCT GGC CCC <u>CTT</u> GTT GCT GTA CAC CG (Reverse)

The DNA template pMD14 (pET-14b plasmid containing *menD* was called as pMD14 in our lab, obtained from Andrea Macova⁴¹) was isolated from the XL1-blue host

according to the protocol in the QIAprep spin miniprep kit manual. The PCR experiments were performed with 50 μ l total reaction volume in 0.5 ml PCR tube as follows:

Molecular biology water (added first), 38.5 μ l

Template DNA (pMD14, 37 ng/ μ l), 1.5 μ l

Primer (forward, 100 ng/ μ l, Alpha DNA), 1.5 μ l

Primer (reverse, 100 ng/ μ l, Alpha DNA), 1.5 μ l

10X *pfuUltra* buffer (Stratagene) 5 μ l

dNTPs (10 mmol, Stratagene) 1 μ l

pfuUltra polymerase (2.5 U/ μ l, Stratagene, added last) 1 μ l

The thermocycler was programmed as follows:

Step1: 95 °C 30 seconds

Step2: 95 °C 30 seconds

55 °C 1 min

72 °C ca. 14 min

After 18 cycles were performed for the amplification, the reaction mixtures were cooled to 4 °C. To each amplification product was added 1 μ l DpnI (restriction enzyme, 20 U/ μ l, New England Biolabs), and the resulting mixture was thoroughly mixed and incubated for 1 hour at 37 °C to digest the parental pMD14.

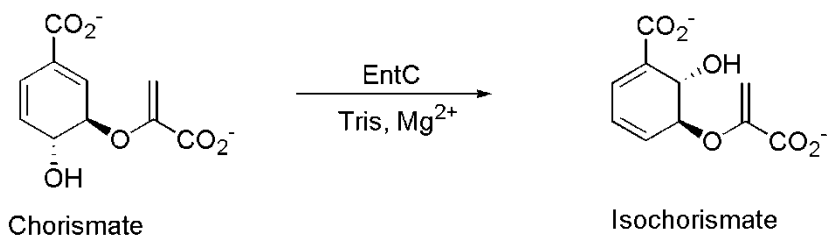
The DpnI-treated DNA (4 μ l) was added to XL1-blue competent cell (100 μ l) in 0.5 ml PCR tube and cooled on ice for 30 min. Once heated at 42 °C for 40 seconds, the mixture in PCR tube was added to a 0.9 ml pre-heated LB media in a sterile 14 ml polypropylene Falcon tube. After 1 hour incubation at 37 °C with shaking at 250 rpm, 50

μl of the culture was plated on a LB-agar plate containing 50 $\mu\text{g}/\text{ml}$ of ampicillin and incubated at 37 °C. A few colonies from each plate appeared after overnight incubation. Several of the colonies (usually 3) were picked out and used to inoculate LB media (6 ml) containing 50 $\mu\text{g}/\text{ml}$ ampicillin at 37 °C with 250 rpm overnight. Each of the grown cultures was harvested to isolate plasmid using QIAprep spin miniprep kit. The plasmids were sequenced to confirm the mutation results.

2.2.2 Gene overexpression and protein purification

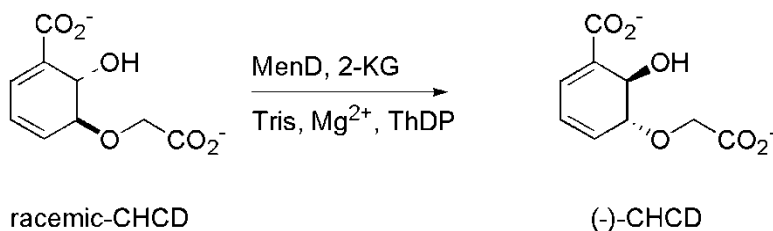
The vectors containing targeted mutant genes were transformed into *E. coli* BL21-Gold competent cells with the same procedure of transformation to XL1-Blue cell described above. One colony of the transformed BL21-Gold cell was used to inoculate LB media (5 ml) containing 50 $\mu\text{g}/\text{ml}$ ampicillin at 37 °C with 250 rpm for 4 hours. The grown culture was inoculated to 250 ml LB with 250 μl ampicillin (50 mg/ml), which was shaken at 37 °C with 250 rpm. When the OD_{600} of the culture reached 0.6 - 0.8 (about 3.5 hours), 100 μl IPTG solution (1.0 M) was added to the culture with a final concentration of 0.4 mM. The IPTG-induced culture was then shaken at 25 °C with 250 rpm overnight (~16 hours). The culture was harvested and protein was purified according to the established protocol⁴¹. The fractions containing MenD or mutants were pooled and dialyzed against MenD dialysis buffer (50 ml Tris (100 mM, pH 7.4; 500 ml glycerol; 450 ml deionized water) for 18-20 hours at 4 °C. The concentrations of proteins were determined by Bradford Assay using BSA as standard. The proteins were separated into 0.4 ml aliquot, frozen in liquid nitrogen and stored at -80 °C.

2.2.3 Preparation of isochorismate (ISC)



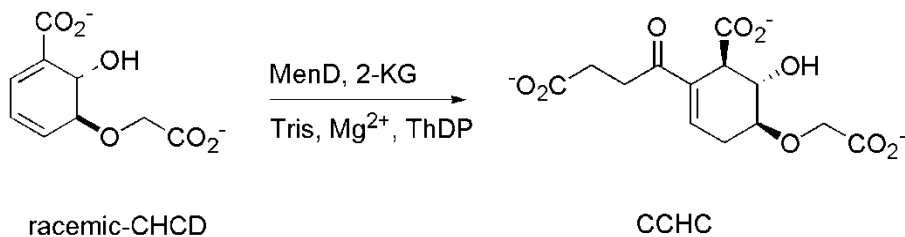
Chorismic acid was prepared biosynthetically from glucose using *Klebsiella pneumoniae* 62-1. The preparation of isochorismate from chorismate using EntC was similar to previous procedure with some modification⁴¹. In a 14 ml polypropylene round-bottom Falcon tube, the solution of chorismic acid (140 mg) in deionized water (2 ml) in a 10 ml was adjusted to pH = ca.7 with NaOH (1 M). To the pH-adjusted solution were added the Tris buffer (0.6 ml, pH 8.0, 1 M) and MgCl₂ (0.18 ml, 1 M). After the addition of EntC (0.5 ml), the reaction mixture was incubated at 30 °C for 1.5-2 hours. After the mixture was cooled on ice, MeOH (2 ml) was added and then acidified to pH < 2 with HCl (5 M). The white precipitate was removed using centrifuge and the supernatant was filtered through a 0.45 µm syringe filter into a round-bottom flask. The filtrate was concentrated *in vacuo* to ca. 2 ml. The solution was loaded to the Lichropep RP-18 column from Merck on the AKTAhplc in a refrigerated chamber. The elution of the column and isolation of isochorismate are the same as previous procedure⁴¹.

2.2.4 Isolation of (-)-5-(carboxylatomethoxy)-6-hydroxycyclohexa-1,3-diene carboxylate ((-)-CHCD)



The lithium salt of (\pm)-CHCD (40 mg), 2-KG (30 mg), ThDP (2 mg) were dissolved in deionized water (1 ml). The resulting mixture was adjusted to pH = 7-8 with NaOH (1 M) to form a clear solution. To the solution were added 0.2 ml Tris buffer (7.4, 1 M) and 0.16 ml MenD (28 μ M), water was then added to obtain a ca. 2 ml reaction mixture which was shaken at room temperature until the UV absorbance at 280 nm (5 μ l of reaction mixture was diluted with 1 ml deionized water) stopped decreasing (ca.12 hours). MeOH (0.5 ml) was added and drops of HCl (5 M) were added to acidify the reaction mixture pH < 2. After filtered through 0.45 μ m syringe filter, the solution was loaded to the Lichropep RP-18 column from Merck on the AKTAhp1c in a refrigerated chamber. Typically, the MeOH/0.1% TFA solution gradient elution procedure was as follows: 0-10% MeOH over 40 min, stay with 10% MeOH until (-)-CHCD peak was eluted. The fractions of (-)-CHCD was monitored at 280 nm and/or using UV scan with a maximal UV absorbance at 278-280 nm. The appropriate fractions were pooled and concentrated *in vacuo* at room temperature. The concentrated solution was frozen and lyophilized to achieve pale brown solid. The ^1H NMR of the product is identical to racemic CHCD. The specific rotation of (-)-CHCD was determined as $[\alpha]_D^{25} = -170 \pm 10$ (c 0.24, H₂O).

2.2.5 Isolation of 5-carboxymethoxy-2-(3-carboxy-propionyl)-6-hydroxy-cyclohex-2-enecarboxylate (CCHC)



The lithium salt of (\pm)-CHCD (232 mg), 2-KG (160 mg), ThDP (10 mg) were dissolved in 3 ml deionized water. The resulting mixture was adjusted to pH = 7-8 with NaOH (1 M) to form a clear solution. To the solution were added 0.4 ml Tris buffer (7.4, 1 M) and 0.1 ml MenD (65 μ M), water was then added to obtain ca. 4 ml reaction mixture which was shaken at room temperature until the UV absorbance at 280 nm (1 μ l of reaction mixture was diluted with 1 ml deionized water) stopped decreasing (ca.35 hours). The reaction mixture was adjusted to pH = 4 with ca. 100 μ l formic acid (96%). MenD was removed by Nanosep centrifugal device with 30 kDa cut-off. The resulting filtrate was isolated with HPLC using a Zorbax SB-C18 (9.4 \times 250 mm) semi-preparative column. The column was eluted with an isocratic eluent combination of 5% acetonitrile and 95% formic acid (0.1%). (-)-CHCD was eluted at ca. 23.5 min and CCHC at ca. 37.5 min. The collected eluents were evaporated *in vacuo* to remove volatiles, the resulting solutions were lyophilized to yield (-)-CHCD (1 HNMR showed the same result as authentic CHCD) as pale brown solid and CCHC as white solid. The component characterized by NMR as Diels-Alder product of CHCD was also isolated (eluted at ca. 42.3 min).

$$[\alpha]_D^{25} = -50 \pm 10 \text{ (c 0.12, H}_2\text{O)}$$

CCHC: $^1\text{H NMR (CD}_3\text{OD): } \delta$ 2.40 & 2.35 (m, m, 1H), 2.49 (t, 1H, dd, 1H, $J = 6.0$ Hz), 2.75 & 2.71 (m, m, 1H), 3.03 (m, 1H) & 2.93 (m, 1H), 3.33 (d, 1H, $J = 6.0$ Hz), 3.62 (m, 1H), 4.10 (m, 3H), 7.11 (br, 1H); .

$^{13}\text{C NMR (CDCl}_3\text{): } \delta$ 27.9, 29.6, 31.8, 47.5, 66.9, 70.2, 76.5, 133.8, 142.1, 174.7, 176.5, 177.4, 201.3;

HRMS(ESI): calcd for $\text{C}_9\text{H}_{15}\text{O}_9$ 315.0722, found 315.0741 ($[\text{M-H}]^-$).

2.2.6 Continuous assay of MenD- or mutant-catalyzed reactions using UV spectrophotometer

The stock solutions of buffer and substrates were prepared as follows: Tris buffer was prepared by dissolving Tris in deionized water. The pH value was adjusted with HCl and determined with pH meter (100 mM, pH 7.4); ThDP and 2-KG were dissolved in Tris buffer and adjusted to pH = 7.4 with NaOH (1M). The typical stock solution for ThDP and 2-KG are 20 mM and good for kinetic assay within a month if stored at -20 °C. The MgCl_2 solution was prepared as described for ThDP and 2-KG solution to obtain 1.0 M solution at pH 7.4. The typical enzyme concentrations were 5-20 μM . The ISC or (\pm)-CHCD solution was prepared and their concentrations were calibrated (refer to **2.2.7**) and good for days. The assay stock solutions of ThDP, 2-KG, ISC or (\pm)-CHCD solution were stored at -20 °C and cooled on ice when the kinetic assay was being done.

All assays were carried out at 25 °C in 1.4-ml quartz cuvettes with 1.0 cm path length using a Beckman Coulter DU 600/700 spectrophotometer and were performed in a 1 ml

(or 0.6 ml) total volume. Usually the reaction mixture containing components except ISC was pre-incubated for 5 min and then blanked before initiated with ISC. The reaction rate was determined by continuously monitoring the absorbance change at 278 nm or 300 nm. The initial rate was calculated on the basis of the extinction coefficients of the substrates (at 278 nm, ϵ (ISC) = 8300 M⁻¹.cm⁻¹,⁸⁶ ϵ ((±)-CHCD) = 4700 M⁻¹.cm⁻¹; at 300 nm, ϵ (ISC) = 3600 M⁻¹.cm⁻¹, ϵ ((±)-CHCD) = 1700 M⁻¹.cm⁻¹;) by the equation 2.1:

$$v = \frac{-\Delta A \times 10^6}{\Delta t \times \epsilon} \text{ (}\mu\text{M/Min)} \quad (2.1)$$

Typically, the reaction mixture has a final concentration of 100 mM Tris-HCl (buffer, pH 7.4), 5 mM MgCl₂, 50 μM ThDP, 100 μM 2-KG, 20 μM ISC and appropriate concentrations of MenD or mutants (10, 30, 60 nM or higher for the low activity mutants). All data points represent the average of at least two experiments.

2.2.7 Determination of the concentrations of ISC and (±)-CHCD

At first the concentration of ISC can be roughly determined. We assumed the ISC solution was pure and containing only ISC. The UV absorbance of 4 μl ISC solution diluted in 596 μl Tris buffer (100 mM, pH 7.4) was measured against the buffer at 278 nm. The apparent concentration was then given according to Beer's law $A = \epsilon lc$.

The more accurate concentration of ISC was then determined by the absorbance at 278 nm by using $\epsilon = 8300 \text{ M}^{-1}\text{cm}^{-1}$ as described below. To a 0.6 ml reaction mixture

containing 100 mM Tris (pH 7.4), 100 μ M 2-KG, 5 mM $MgCl_2$, 50 μ M ThDP and 100 nM MenD was added ISC (30 μ M, apparent conc. determined as described above) to initiate the reaction. The complete depletion of ISC monitored at 278 nm was related to the amount of ISC and therefore the concentration of ISC can be determined according to the ISC solution volume added and Beer's law $A = \epsilon lc$.

The concentration of (\pm)-CHCD was determined in the same way using $\epsilon_{278} = 4700 M^{-1}.cm^{-1}$ which was determined from the standard (\pm)-CHCD solutions prepared in volumetric flasks.

2.2.8 HPLC analysis of the MenD reaction

The reaction was performed at 25 $^{\circ}C$ in a 4 ml solution with a final concentration of 100 mM Tris (pH 7.4), 2 mM $MgCl_2$, 100 μ M 2-KG, 50 μ M ThDP, 60 nM MenD, 20 μ M 3,4-dihydroxybenzene (3,4-DHB, as internal standard). From the reaction mixture, 1 ml solution was transferred to a cuvette as blank solution for UV monitoring. After incubation for 5 min, the reaction was initiated by adding 7.5 μ l ISC (6.4 mM, final conc. 16 μ M) to the 3 ml reaction mixture. From the 3 ml solution, 1 ml solution was transferred to a cuvette which was monitored on UV spectrophotometer with the blank solution at 278 nm. At the same time, every 3 min, 150 μ l of the solution was taken out from the remaining 2 ml reaction solution and quenched with 1 μ l formic acid solution (v/v, 10%) to pH = ca. 4. These quenched fractions were filtered through Nanosep centrifugal device with 30 kDa cut-off and cooled on ice prior to HPLC analysis. The HPLC analysis condition is as follows: Zorbax SB-C18 (4.6 \times 250 mm) analytical RP

column, isocratic elution with 10% acetonitrile out of 0.1% formic acid (v/v), 25 °C, 1 ml/min flow rate, injection of 50 µl sample. All components were identified by comparison with authentic compounds. The 3,4-DHB and ISC were eluted at 7.3 min and 8.0 min respectively. The concentration of ISC was quantified based on the ratio of integral area of 3,4-DHB and ISC peaks according to the response factor between the two compounds which was determined under the same conditions.

2.2.9 Determination of K_m^a and V_{max}^a of the MenD reaction

The MenD reaction was assayed as described in 2.2.6. The kinetic constants of the MenD reaction for individual substrate (2-KG and ISC) or cofactor (ThDP and Mg^{2+}) were determined with the varied concentrations at the saturating concentrations of the other substrates or cofactors. The reaction was usually initiated with various concentrations of ISC. Kinetic constants were determined using the program Leonora⁷¹ by nonlinear least-squares fitting of the data to Michaelis-Menten equations 2.2 (v vs. $[S]$). In the cases where the initial rates at the full range of substrate concentrations for saturation curve were not achievable experimentally, the kinetic parameters were estimated by the Hanes-Woolf plot ($[S]/v$ vs. $[S]$) according to the equation 2.3.

$$v = \frac{V_m[S]}{K_m + [S]} \quad (2.2)$$

$$\frac{[S]}{v} = [S] \left(\frac{1}{V_m} \right) + \frac{K_m}{V_m} \quad (2.3)$$

where [S] represents the concentration of substrate, K_m is Michaelis constant, V_{max} is the maximal rate.

The same procedure was applied to the kinetic assay using CHCD as substrate instead of ISC. Since only (+)-enantiomer of racemic CHCD can react in the reaction, the actual working concentration of CHCD is a half of the concentration of the racemic CHCD solution.

2.2.10 Inhibition study of 2-KG phosphonate analogues with respect to 2-KG

The reaction mixture contained all components and appropriate inhibitors except 2-KG. MenD with a final concentration of 60 nM was used and [ISC] was fixed at 20 μ M for the assay. After pre-incubation at 25 °C for 5 minutes, the reaction was initiated by addition of 2-KG with various concentrations (10, 15, 20, 40 μ M) at 5 fixed concentrations of each inhibitors. The inhibition type and the inhibition constants were determined graphically by a Dixon plot⁶⁸ (1/v vs. [inhibitor] at four different [2-KG]) and Cornish-Bowden plot (plot [2-KG]/v vs. [inhibitor] at four different [2-KG]), based on the equation 2.4.

$$v = \frac{V_{max} [S]}{[S] + K_m \left(1 + \frac{[I]}{K_i} \right)} \quad (2.4)$$

where [I] is the inhibitor concentration, K_i is the inhibitor constant, S is the substrate 2-KG.

2.2.11 Determination of the reversibility of the 2-KG phosphonate inhibition

A fast dilution method was performed to test the reversibility of MMSP inhibition. Three parallel continuous assays were conducted: (1) to a 1 ml reaction mixture with 100 mM Tris (pH 7.4), 5 mM MgCl₂, 50 μM ThDP and 10 μM MMSP was added 60 nM MenD. The mixture was pre-incubated at 25 °C and finally initiated by 20 μM 2-KG; (2) Same as (1) except that there is no MMSP added and MenD was pre-incubated with water (30 μl MenD (28 μM) was mixed with 10 μl water) for 30 min before added to the reaction mixture, the final concentration of MenD is still 60 nM; (3) Same as (2), but MenD was pre-incubated with MMSP instead of water (30 μl MenD (28 μM) was mixed with 10 μl MMSP (40 μM)) for 30 min before added to the reaction mixture; the final concentration of MenD is still 60 nM.

2.2.12 Kinetic mechanism study of the MenD reaction using CHCD

The reaction rate was determined with 30 nM MenD, 100 mM Tris (pH 7.4), 5 mM MgCl₂ and 50 μM ThDP by varying the concentrations of 2-KG (4, 8, 16, 32, 64 μM) with the constant concentration of CHCD at 5, 10, 20, 50 μM respectively. The pattern of kinetic mechanism was distinguished as ping-pong bi bi enzymatic reaction by the double reciprocal plots (1/v vs. [2-KG] or [CHCD]). Kinetic constants were determined using the program Leonora by non-linear least-squares fitting of data to the rate equation as 2.5, which describes the initial rate in the absence of products for a ping-pong bi bi enzymatic reaction:

$$v = \frac{V_{\max} [A][B]}{K_m^B [A] + K_m^A [B] + [A][B]} \quad (2.5)$$

where [A] is the concentration of the substrate (2-KG) that first binds to MenD, [B] is the concentration of the second substrate (ISC or CHCD), K_m^A and K_m^B are the respective Michaelis constants for substrate A and B, and V_{\max} is the maximal velocity when both substrates are at saturating concentrations.

The dead-end competitive inhibitor monomethyl succinylphosphonate (MMSP) was used as a mechanistic tool to investigate the kinetic mechanism of MenD reaction with CHCD as an alternative substrate and substrate 2-KG was at the fixed non-saturating concentration ($\sim K_m^a$). The inhibition of MMSP with respect to CHCD was similarly determined by a Dixon plot ($1/v$ against [inhibitor] at four different [CHCD]) and Cornish-Bowden plot ($[CHCD]/v$ against [inhibitor] at four different [CHCD]). The reaction rate was determined with 60 nM MenD, 100 mM Tris (pH 7.4), 5 mM MgCl₂, 50 μM ThDP. [2-KG] was fixed at 6 μM and [CHCD] was at 3 μM, 6 μM, 9 μM, 18 μM. [MMSP] was varied at 10 μM, 20 μM, 30 μM and 40 μM.

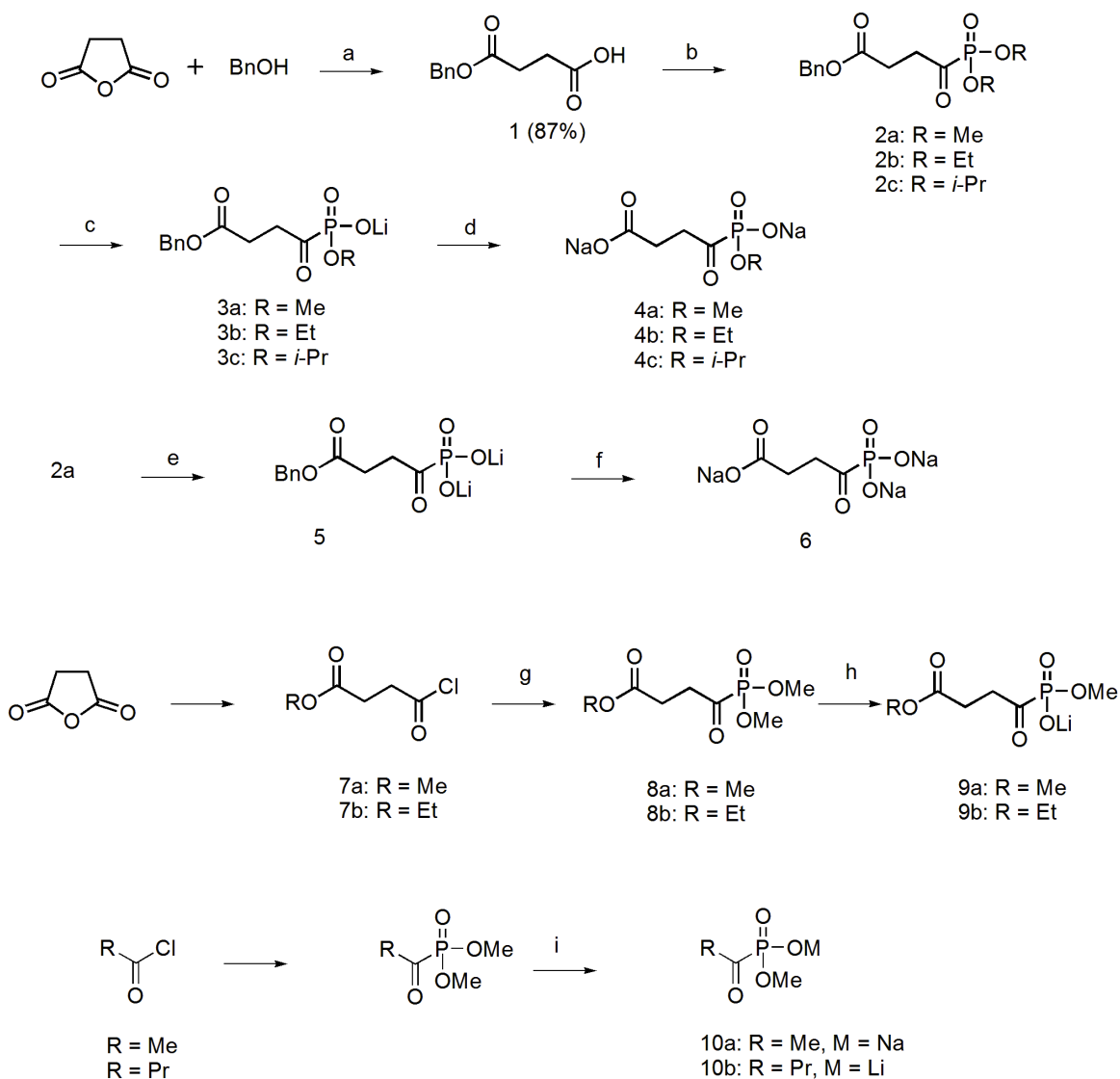
3. RESULTS AND DISCUSSION

3.1 Chemical synthesis

3.1.1 Chemical synthesis of phosphonate analogues of 2-KG

At the beginning of synthesis of phosphonate analogues of 2-ketoglutarate (2-KG), a synthetic route which is coincidentally the same as reported by Bunik *et al.* later⁵⁹, was explored. However, in our hands, the condition for the saponification of the carboxylate ester with NaOH or conc. HCl solution caused cleavage of the C-P bond to yield succinic acid.

Fortunately, a modified route to the phosphonate analogues of 2-KG was developed successfully (Scheme 3.1). Succinic acid monobenzyl ester (**1**), prepared from succinic anhydride and benzyl alcohol according to the literature method⁷³, was cleanly converted to the reactive acid chloride using oxalyl chloride in the presence of a catalytic amount of DMF. The resulting acid chloride, in no need of further purification, readily reacted with trialkyl phosphite to yield the benzyl diester of succinyl phosphonate (**2a-c**) quantitatively from **1**. The specific removal of one alkyl group from the phosphonate diester with 1.0 equivalent of LiBr turned out to be very effective and the resulting lithium salt product was easy to isolate as a white precipitate (**3a-c**).



Scheme 3.1: Synthesis of phosphonate analogues of 2-KG. Reagents and conditions: a) benzyl alcohol, DMAP (cat.), anhydrous THF, reflux 12 h; (b) (1) oxalyl chloride (2 M in DCM), DMF (cat.), DCM, 1.5h; (2) trialkyl phosphite, 2 h; (c) LiBr (1.0 equiv.), acetonitrile; (d) EtOAc, formic acid, H₂, Pd/C; Dowex [Na⁺]; (e) LiBr (2.2 equiv.), acetonitrile; (f) EtOAc, formic acid, H₂, Pd/C; Dowex [Na⁺]; (g) trimethyl phosphite, 2 h; (h) LiBr (1.0 equiv.), acetonitrile; (i) **10a**: NaI (1.0 equiv.), acetonitrile; **10b**: LiBr (1.0 equiv.), acetonitrile.

An initial attempt to hydrogenolyse the benzyl group with Pd/C in methanol was not successful possibly due to poor solubility of the lithium salts (**3a-c**) in organic solvents.

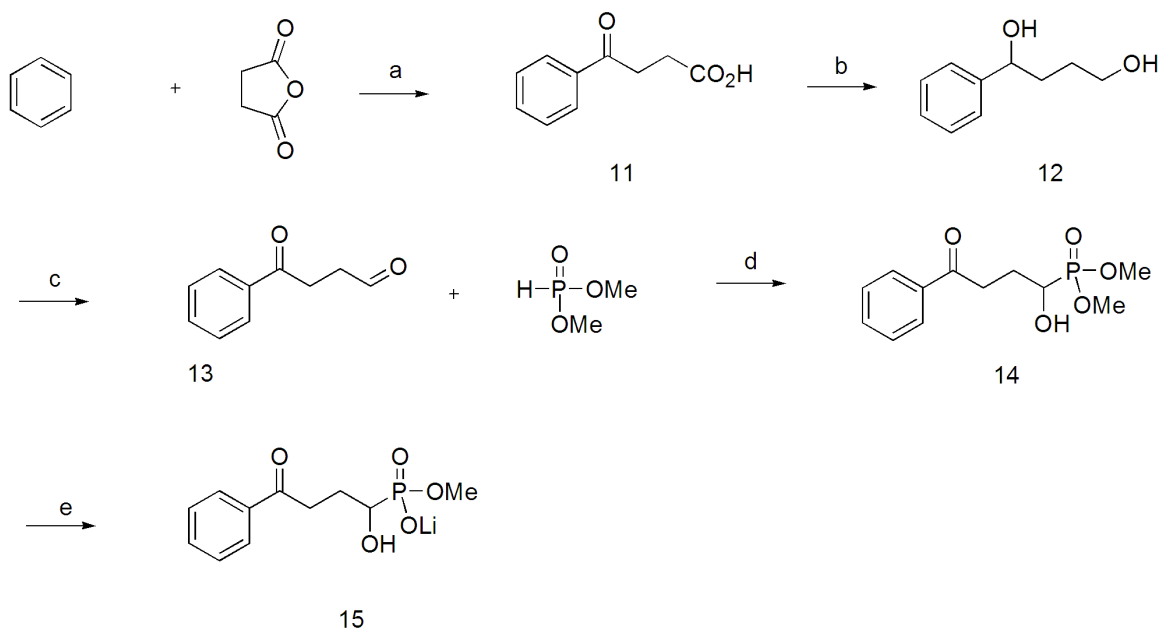
The removal of the benzyl group was successfully achieved by adding formic acid, which helped solubilize lithium salts and facilitate hydrogenolysis as well, but the yielded product was found to be the phosphonate methyl ester resulting from acid-catalyzed esterification with methanol. This problem was then overcome by using a combination of formic acid and ethyl acetate. It turned out that formic acid and ethyl acetate worked very well to achieve the hydrogenolysis of benzyl ester in **3a-c** without affecting the phosphonate ester. Crude products of **4a-c** were purified with Dowex cation exchange resin to yield the pure sodium salt of **4a-c**. Excess LiBr realized complete hydrolysis of the phosphonate diester to prepare compound **5**. In the same way, the hydrogenolysis of **5** in formic acid and ethyl acetate yielded succinyl phosphonate **6**.

For compounds **4a-c** and **6**, a fast H/D exchange of the 3-position (α to 2-keto) in D₂O was observed on ¹H NMR spectra. The signal due to H-3 gradually disappeared in hours. As a consequence, the ¹³C NMR signal of the 3-carbon of compounds **4a-c** and **6** was not detected due to the deuterium coupling. These lithium salts are not soluble in common deuterated solvents including DMSO-d₆. However, H/D exchange was not observed for compounds containing 4-carboxylic esters such as **3a-c**. Therefore, the fast H/D exchange seems to be due to the 4-carboxylate group of **4a-c** and **6**, **which** facilitates the exchange at the 3-position.

Compound **9a-b** and **10a-b** were prepared using the same strategy. All the phosphonate analogues including **3a-c**, **4a-c**, **6**, **9a-b** and **10a-b** were chemically synthesized with good purity (>95%, NMR) in salt form, which are all water soluble and therefore convenient for the kinetic assay of MenD enzyme. As a result, our approaches

represent a versatile synthesis for an array of acylphosphonate analogues with varied carboxylate and phosphonate moieties.

The 2-KG phosphonate analogues with a 2-hydroxyl group in place of the ketone were also synthesized, for instance, as compound **15** and **21** (Scheme 3.2 and Scheme 3.3). In compound **15**, the carboxyl group was also substituted with a phenyl ketone; in compound **16**, the carboxyl group was changed to an amide. Starting from benzene and succinic anhydride, aldehyde **13** was prepared by LiAlH₄ reduction and Swern oxidation via **11** and **12**. The reaction of aldehyde **13** and dimethyl phosphite yielded compound **14**, which was treated with 1.0 equiv. LiBr to afford 2-hydroxy monoester phosphonate **15**.

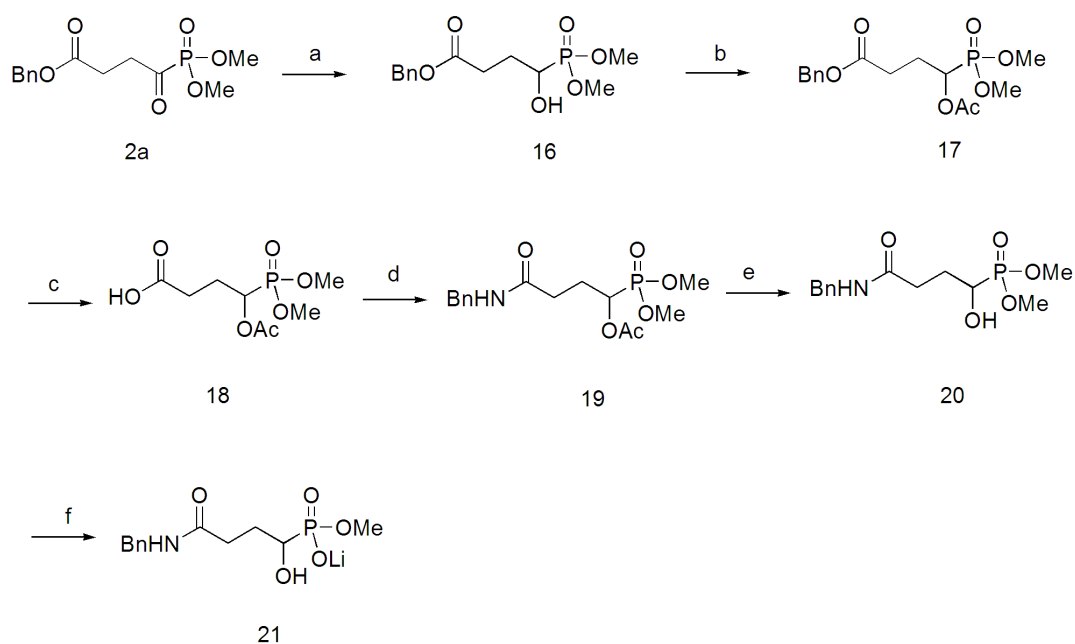


Scheme 3.2: Synthesis of phosphonate analogue **15**. Reagents and conditions: (a) AlCl₃, lit.76-77, 95%; (b) LiAlH₄, THF, lit.78, 85%; (c) Swern [O], -78 °C, 96%; (d) DBU, THF, lit.80, 74%; (e) 1.0 equiv. LiBr, acetonitrile, 70 °C, 76%.

Reduction of benzyl dimethyl phosphonate **2a** by NaBH₄ afforded the 2-hydroxyl product **16** (Scheme 3.3), which was then acetylated to protect the 2-hydroxyl group.

Hydrogenolysis of **17** freed the carboxyl group and got ready for forming amide **19**, which was then deprotected to regenerate the alcohol. The phosphonate monoester **21** was readily prepared using 1.0 equiv. LiBr.

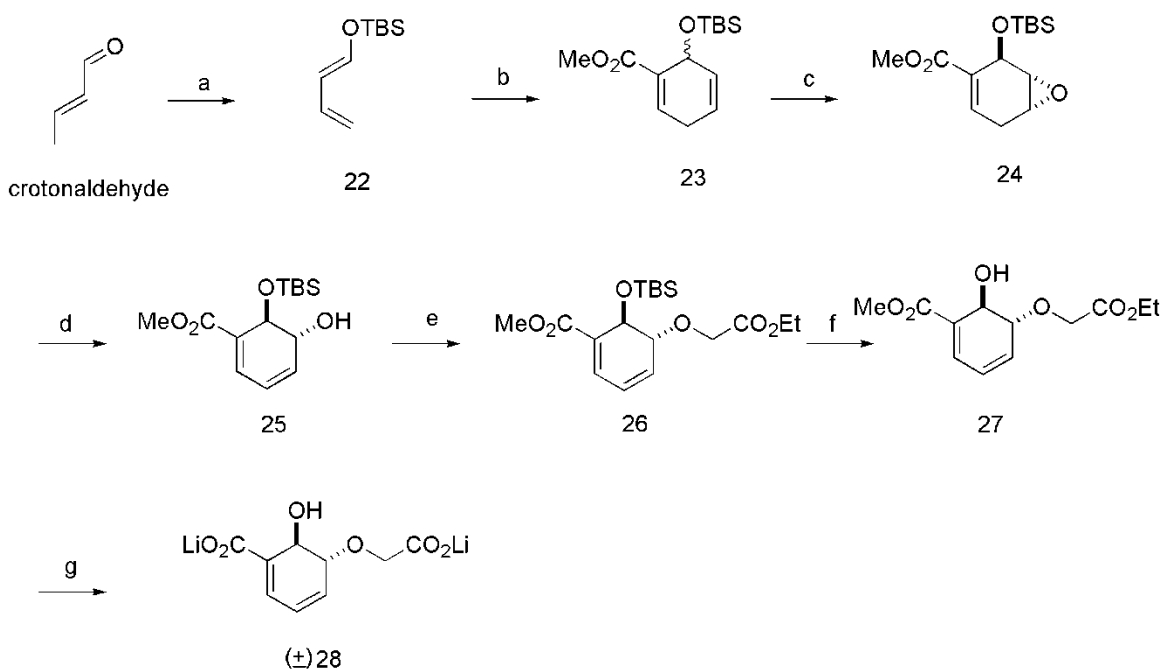
2-Hydroxyl phosphonates **15** and **21** are both water-soluble lithium salts and provide structural variety for the aforementioned 2-keto phosphonates, adding to a library of phosphonate analogues available for inhibition screening of MenD enzyme.



Scheme 3.3: Synthesis of phosphonate analogues **21**. Reagents and conditions: a) NaBH₄, KH₂PO₄, H₂O, 69%; b) Ac₂O, pyridine, 96%; c) H₂, Pd/C, EtOAc, ca. 100%; d) Oxalyl chloride, DMF (cat.), CH₂Cl₂, benzylamine, Et₃N, 33%; e) Et₃N, MeOH, 36%; f) LiBr, acetonitrile, 70 °C, 68%.

3.1.2 Chemical synthesis of the analogues of ISC

The synthesis of ISC analogues (\pm)-CHCD (**28**) started with the formation of the Diels-Alder product **23**, which reacted with *meta*-chloroperoxybenzoic acid (*m*-CPBA) to afford epoxide **24** (Scheme 3.4).

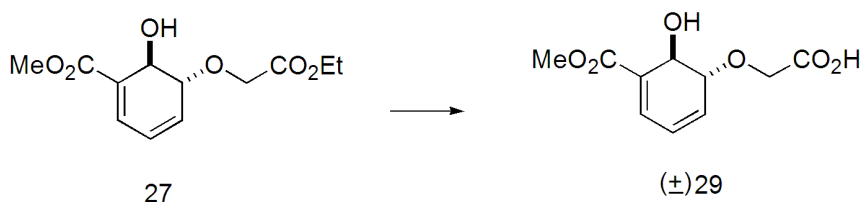


Scheme 3.4: Synthesis of (±)-CHCD. Reagents and conditions: (a) Et₃N, *t*-butyldimethylsilyl chloride, NaI, acetonitrile, 72%; (b) methyl propionate, 60%; (c) *m*-CPBA, NaHCO₃, CH₂Cl₂, 71%; (d) DBU (5.0 equiv.), CH₂Cl₂, 85%; (e) N₂CHCOEt, Rh₂(OAc)₄, CH₂Cl₂, 71%; (f) AcOH/H₂O (v/v 3:2), 84%; (g) LiOH (6 equiv.), THF/H₂O (v/v 4:1), Dowex [H⁺] or anion exchange resin, LiCl.

Commercially available *m*-CPBA usually contains water as stabilizer and was found to cause low yield (ca. 10-15%). The yield was remarkably improved to 71% using dried *m*-CPBA that was prepared by dissolving wet *m*-CPBA in CH₂Cl₂ and drying over anhydrous Na₂SO₄ before use. Opening of the epoxide ring in **24** by DBU formed the cyclohexadiene isomer **25** at room temperature. Introduction of the side chain was achieved by the Rh-catalyzed reaction with ethyl diazoacetate. The resulting compound **26** was then deprotected by removing the *t*-butyldimethylsilyl group under acidic conditions, and hydrolyzed by excess LiOH in a mixture of THF and water to yield crude (±)-CHCD **28**. The purification with a cation exchange resin column or anion exchange resin column afforded the acid form or lithium salt of CHCD, which are both water-

soluble and convenient for kinetic assay. The ion exchange resin method enables a simple and scalable purification of usually unstable ISC analogues, eliminating tedious HPLC isolation. It was observed that (\pm)-CHCD demonstrated higher stability than ISC.

Furthermore, this new CHCD synthetic strategy could be adapted to prepare different isochorismate analogues with a 1,3-dienebenzoate structure, for instance, *trans*-2,3-dihydroxy-2,3-dihydrobenzoate or 3-hydroxy-2,3-dihydrobenzoate⁶⁵.

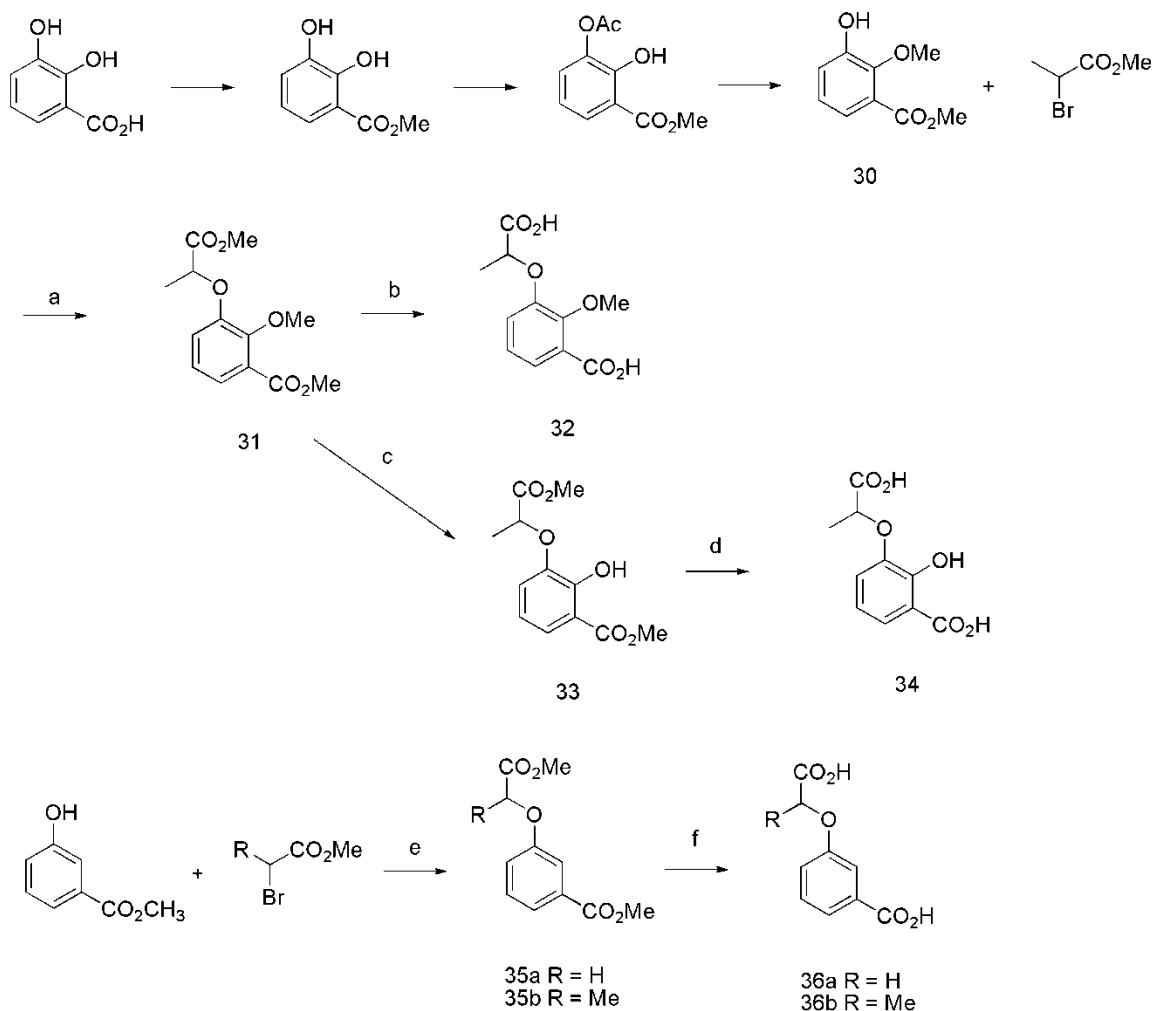


Scheme 3.5: Synthesis of (\pm)-CHCD methyl ester ((\pm)-CHCDMe). Reagents and conditions: *Candida antarctica* Lipase B, acetonitrile/H₂O.

Initially, *Candida antarctica* Lipase B was tried in order to develop a mild condition to hydrolyze compound **27** to prepare (\pm)-CHCD (**28**), or the optically active compound. However, the experimental results showed that the product was the methyl ester (\pm)-CHCDMe (**29**, Scheme 3.5). Steric hindrance may be accountable for selective hydrolysis of esters by lipase. (\pm)-CHCDMe is water-soluble and was also tested in a kinetic assay of MenD enzyme as an ISC analogue.

Several ISC analogues bearing a benzene core were prepared from the compound **30** which was reported by Coleman *et al.* (Scheme 3.6)⁸⁴. Methyl 2-bromopropanoate and methyl bromoacetate were used to introduce a side chain to the benzene core. Hydrolysis of compounds **31**, **33** and **35a-b** resulted in the carboxylic acid compounds **32**, **34** and **36a-b** respectively. The removal of the methyl group from compound **31** was achieved

using BBr_3 at $-78\text{ }^\circ\text{C}$. These analogues were prepared as pure acid compounds that are soluble in the buffers for MenD assay and therefore could be tested as inhibitors or alternative substrates in the MenD reaction.



Scheme 3.6: Synthesis of ISC analogues with benzene core. Reagents and conditions: a) **3084**, NaI, K_2CO_3 , MeCN, reflux, 77%; (b) LiOH, THF/ H_2O (v/v 2:1), 83%; (c) BBr_3 , CH_2Cl_2 , $-78\text{ }^\circ\text{C}$, 70%; (d) LiOH, THF/ H_2O (v/v 2:1), 56%; (e) NaI, K_2CO_3 , MeCN, reflux, ca. 100%; (f) LiOH, THF/ H_2O (v/v 1:1). **36a**: 82%; **36b**: 76%.

3.2 Mutagenesis and protein expression

The wild type MenD and some mutants including S32A, S32D, R33K, R33Q, E55D, Q118E, S391A, R395A, R395K, and I418L were prepared previously in our lab, the plasmids (pMD14) harboring the genes for MenD and mutants were stored in XL1-Blue cell at -80 °C. MenD and mutants were all prepared by overexpression of individual plasmids (refer to 2.2.2). Four new mutants *R107K*, *K293Q*, *R293K* and *R413K* were prepared in the same PCR thermocyclic program (refer to 2.2.1) and the corresponding gene sequences were determined. The determined sequences were aligned with the wild type *menD* to identify the desired plasmids. All the four new mutants were confirmed as expected and the plasmids containing mutant genes were transformed to *E. coli* BL21-Gold cell and overexpressed with IPTG induction. The plasmids containing the desired mutants were all successfully expressed and purified with Ni-affinity columns to homogeneous solution (refer to 2.2.2).

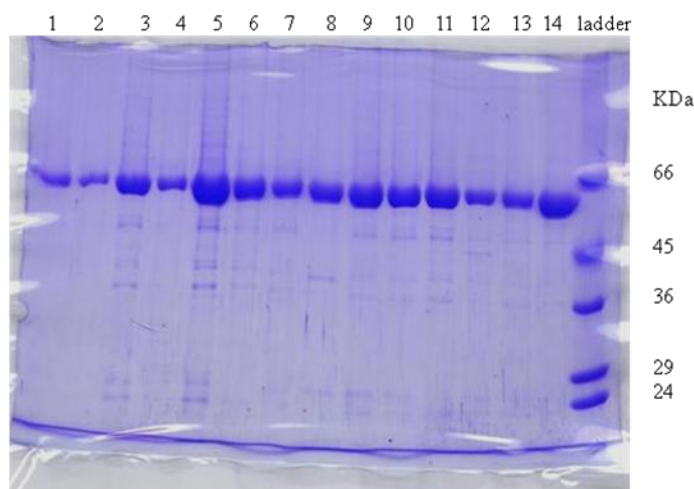


Figure 3.1: SDS-PAGE gel of purified MenD mutants: 1. S32A; 2. S32D; 3. R33K; 4. R33Q; 5. E55D; 6. R107K; 7. Q118E; 8. R293K; 9. S391A; 10. S395A; 11. R395K; 12. R413K; 13. I418L; 14. K292Q; Ladder (Sigma-Aldrich).

These four new mutants, together with freshly prepared mutants S32A, S32D, R33K, R33Q, E55D, Q118E, S391A, R395A, R395K and I418L from the stored plasmids in our lab were shown in one SDS-PAGE gel (Figure 3.1) with a MW= ca. 64 kDa (the wt-MenD has 556 residues with MW= 61367 Da, plus N-terminal his-tag residues, the molecular weights of the enzymes used in all experiments amount to ca. 64 kDa.).

3.3 Preparation of isochorismate (ISC)

Although the preparation of isochorismate from chorismate catalyzed by EntC was performed previously in our lab, the scale of the reaction and purification seemed to have room for further optimization. In the step of acidification with HCl (refer to **2.2.3**), it was found that the desired acid form of ISC might form a precipitate that would be removed by subsequent filtration. This could cause considerable loss of the desired ISC. Therefore, MeOH was added to dissolve more ISC so that all the ISC in the crude mixture could escape the filtration prior to FPLC purification. The yield was improved from 10-15% to 40-45%. Because the conversion of chorismic acid to ISC by EntC is a thermodynamic equilibrium, the isolation yield is very satisfactory.

3.4 Isochorismate analogues were tested for the MenD reaction

In attempts to design inhibitors structurally analogous to isochorismate, *trans*-(±)-5-carboxymethoxy-6-hydroxy-cyclohexa-1,3-dienecarboxylate ((±)-CHCD, **28**) was synthesized as a racemic mixture (refer to **3.1.2**). Experimental results indicated that (±)-CHCD is not an inhibitor, but is recognized as a substrate by MenD. In Figure 3.2A, it is

shown that the drop of UV absorbance at 278 nm (the maximal UV absorbance wavelength of CHCD) corresponds to half of the quantity of CHCD used ($A = 1/2 \times 30 \times 10^{-6} \text{ M} \times 1 \text{ cm} \times 4700 \text{ M}^{-1} \cdot \text{cm}^{-1}$) and remains substantially constant after the progress curve levels off; HPLC analysis clearly indicated that half the quantity of CHCD was consumed and the other half was unreactive (Figure 3.2B and Figure 3.2C).

This apparently suggests that only one enantiomer of the racemic mixture was involved in the reaction, consistent with the high stereospecificity of enzyme reactions. In order to prove this assumption, unreacted CHCD was isolated with a preparative HPLC column (see 2.2.4) and its specific rotation was measured as $[\alpha]_{\text{D}} = -170 \pm 10$ (c 0.24, H₂O), while for the synthetic racemic CHCD, $[\alpha]_{\text{D}} = -2 \pm 2$ (c 0.24, H₂O) and for physiological substrate ISC, $[\alpha]_{\text{D}} = 220 \pm 10$ (c 0.18, H₂O) as determined in our lab. These results strongly support that *trans*-(+)-CHCD is the substrate species involved in the MenD-catalyzed reaction, and thus acts as alternative substrate. Naturally, our interest turned to the kinetics of *trans*-(+)-CHCD transformation by MenD reaction and whether the unrecognized *trans*-(-)-CHCD inhibits the MenD reaction. Fortunately, it turned out that (-)-CHCD made no difference to MenD activity in the presence of ISC, thus racemic CHCD can be used in MenD reactions. As shown in Figure 3.2A, the reaction progress curve of the MenD reaction utilizing racemic CHCD (UV absorbance at 278 nm of CHCD over time in minutes) is essentially the same as using ISC, therefore kinetics of the MenD reaction utilizing CHCD can be determined as a regular MenD assay, i.e. monitoring the depletion of CHCD over time by UV spectrophotometer (refer to 2.2.6).

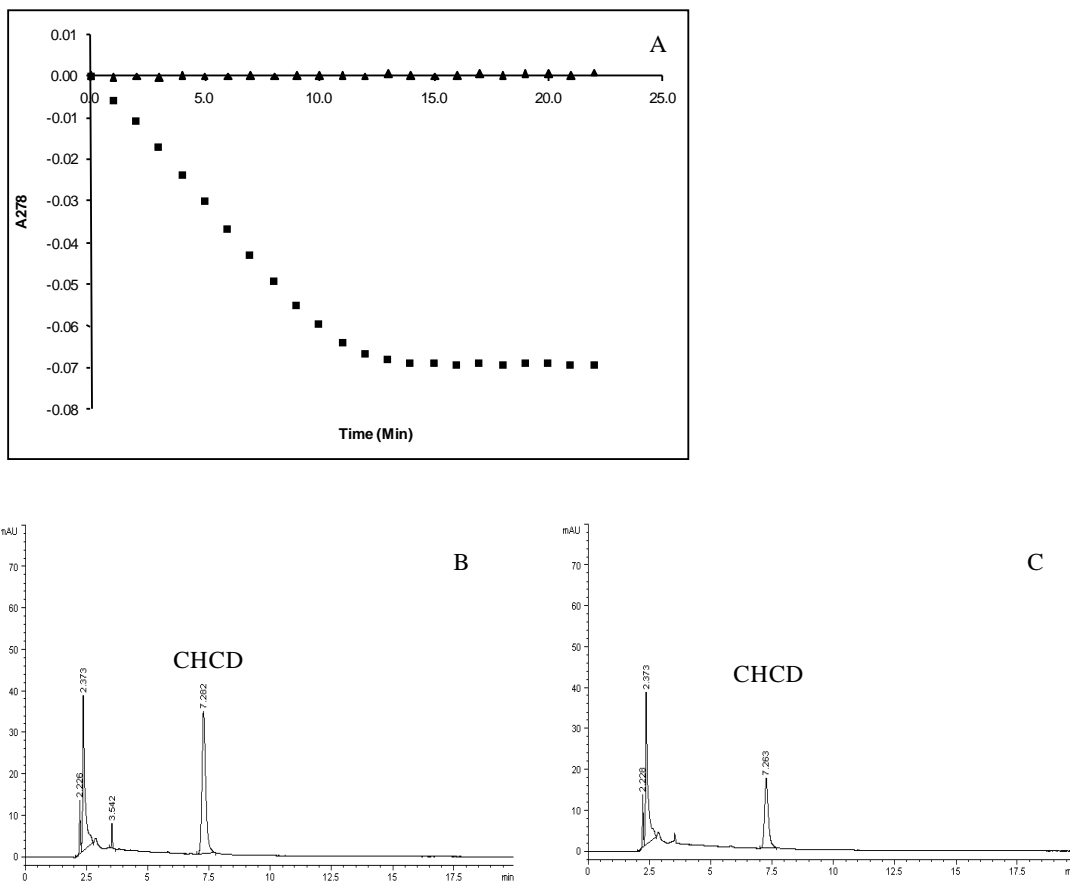


Figure 3.2: Comparison of HPLC and spectrophotometric analysis of the MenD reaction utilizing *trans*-(±)-CHCD. The reaction was performed with 60 nM MenD, 100 mM Tris (pH 7.4), 5 mM MgCl₂, 50 μM ThDP, 100 μM 2-KG and 30 μM (±)-CHCD. The HPLC elution buffer was 5% ACN, 95% formic acid solution (0.1%, v/v) and the detection wavelength was 278 nm. (A) A progress curve detected spectrophotometrically at 278 nm. ▲ Blank reaction mixture containing all components but 2-KG; ■ reaction mixture initiated with 2-KG; (B) reaction mixture before initiation with 2-KG, the area of CHCD (retention time: 7.28 min) was 379.5 mAU*s; (C) reaction mixture quenched at 30 min after the initiation with 2-KG, the area of CHCD was 188.6 mAU*s.

The methyl ester of *trans*-(±)-CHCD (i.e. CHCDMe, compound **29**, refer to **2.1.2**) was tested as a substrate of MenD. In contrast to CHCD, CHCDMe was found not to be accepted by MenD; no change in UV absorbance was detected. The methyl ester of the side chain is probably not compatible with the basic residues surrounding where carboxylates of ISC presumably locate in the active site of MenD (Figure 1.13). This

suggests the involvement of unsaturated carboxylic moiety of ISC in the enzyme-substrate interaction.

Several isochorismate analogues with a benzene ring core (compound **32**, **34**, and **36a&b**, refer to **3.1.2**) were also tested as inhibitors of the MenD reaction. Unlike the inhibitory efficacy they (or close analogues) exhibited for salicylate synthase or isochorismatase^{64,66}, compounds **32**, **34**, **36a** and **36b** were neither substrate nor inhibitor for MenD. This suggests that the active site of MenD is unable to accommodate the flat benzene core.

3.5 Characterization and analysis of CCHC

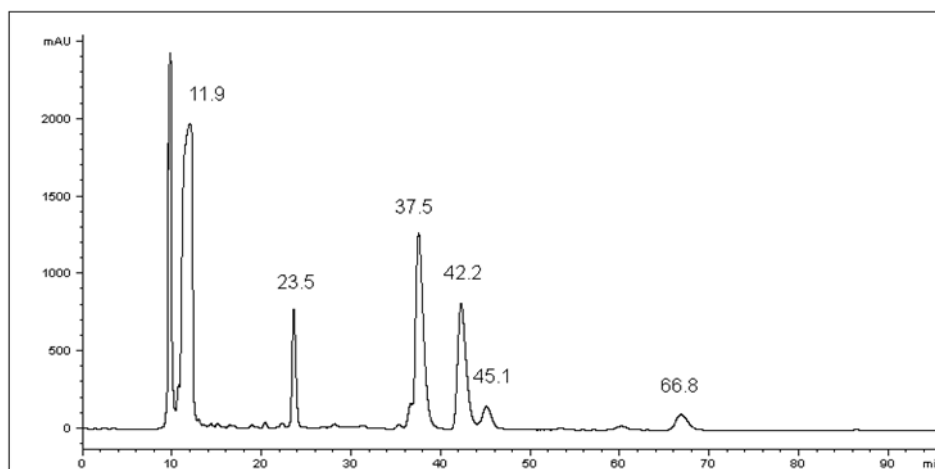


Figure 3.3: HPLC chromatogram of MenD reaction mixture using CHCD as substrate. Conditions: detector wavelength at 210 nm; Zorbax SB-C18 (9.4 × 250 mm) semi-preparative column; isocratic elution with 5% acetonitrile and 95% formic acid (0.1%).

As noted above, *trans*-(+)-CHCD is recognized as an alternative substrate by MenD, therefore it is reasonable to assume the formation of an SEPHCHC-like product from the reaction. However, ¹HNMR analysis of the MenD reaction mixture using CHCD failed to

detect the signal of predicted SEPHCHC-like product; HPLC isolation with semi-preparative column was not successful either, although several unexpected peaks were found in the chromatogram (Figure 3.3). The peak with a retention time 23.5 min was attributed to unreacted (-)-CHCD by comparison with a sample spiked with authentic CHCD. The fractions at 37.5 min, 42.2 min and 66.8 min were unknown and were collected. The fractions at both 37.5 min and 42.2 min yielded white solids after lyophilization.

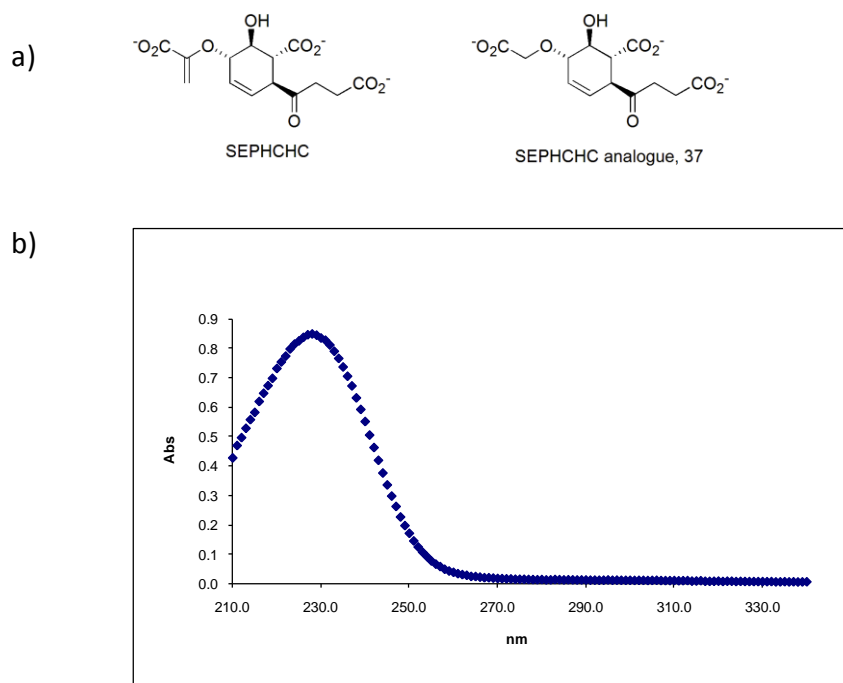


Figure 3.4: The product from fraction at 37.5 min (refer to Figure 3.3). a) SEPHCHC and analogue **37**; b) UV scan of the product.

The UV scan of the product from the fraction at 37.5 min revealed a maximal absorbance at 228 nm with an extinction coefficient of $12000 \text{ M}^{-1} \cdot \text{cm}^{-1}$, suggesting a conjugated structure different from the expected SEPHCHC-like product (compound **37**, Figure 3.4), which is expected to be UV inactive, as observed for SEPHCHC, due to the

absence of a conjugated π -system. Extensive analysis using NMR was then conducted to determine the chemical structure of the compound. Structural analysis including ^1H NMR, COSY, Jmod- ^{13}C NMR and HMQC as shown below (Figure 3.5, Figure 3.6, Figure 3.7 and Figure 3.8) clearly suggest that the compound is actually 5-carboxymethoxyl-2-(3-carboxypropionyl)-6-hydroxy-cyclohex-2-enecarboxylate (CCHC). Its configuration was assumed to be the same as that of SEPCHC, in accordance with the specific nature of enzyme reactions¹⁵. Furthermore, high resolution mass spectrometry also supported this assignment (see 2.2.5).

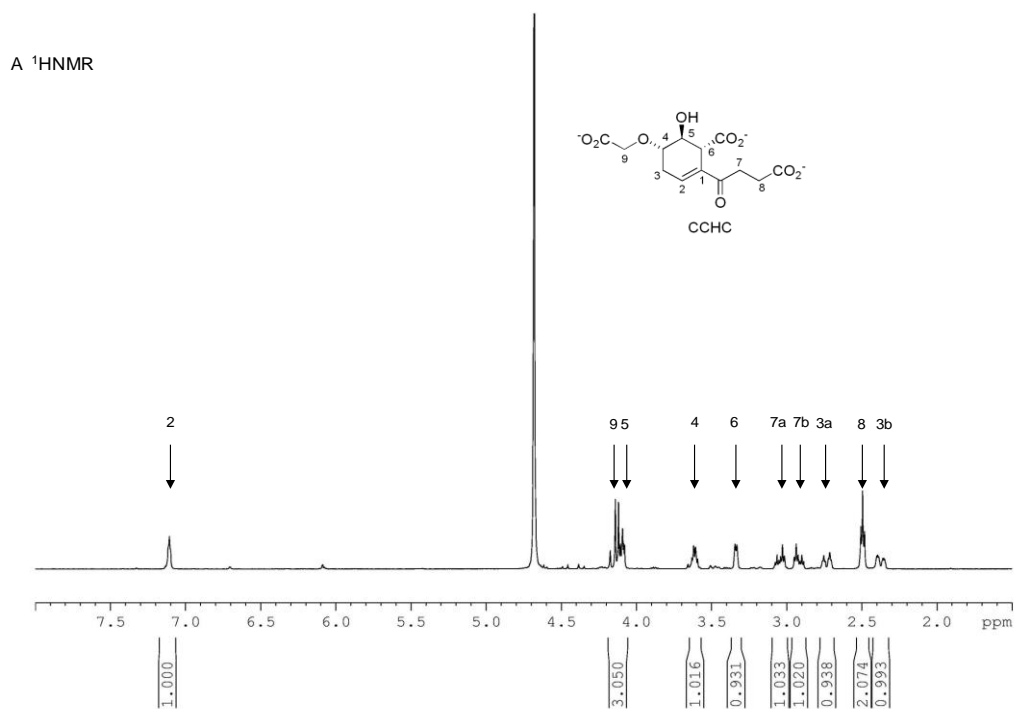


Figure 3.5: ^1H NMR spectroscopy of CCHC.

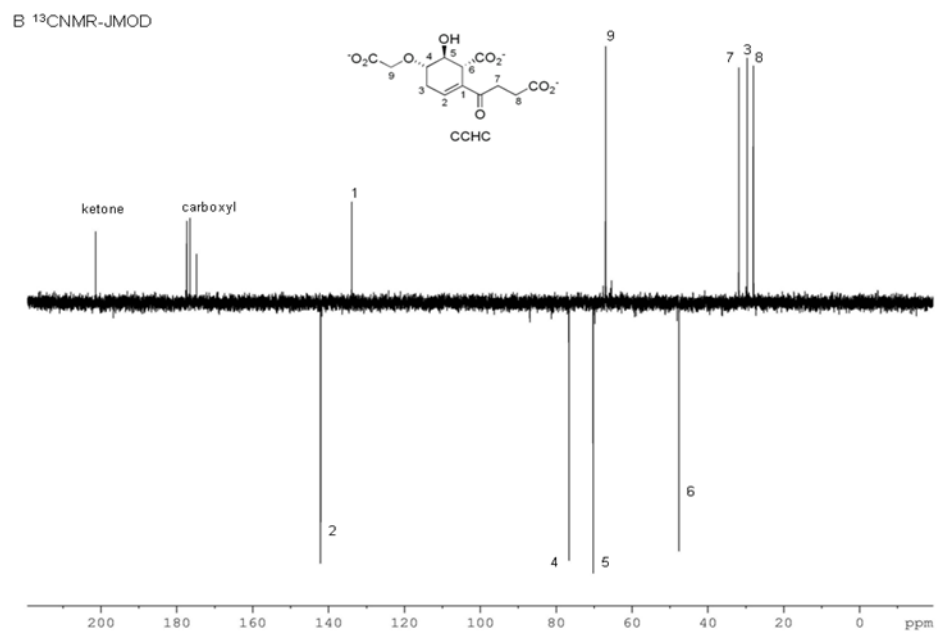


Figure 3.6: Jmod- ^{13}C NMR spectroscopy of CCHC.

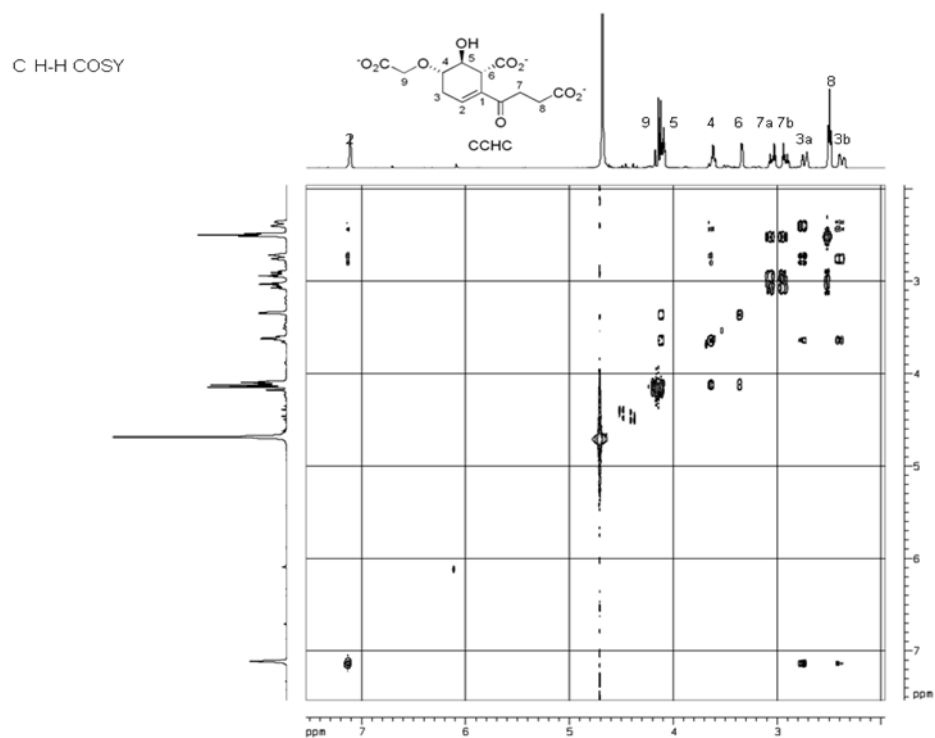


Figure 3.7: H-H COSY spectroscopy of CCHC.

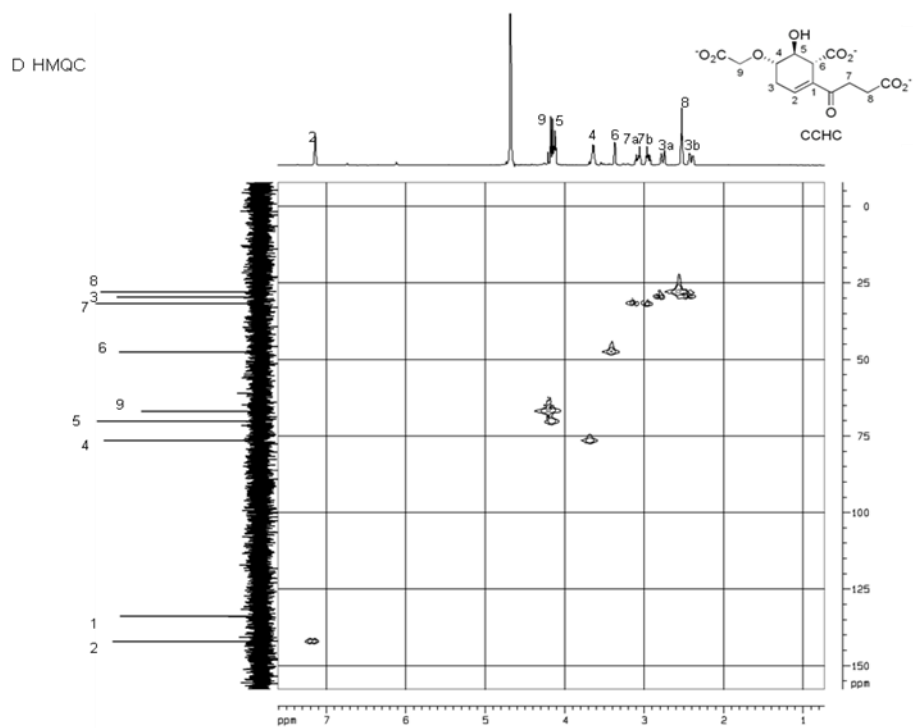


Figure 3.8: HMOC spectroscopy of CCHC.

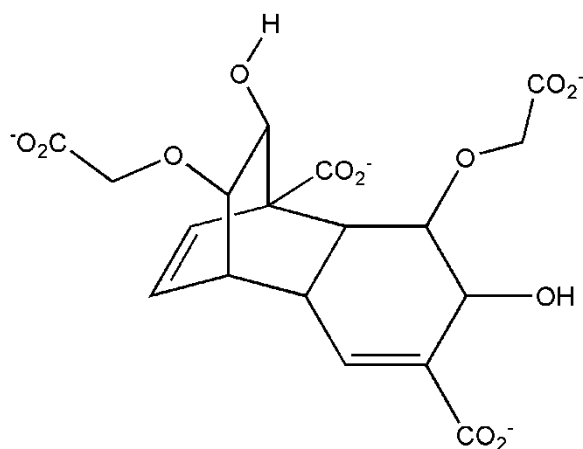


Figure 3.9: Proposed Diels-Alder product of CHCD. The fraction at 42.2 min (refer to Figure 3.3).

The fraction at 42.2 min as shown in Figure 3.3 is identified as the Diels-Alder product of two CHCD molecules according to the NMR analysis (NMR spectra were attached in **Appendix**), but the relative configuration was not fully determined (Figure 3.9). This finding could account for the instability of a CHCD stock solution and why

the freshly prepared solution must be calibrated in concentration by full MenD-catalyzed conversion before the kinetic assay.

In conclusion, CCHC was isolated as the product from the MenD-catalyzed reaction using CHCD as substrate and its structure was well characterized on the basis of NMR and MS in good agreement with its UV scan.

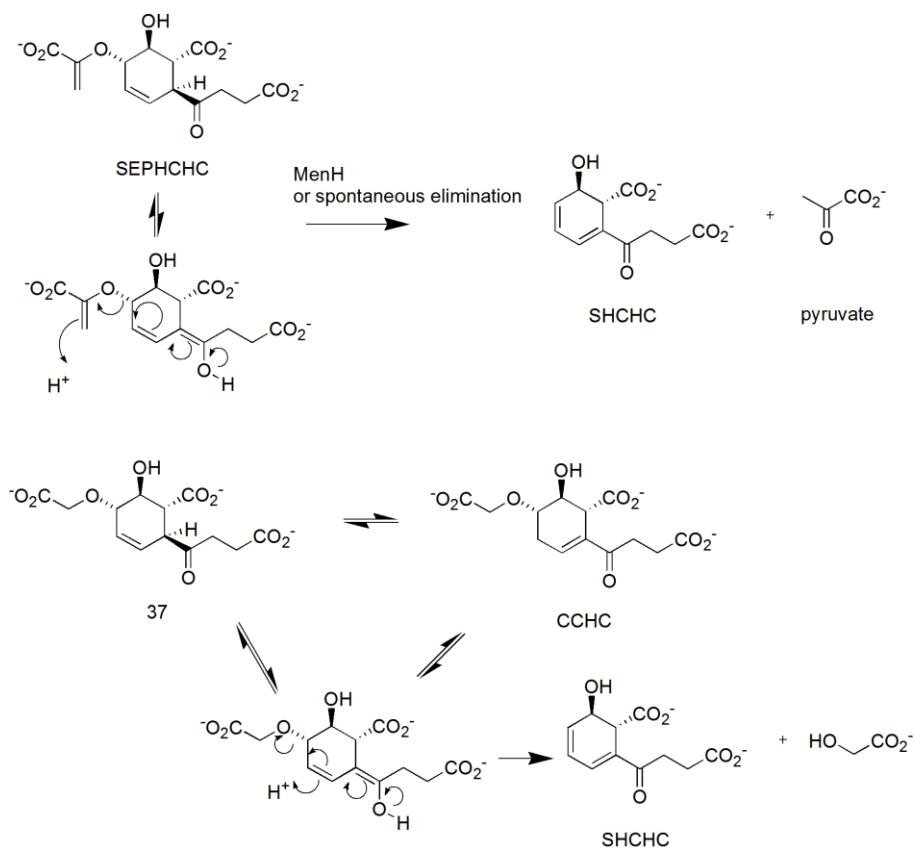


Figure 3.10: Proposed mechanism of CCHC formation.

Questions arose here why the isolated product is CCHC but not compound **37** when CHCD was used in the MenD reaction. A plausible answer is that CCHC comes from **37** by allyl isomerization (Figure 3.10). As noted earlier (refer to **1.2**), MenD was long annotated as SHCHC synthase until Guo *et al.* suggested that the real product is

SEPHCHC and SHCHC is formed by spontaneous elimination or upon catalysis of enzyme MenH from SEPHCHC^{13,14,15}. This might be due to the fact that SEPHCHC is a base-labile compound and elusive from UV detection. Following this idea, a mechanism for CCHC formation was proposed (Figure 3.10). As with the formation of SEPHCHC from ISC, the SEPHCHC-like analogue **37** is supposed to be produced from CHCD by MenD, but due to the acidic α -proton of the ketone, this analogue readily enolizes to facilitate subsequent elimination and therefore lead to CCHC or even SHCHC. In the case of SEPHCHC, the formation of SHCHC is thermodynamically favored because of the superior leaving inclination of the enolpyruvyl side chain in SEPHCHC, but in the case of compound **37**, the formation of CCHC becomes favored.

In order to confirm our assumption, MenD reaction mixtures using racemic CHCD as the substrate were analyzed by HPLC. As shown in Figure 3.11, identical volumes from the same reaction mixture taken immediately after the reaction finished, and 16 hours later, were analyzed by HPLC. In the upper chromatogram, unreacted (-)-CHCD and very small CCHC peaks can be seen, while over 16 hours (lower chromatogram) CHCD peak remained the same but the CCHC peak significantly increased, i.e. thermodynamically more stable CCHC was formed from the undetected intermediate slowly and spontaneously. The undetected intermediate is proposed to be compound **37**. Similarly, in the case of MenD reaction utilizing ISC, Guo *et al.* indicated asynchronous substrate consumption and SHCHC formation⁶. Furthermore, when isolated pure CCHC was dissolved in pH 12-13 solution overnight on the bench, HPLC analysis clearly showed formation of SHCHC by this treatment (Figure 3.12, the upper chromatogram is pure CCHC solution, the lower is NaOH-treated CCHC solution).

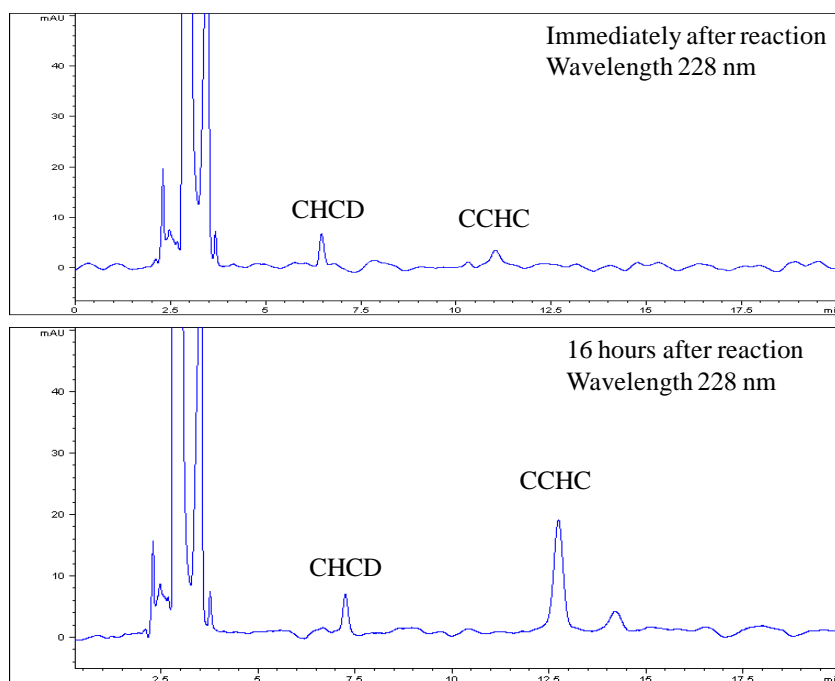


Figure 3.11: HPLC analysis of MenD reaction using CHCD. Conditions: Zorbax SB-C18 analytical column; isocratic elution with 5% acetonitrile and 95% formic acid (0.1%); flow rate at 1.0 ml/min.

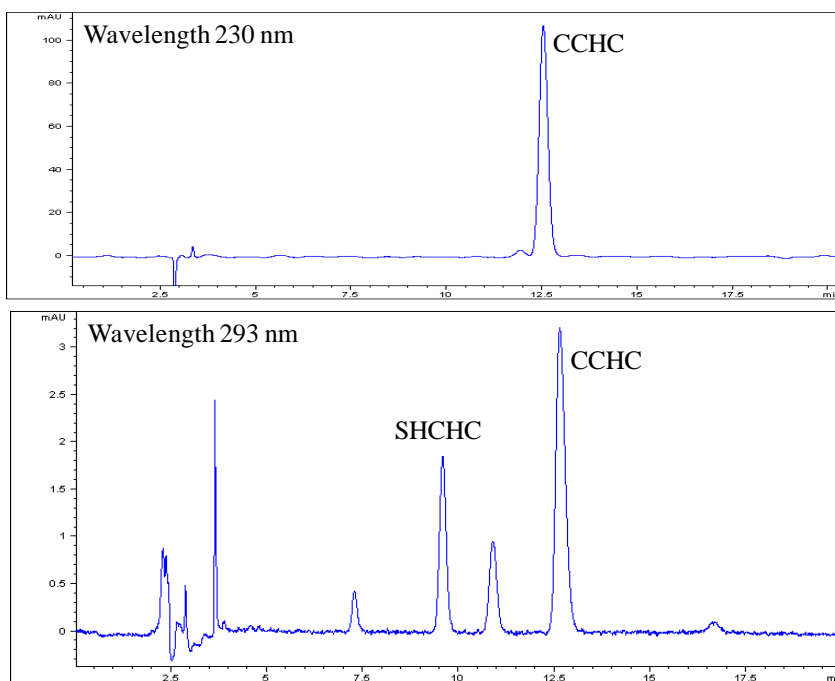


Figure 3.12: HPLC analysis of CCHC solution at pH 12-13. Conditions: Zorbax SB-C18 analytical column; isocratic elution with 5% acetonitrile and 95% formic acid (0.1%); flow rate at 1.0 ml/min.

As a result, these evidences strongly support the proposed conversion mechanism of compound **37** to CCHC and SHCHC (Figure 3.10). Interestingly, after we finished studies of CHCD-utilized MenD reaction, similar work by Müller *et al.* emerged in the literature and a CCHC-like product was reported⁶⁵. MenD was found to turn over (2S,3S)-2,3-dihydroxy-2,3-dihydrobenzoate (2,3-CHD), a simple compound lacking the side chain of CHCD or ISC. The authors successfully observed SEPHCHC-like product and slowly formed CCHC-like stable compound by NMR spectroscopy (Figure 3.13).

Moreover, according to this report MenD has a much broader substrate scope than expected. Considering racemic *trans*-CHD and *trans*-CHCD can be prepared using our CHCD synthetic route in large lab scale, the combination of MenD and CHCD synthesis strategy is of great interest in chemoenzymatic synthesis of certain optically pure molecules. For example, it is certain that MenD can be used in preparing optically pure *trans*-(-)-CHCD and (2R,3R)-2,3-CHD from their racemates.

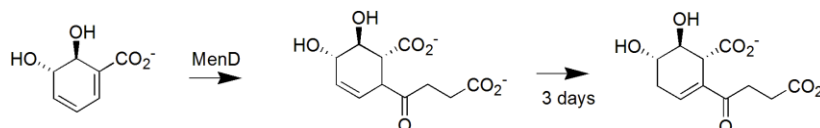


Figure 3.13: (2S,3S)-2,3-dihydroxy-dihydrobenzoate (2,3-CHD)-utilized MenD reaction⁶⁵.

3.6 The continuous and HPLC assay of the MenD reaction using ISC

When MenD was considered an SHCHC synthase, kinetic assay was performed in a coupled assay by determining NADH depletion rate in conversion of concomitantly formed pyruvate to lactic acid by lactate dehydrogenase (LDH)¹⁴. When MenD was demonstrated to be an SEPHCHC synthase producing SEPHCHC and carbon dioxide, Guo *et al.*

conducted kinetic assays by monitoring UV absorbance of substrate ISC at 278 nm⁶. This assay method is very attractive due to features of being handy and not disturbing reaction mixture. To ensure the validation of the continuous assay by UV spectrophotometer, and to confirm the new functional assignment of MenD, the MenD reaction was carefully evaluated by UV spectroscopy and HPLC analysis.

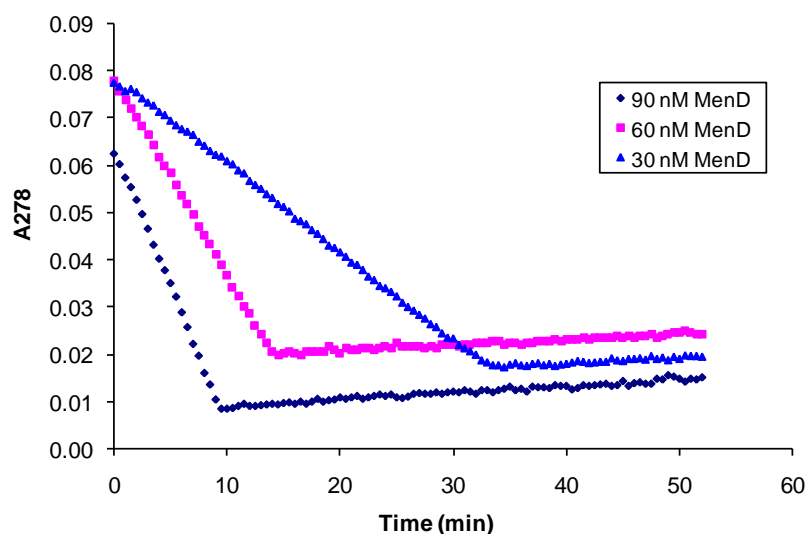


Figure 3.14: The MenD-catalyzed reaction progress curve monitored at 278 nm by UV spectrophotometer. Conditions: 100 mM Tris buffer (pH 7.4), 5 mM MgCl₂, 50 μ M ThDP, 100 μ M 2-KG and 8 μ M ISC, at 25 °C. The concentrations of MenD were 90 nM, 60 nM and 30 nM respectively.

In continuous assays, the time-dependent depletion of ISC was monitored by observing the UV absorbance at 278 nm. Unlike the usual exponential progress curve for first-order reactions, the disappearance of substrate proceeds in a linear fashion as shown in Figure 3.14, suggesting a zero-order dependence on this substrate, perhaps due to the very small saturating concentration for ISC. After the depletion of ISC, the progress curve levels off sharply, then increases slowly, interpreted to represent a slow and spontaneous formation of SHCHC⁶.

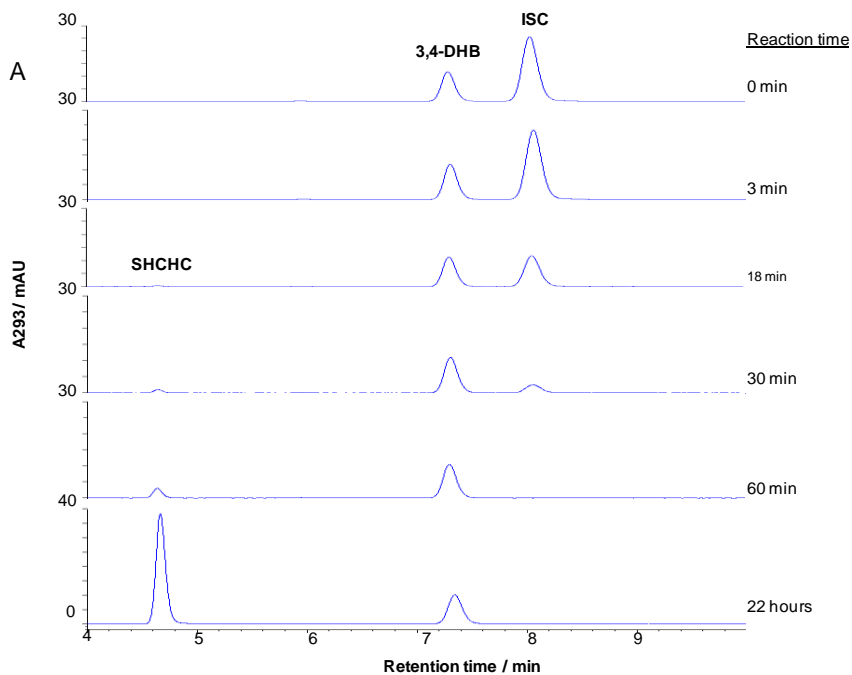


Figure 3.15: HPLC analysis of the MenD reaction using ISC. Conditions: refer to **2.2.8**, the detection wavelength for HPLC was 293 nm.

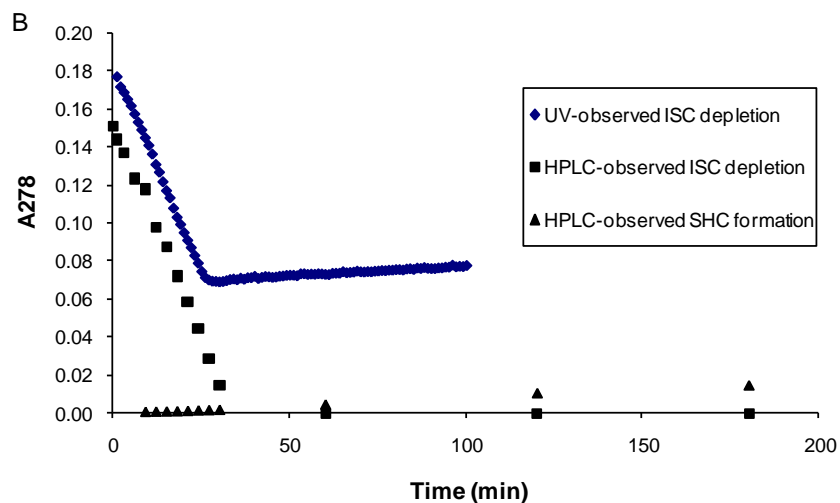


Figure 3.16: Comparison of UV and HPLC-observed progress curve of the MenD reaction using ISC. Conditions: refer to **2.2.8**, the detection wavelength for HPLC was 293 nm.

In order to validate the continuous assay by a UV spectrophotometer, concentrations of ISC during the process of reaction were determined by HPLC analysis. Aliquots of the

reaction mixture were quenched by formic acid to pH = ca. 4-5 at certain intervals and then analyzed in parallel by HPLC under the same conditions. Quenching the reaction mixture aliquots with formic acid to pH = ca. 4-5 did not decompose ISC within the analysis time period, or else faster ISC depletion would be mistakenly observed in comparison with UV detection. The internal standard 3,4-dihydroxy-benzoic acid (3,4-DHB) was used to quantify the concentration of ISC (Figure 3.15). It was observed that the ISC peak was decreasing during the reaction process, while SHCHC was formed slowly, obviously asynchronous to the ISC depletion. After ISC was depleted completely at ca. 30 min, SHCHC still slowly accumulated over 22 hours. This observation is consistent with Guo's proposal that SHCHC forms from UV-inactive SEPHCHC irrelevant of MenD catalysis under assay conditions, and the progress curve after ISC depletion moves up because of SHCHC accumulation⁶. The parallel experiments (Figure 3.15 and Figure 3.16) demonstrate the same rates of ISC consumption, which was represented by the slope of linear dropping progress curves. These results clearly indicate that the UV absorbance change at 278 nm of MenD reaction mixture is due to ISC consumption and the slope of this line represents MenD-catalyzed activity.

In the presence of saturating 2-KG, MgCl₂ and ThDP, the MenD reaction can be considered a pseudo-first-order reaction, according to rate = $k_{\text{cat}}[\text{E}]$, reaction rates should be proportional to enzyme concentrations. Figure 3.14 indeed demonstrates the slopes of the dropping linear part are proportional to the enzyme concentrations (slope ratio = -0.0019: -0.0042: -0.0059 = 1:2:3, concentration ratio = 30 nM: 60 nM: 90 nM = 1:2:3), supporting the validation of using ISC consumption rate to represent turnover rate.

In conclusion, UV absorbance change of the MenD-catalyzed reaction mixture at 278 nm as a function of time was confirmed to be the rate of ISC consumption; SHCHC is not the direct turnover product of MenD catalysis. In section 3.4, *trans*-(+)-CHCD was found to be an alternative substrate of MenD. Considering that *trans*-(+)-CHCD has almost the same UV absorbance spectroscopy as ISC, the continuous assay of MenD reaction using ISC can be expanded to the case of MenD-catalyzed CHCD consumption.

3.7 Determining concentration and ϵ_{300} of ISC and (\pm)-CHCD

Because ISC and (\pm)-CHCD are not stable in solution, it is necessary to use freshly prepared solutions to determine accurate kinetic constants. Initially, the ISC solution concentration was calibrated by determining its absorbance at 278 nm, but this method proved to be problematic. As shown in Figure 3.14 and Figure 3.16, referring to blank solution containing all components but ISC, after full consumption of ISC the UV-observed progress curve should reach the X-axis as HPLC-observed curve shows. But the UV absorbance does not drop to zero in the spectrophotometric assays. The use of fresh ISC solution reduced but could not eliminate this problem. Therefore it was reasoned that the absorbance of ISC solution at 278 nm could not be attributed solely to ISC.

In order to determine accurate concentrations of ISC and (\pm)-CHCD, full enzymatic conversion of MenD in the presence of excess 2-KG is a suitable strategy⁸⁶. By using $\epsilon_{278} = 8300 \text{ M}^{-1}.\text{cm}^{-1}$ for ISC⁸⁶ and $\epsilon_{278} = 4700 \text{ M}^{-1}.\text{cm}^{-1}$ for (\pm)-CHCD (refer to 2.2.7), UV absorbance drops measured from reactions can be used to determine substrate concentrations.

In the cases of assaying some mutants, higher concentrations of enzyme, ThDP or substrates were needed. These species have moderate or high absorbance at 278 nm, causing too high background noise of the reaction mixture to determine the absorbance decrease due to ISC or CHCD consumption; hence the absorbance at 300 nm was usually measured to circumvent the problem. Thus, it was required to determine the extinction coefficients of ISC and CHCD at 300 nm. Since the ϵ_{278} of ISC and CHCD were already known, the experiment as follows was designed: in a 1.4 ml quartz cuvette, 0.6 ml total volume reaction mixture containing 100 mM Tris buffer (pH 7.4), 5.0 mM MgCl₂, 50 μ M ThDP, 100 μ M 2-KG, 150 nM MenD and 10 μ M ISC was scanned spectrophotometrically in a range of 240-320 nm at an interval time of 1 min (Figure 3.17). In Figure 3.17A, it shows that the UV absorbance of the enzymatic reaction mixture decreased due to the ISC depletion and stopped at ca. 7 min. The UV absorbances at 278 nm and 300 nm were extracted from each scan and plotted with respect to time, as shown in Figure 3.17B. The results clearly indicate that the monitoring at 278 nm and 300 nm is representing ISC depletion at the same pace and therefore it is valid to assay the reaction monitoring UV absorbance at 300 nm. Furthermore, because the absorbance decrease of the full enzymatic conversion of ISC at 278 nm represents the same amount, the ϵ_{300} of ISC could be derived according to $\frac{\Delta A_{300}}{\Delta A_{278}} \times 8300 \text{ (M}^{-1} \cdot \text{cm}^{-1}\text{)}$.

From three repetitions of the experiments as above, the average ϵ_{300} of ISC was determined as 3600 M⁻¹ cm⁻¹. The value was used in all the kinetic assays when applicable.

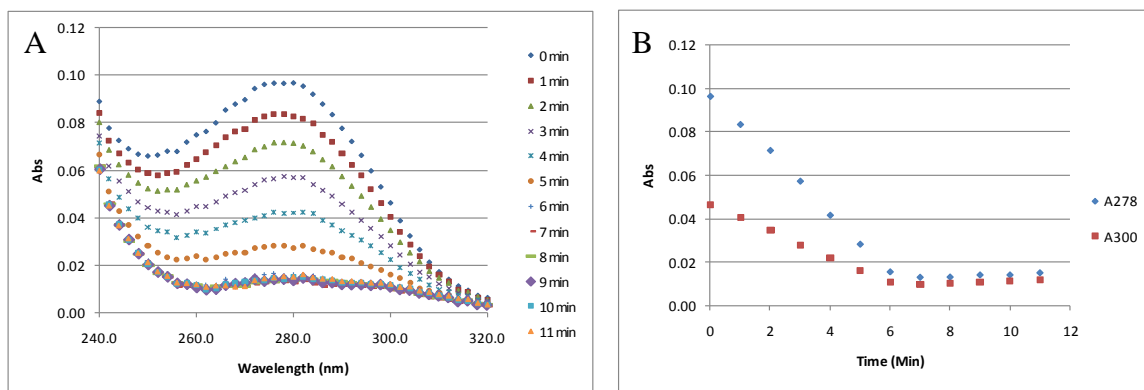


Figure 3.17: Determination of the extinction coefficient of ISC at 300 nm. A) Time-dependent UV scans of MenD reaction mixture using ISC as substrate; B) UV absorbance decreases at 278 nm and 300 nm using the data extracted from A.

Similar experiments were also conducted for enzymatic conversion of (\pm)-CHCD, and the same conclusion was drawn. The ϵ_{300} for (\pm)-CHCD was determined to be $1700 \text{ M}^{-1} \cdot \text{cm}^{-1}$ (Figure 3.18). Recall, because only one enantiomer of CHCD is reactive in MenD-catalyzed (or some mutants) reactions, reactive concentrations of CHCD are half of the racemic CHCD solution used for assays.

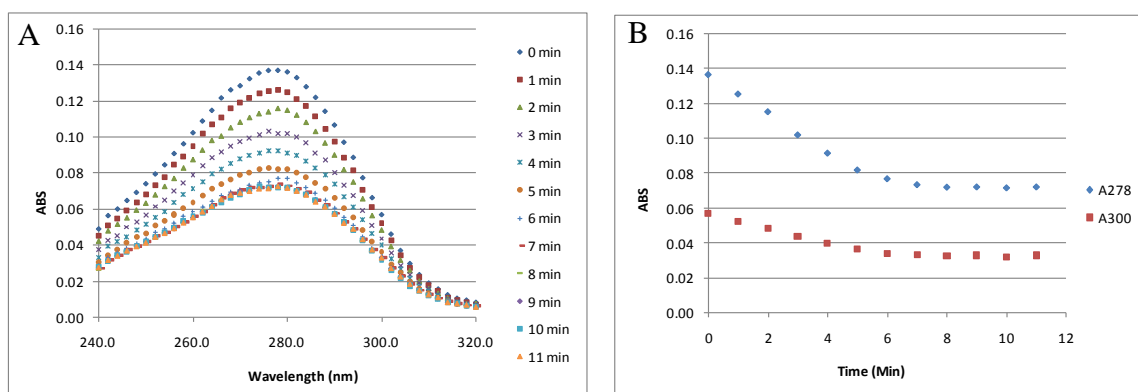


Figure 3.18: Determination of the extinction coefficient of ISC at 300 nm. A) Time-dependent UV scans of MenD reaction using (\pm)-CHCD as substrate; B) UV absorbance decrease at 278 nm and 300 nm using the data extracted from A.

3.8 Activity assays of MenD and mutants

Although the MenD-catalyzed reaction is a bi-substrate reaction, it becomes a pseudo uni-substrate reaction when all the other substrates and cofactors are at saturating concentrations. The activities of MenD and mutants were assayed using continuous UV monitoring of the consumption of ISC and (\pm)-CHCD at 278 nm or 300 nm. All the apparent kinetic parameters including K_m^a , k_{cat}^a , k_{cat}^a / K_m^a were derived from the saturation curves or Hanes-Woolf plots of the substrates (2-KG, ISC and CHCD) and cofactors (MgCl₂ and ThDP).

The very small saturating concentration or K_m^a observed for ISC makes it easy to obtain a linear ISC depletion curve (refer to Figure 3.14), but almost impossible to determine the initial rate at a very low concentration of ISC due to the short time period allowed for measurement and the background absorbance noise (applied to MenD and most but not all mutants studied). Guo *et al.* reported K_m^a value of ISC measured for wt-MenD is $0.053 \pm 0.003 \mu\text{M}$, corresponding to < 0.00083 AU UV absorbance⁶. This small value precludes accurate measurement of initial rates with varied ISC concentrations below K_m^a of ISC, which is required to obtain saturation curve of ISC. For the mutants having a very large saturation concentration for ISC or CHCD, the UV absorbance is too high to measure with a UV spectrophotometer. The apparent kinetic parameters were hence unable to be determined. In such cases, kinetic constants were estimated from Hanes-Woolf plot.

The saturation curves for 2-KG, ThDP and Mg²⁺ of wild type MenD reaction, typical of Michaelis-Menten kinetics, are shown in Figure 3.19 and kinetic constants were

derived from them. The kinetic parameters of mutant S32A, S32D, R33K, R33Q, E55D, R107K, K292Q, R293K, S391A, S395A, S395K, R413K, and I418L were measured in the same way.

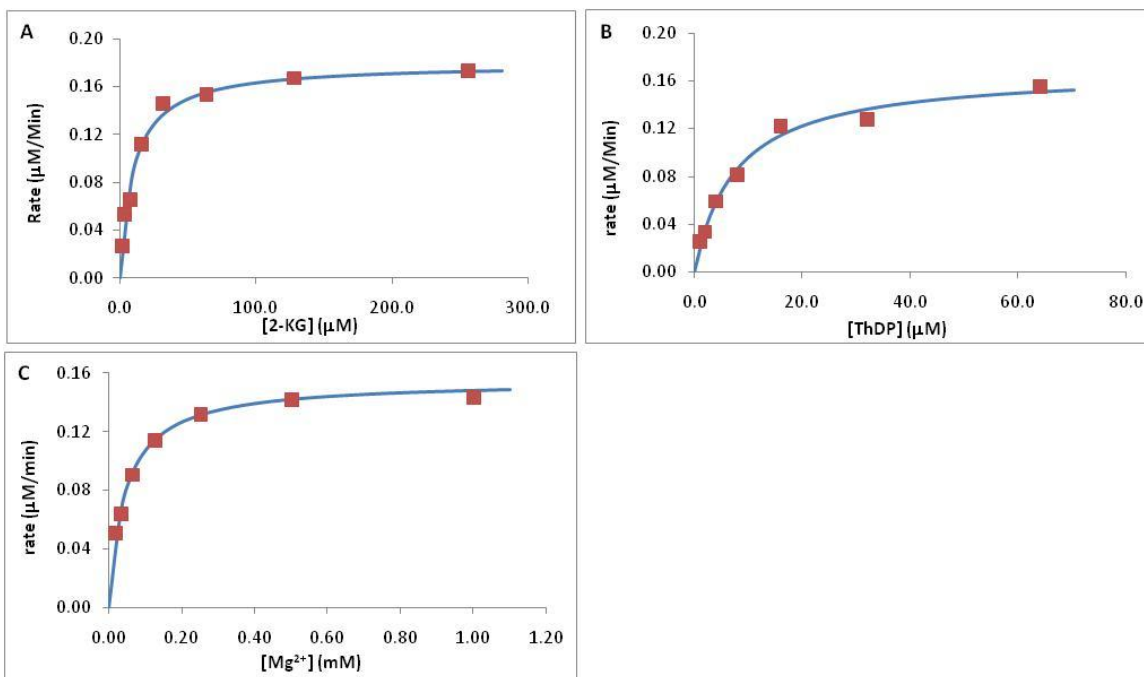


Figure 3.19: Saturation curves of the MenD-catalyzed reaction. (A) 2-KG Saturation curve of MenD. The reaction rate was determined with 10 nM MenD, 100 mM Tris (pH 7.4), 5 mM MgCl_2 , 50 μM ThDP and 16 μM ISC; (B) ThDP Saturation curve of MenD. The reaction rate was determined with 10 nM MenD, 100 mM Tris (pH 7.4), 5 mM MgCl_2 , 16 μM ISC and 100 μM 2-KG; (C) MgCl_2 Saturation curve of MenD. The reaction rate was determined with 10 nM MenD, 100 mM Tris (pH 7.4), 50 μM ThDP, 16 μM ISC and 100 μM 2-KG.

3.9 Inhibition of the MenD-catalyzed reaction with phosphonate analogues of 2-KG

In line with pioneering work by Kluger and Pike using a phosphonate analogue of pyruvate (MAP, refer to section 1.7.1) to study pyruvate dehydrogenase (PDH-E1)⁵¹, 2-keto phosphonate analogues, which are close steric analogues of 2-KG, were surmised to

behave as inhibitors of MenD. Eleven 2-keto phosphonate compounds were synthesized and assayed as inhibitors of the MenD reaction. As expected, it was found that these phosphonates demonstrate inhibition of MenD with varied efficiencies.

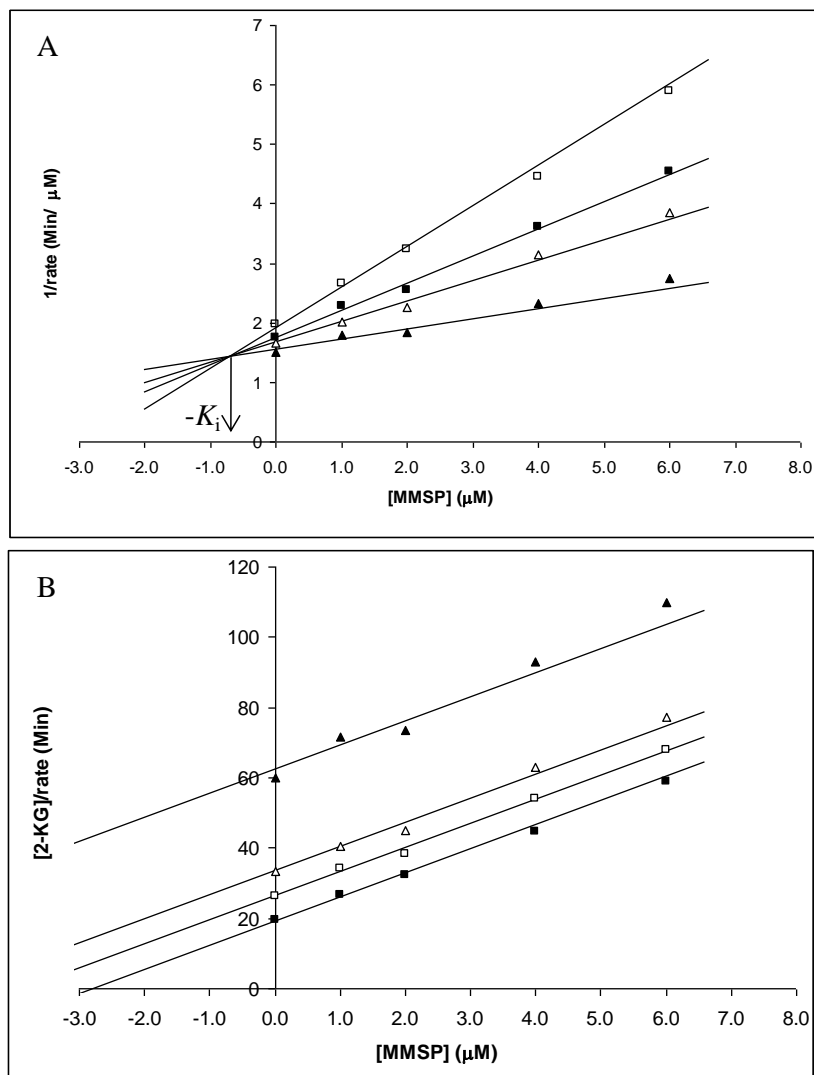


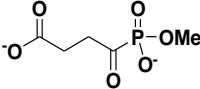
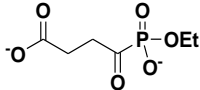
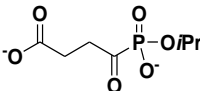
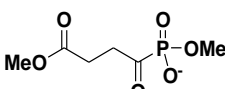
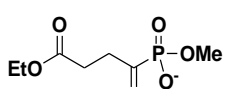
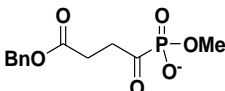
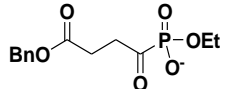
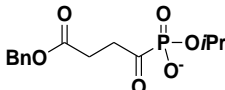
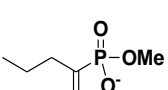
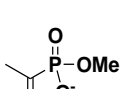
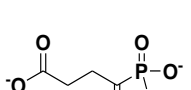
Figure 3.20: Graphic determination of MMSP inhibition of the MenD-catalyzed reaction. (A) Dixon plot (1/rate vs. [MMSP]); (B) Cornish-Bowden plot ([2-KG]/rate vs. [MMSP]). The reaction rate was determined with 60 nM MenD, 100 mM Tris (pH 7.4), 5 mM MgCl₂, 50 μM ThDP and 16 μM ISC. [2-KG] was at 10 μM (▲), 15 μM (△), 20 μM (■), 40 μM (□).

Inhibition type and inhibition constants were determined graphically by a combination of Dixon plot ($1/v$ vs. [inhibitor] at four different [2-KG]) and Cornish-Bowden plot ($[2\text{-KG}]/v$ vs. [inhibitor] at four different [2-KG]). For instance, the Dixon plot and Cornish-Bowden plot as shown in Figure 3.20 suggest that monomethyl succinyl phosphonate (MMSP) is a reversible, competitive inhibitor with respect to 2-KG in the MenD reaction (refer to section **1.8**). The inhibition constant (K_i) of MMSP is 0.7 ± 0.1 μM as indicated in Figure 3.20A, showing very potent inhibition in terms of Michaelis constant of 2-KG (9.9 ± 0.6 μM , Table 3.1).

The structures of the 2-KG phosphonates tested and the inhibition results are summarized in Table 3.1. Among these phosphonates, succinylphosphonate (SP) was determined as an inhibitor with K_i of 150 ± 10 μM . Careful inspection of the HNMR spectrum of SP revealed the presence of residual MMSP (ca. 0.5%). Since SP has one more negative charge than 2-KG, very likely the observed inhibition is due to a small amount of the potent MMSP. The same observation was reported by Kluger and Pike in their inhibition study of PDH using acetyl phosphonate (AP)⁵¹.

Following the successful example of MMSP as inhibitor, phosphonates with varied phosphonate ester and carboxyl groups were tested (Table 3.1). Compounds MMSP, MESP and MISP, bearing same number of charges as 2-KG, demonstrate varied potency of inhibition. Increasing the size of the phosphonate monoester causes one order of magnitude dropping of inhibition potency. Steric hindrance appears to be accountable for weaker binding affinity between MenD and inhibitor, implying close recognition of the 1-carboxylate of 2-KG (the counterpart of the phosphonate monoester moiety) by the active site.

Table 3.1: Inhibition constants of 2-KG phosphonate analogues for MenD reaction. * ca. 0.5% MMSP contained.

Compounds	Structure	K_i (μM)
Monomethyl succinylphosphonate (MMSP)		0.7 ± 0.1
Monoethyl succinylphosphonate (MESP)		16 ± 1
Monoisopropyl succinylphosphonate (MISP)		170 ± 10
Methyl monomethyl succinylphosphonate (MMMP)		240 ± 20
Ethyl monomethyl succinylphosphonate (EMMP)		1630 ± 90
Benzyl monomethyl succinylphosphonate (BMMP)		160 ± 10
Benzyl monoethyl succinylphosphonate (BMEP)		1320 ± 60
Benzyl monoisopropyl succinylphosphonate (BMIP)		6700 ± 400
Monomethyl butyrylphosphonate (MMBP)		-
Methyl acetylphosphonate (MAP)		-
Succinylphosphonate (SP)		$150 \pm 10^*$

Surprisingly, the phosphonates bearing a carboxylic ester as MMMP, EMMP, BMMP, BMEP and BMIP also inhibit MenD with appreciable potency. It appears that the active site of MenD allows flexibility for recognizing the 4-carboxylate anion of 2-KG, tolerant of neutral carboxylic esters. In order to study the role of the carboxyl group in inhibition, analogues MMBP and MAP, which lack a carboxyl moiety, were prepared and tested as inhibitors. It was found that neither of the two analogues inhibits the MenD reaction at concentrations up to 10 mM, implying that the 4-carbonyl group is necessary for binding.

BMMP, BMEP and BMIP demonstrate the same trend as MMSP, MESP and MISP: inhibition constants increase with increasing size of the alkyl group of the phosphonate esters. Unexpectedly, although BMMP has a benzyl ester, which is bulkier than the methyl ester of MMMP and the ethyl ester of EMMP, BMMP exhibits a slightly lower inhibition constant than MMMP and a 10-fold lower inhibition constant than EMMP.

Structural analysis of 2-keto acid-utilizing ThDP-dependent enzymes with bound intermediates or intermediate phosphonate analogues revealed a common three-centered binding mode for 2-keto acid substrates, including the interactions specific for leaving group (1-carboxylate), 2-carbonyl/carbinol and substrate substituents^{55,56,87}. In POX, the methyl substituent of LThDP is located in a hydrophobic pocket formed by V394, F121, W479 and isoalloxazine of FAD, whereas, for BFDC and BAL, the larger substituents of their substrates are accommodated in a wider pocket consisting of several aromatic residues^{39,52,53}. In contrast, the solved MenD structure indicated that the possible binding pocket for the carboxyethyl substituent of 2-KG consists of basic residues such as arginines and lysines. Stabilization of π - π stacking or cation- π interaction, between the

phenyl group of BMMP and the binding pocket as shown in MenD structure³¹, may account for the inhibition enhancement. In conclusion, inhibition results of the 2-KG phosphonates indicated that appreciable variation is allowed by the 2-KG substituent binding pocket, implying a broad scope of accepted substrates. This is consistent with the report that MenD catalyzed unphysiologically C-C forming reaction for a variety of 2-keto acids⁶⁵. Undoubtedly, an X-ray structure of MenD with a trapped ThDP-phosphonate adduct will reveal more information about this binding pocket. This kind of study will be greatly instructive not only for understanding catalysis mechanism, but also for identification and modification of the relevant residues in order to favorably alter MenD's substrate specificity.

Both compound **15** and **21**, different from the 2-keto phosphonate analogues above (refer to section **3.1.1**), are 2-hydroxy phosphonate monoesters. The former has a phenyl ketone and the latter has a benzyl amide. Inhibition assays indicated that neither of them inhibited the MenD reaction although they have very similar structures as the inhibitory 2-keto phosphonates. This outcome may be rationalized by the underlying principle that 2-keto analogues form a covalent adduct with ThDP, and the 2-keto function is necessary for this.

MenD is a proposed drug target, particularly for antituberculosis drugs⁴**Error! Bookmark not defined.** The inhibitory phosphonate analogues mentioned above are the first reported inhibitors of MenD, therefore these compounds were tested for inhibition of mycobacterial growth. Unfortunately, these inhibitors did not show significant inhibition of *M. tuberculosis* growth in vitro under aerobic and hypoxic conditions⁸⁸.

3.10 Reversibility of the inhibition by 2-KG phosphonate

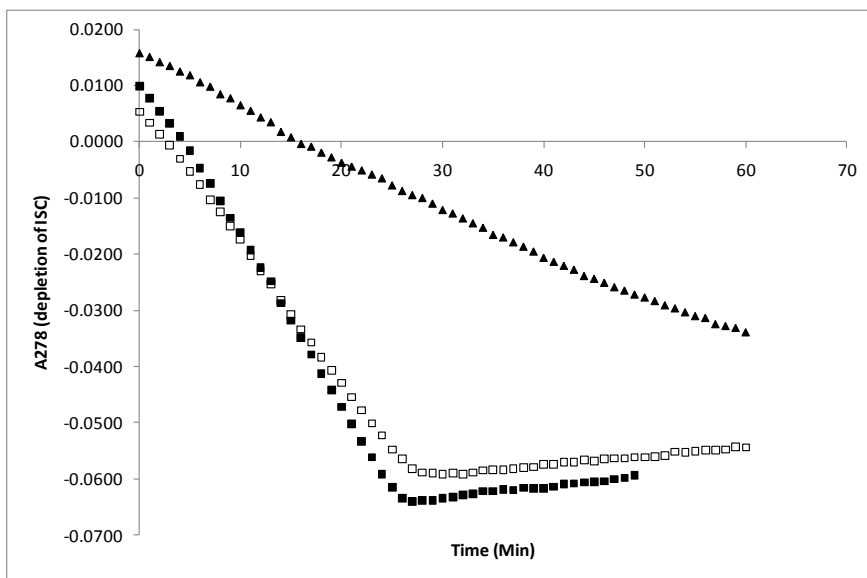


Figure 3.21: Progress curves of MenD reaction for test of inhibition reversibility. Assay conditions: at 25 °C, Tris (pH 7.4) 100 mM, MgCl₂ 5 mM, ThDP 50 μM, ISC 10 μM and MenD 60 nM. (▲) reaction mixture containing 10 μM MMSP was initiated with 2-KG; (□) MenD was pre-incubated with water for 30 min, reaction mixture was initiated with 2-KG; (■) MenD was pre-incubated with MMSP for 30 min, reaction was initiated with 2-KG.

Kinetic analysis of the MenD reaction indicated graphically that succinylphosphonates are inhibitors of MenD in a reversible, competitive manner. In order to further investigate the reversibility of the inhibitions, MenD pre-equilibrated with MMSP was diluted as described in section 2.2.11. In the experiment, MenD (30 μL MenD (28 μM)) was preincubated with MMSP (10 μL MMSP (40 μM)) over 30 min at room temperature, so in the mixture, [MenD] = 21 μM and [MMSP] = 10 μM; then 6.29 μL of the mixture was added to a reaction mixture of 2200 μL, so the actual [MMSP] in the final reaction mixture was 0.029 μM (only 4% of K_i 0.7 μM of MMSP). As shown in Figure 3.21, MenD pre-incubated with only water (□) and with MMSP (■) were

compared. Progress curves indicated the same reaction rate within experimental error, suggesting that the activity of MenD pre-incubated with MMSP was recovered quickly due to dilution of inhibitor. In contrast, obvious inhibition was observed with 10 μM of MMSP (\blacktriangle). Thus, the dilution method demonstrated that MMSP binds reversibly to MenD.

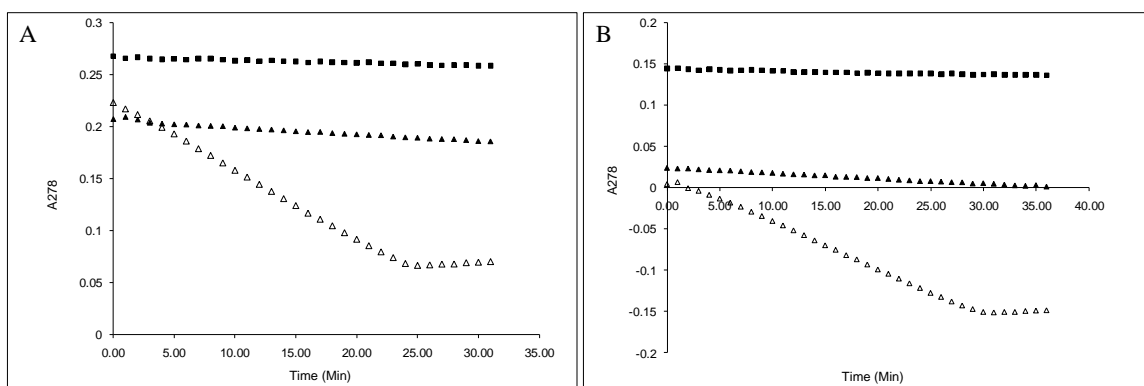


Figure 3.22: Test for time-dependence of MMSP inhibition. Reaction conditions: at 25 $^{\circ}\text{C}$, Tris (pH 7.4) 100 mM, MgCl_2 5 mM, ThDP 50 μM , ISC 20 μM and MenD 60 nM. (A) Reactions were initiated with 2-KG after 5 min incubation of MenD and MMSP. (B) Reactions were initiated with MenD after 5 min incubation of all reagents but MenD. (\blacksquare) [MMSP] 400 μM ; (\blacktriangle) [MMSP] 100 μM ; (\triangle) [MMSP] 0 μM .

In order to test time-dependence of inhibition, parallel experiments of kinetic assay in the presence and the absence of MMSP were performed. As shown in Figure 3.22, when [MMSP] = 100 or 400 μM in the presence of saturating [2-KG], almost full inhibition of MenD activity was observed equally regardless of 2-KG or ISC initiation. All the progress curves are linear without time-dependent increase of inhibition within the steady-state assay time period. In addition, no time lag was observed with MenD initiation, ruling out significant time-dependent inhibition caused by slow binding

between MMSP and MenD. This observation is consistent with previous studies in PDH^{23,51} and BFDC⁵².

In summary, the kinetic analysis, including the dilution method and alteration of initiation order of substrates, suggests that these phosphonates inhibit MenD by establishing a rapid, reversible equilibrium with the ThDP-MenD complex.

3.11 Kinetic mechanism of the MenD reaction

In the proposed mechanism of the MenD-catalyzed reaction (Figure 1.5), a ping-pong bi bi mechanism was surmised. It seems to be very likely that 2-KG must bind to MenD first, and only after carbon dioxide is released, and the resulting post-decarboxylation product can subsequently react with isochorismate. Usually, the double reciprocal plot for ping-pong bi bi reaction results in a set of parallel lines when one substrate concentration is varied at several constant concentrations of the other substrate (Figure 1.23B).

For the MenD-catalyzed reaction of CHCD, it was found that the K_m^a of (+)-CHCD ($12.0 \pm 0.6 \mu\text{M}$, Table 3.2), in contrast to that of ISC, is a spectrophotometrically measurable value. This value allows determination of reaction rate at several different concentrations of (+)-CHCD below value of K_m^a , so that an accurate value can be determined.

As shown in Figure 3.23, when both [2-KG] and [CHCD] are varied around their individual K_m^a values, the double reciprocal plots of either 1/rate vs. 1/[2-KG] or 1/rate vs. 1/[CHCD] exhibited parallel lines. This demonstrated kinetically for the first time that

the reaction catalyzed by MenD follows a ping-pong bi bi mechanism if 2-KG was assumed to bind to MenD first based on the proposed mechanism.

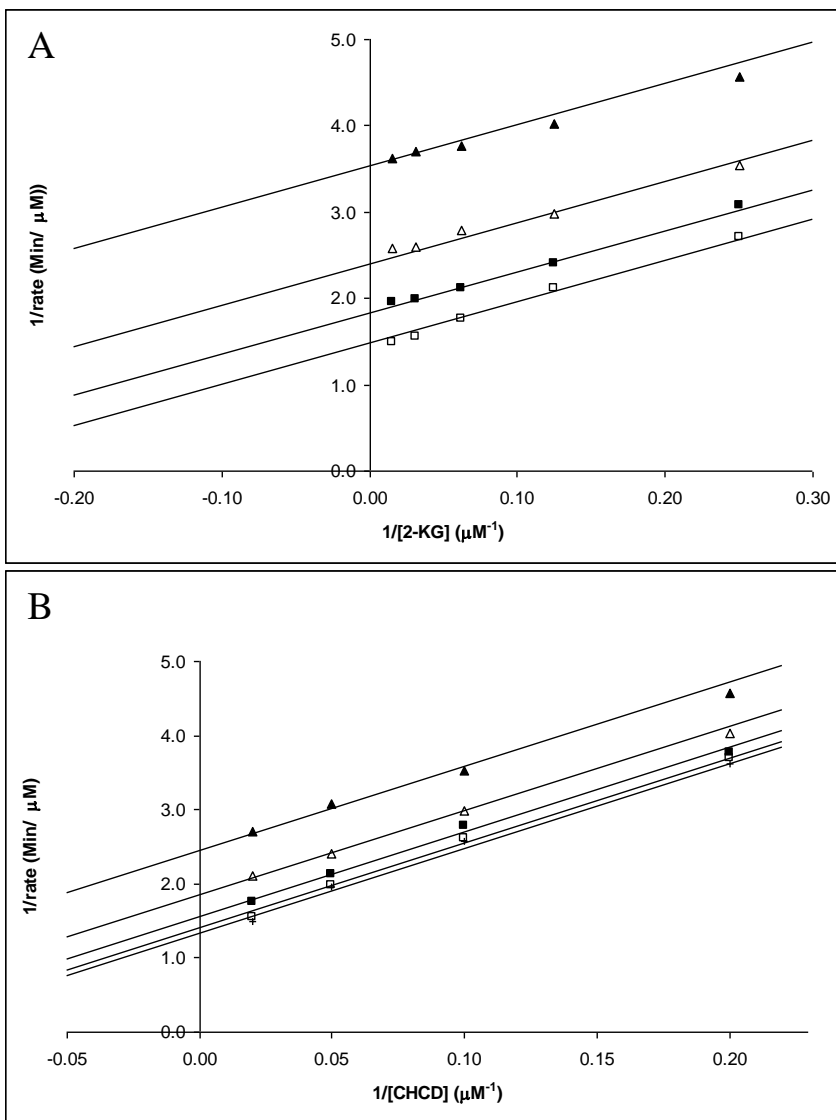


Figure 3.23: Double reciprocal plots of the MenD-catalyzed reaction of CHCD. For reaction conditions, refer to section 2.2.12. (A) Double reciprocal plot ($1/\text{rate}$ vs. $1/[2\text{-KG}]$). Concentrations of 2-KG (4 μM , 8 μM , 16 μM , 32 μM , 64 μM) varied at each concentration of CHCD (5 μM (\blacktriangle), 10 μM (\triangle), 20 μM (\blacksquare), 50 μM (\square)). (B) Double reciprocal plot ($1/\text{rate}$ vs. $1/[\text{CHCD}]$). Concentrations of 2-KG (4 μM (\blacktriangle), 8 μM (\triangle), 16 μM (\blacksquare), 32 μM (\square), 64 μM ($+$)) varied at each concentration of CHCD (5 μM , 10 μM , 20 μM , 50 μM).

Furthermore, these plots can also give the real (not apparent) kinetic constants such as K_m , V_{max} and k_{cat} according to equation 2.5. The apparent and real kinetic constants for the CHCD-utilizing MenD reaction were summarized in Table 3.2.

Table 3.2: Kinetic constants of the CHCD-utilizing MenD reaction. Noted that (±)-CHCD was used, but only half amount of [(±)-CHCD] was used for deriving kinetic constants.

Substrate	K_m^a (μM)	V_{max}^a (μM/min)	k_{cat}^a (min ⁻¹)	K_m (μM)	V_{max} (μM/min)	k_{cat} (min ⁻¹)
2-KG	2.8 ± 0.4	0.68 ± 0.03	23 ± 1	3.8 ± 0.2		
CHCD	12.0 ± 0.6	0.74 ± 0.02	25 ± 1	9.1 ± 0.4	0.80 ± 0.02	27 ± 1

By analogy, the 2-KG phosphonates are assumed to be competitive inhibitors with respect to 2-KG when CHCD is utilized as alternative substrate of MenD, given that these analogues, in mimicking of 2-KG, compete for the binding site of 2-KG, not ISC. From the phosphonates tested for the ISC-utilizing MenD reaction, the most potent inhibitor MMSP was chosen to test for this. The Dixon and Cornish-Bowden plots (Figure 3.24) demonstrate that MMSP is still a reversible, competitive inhibitor with respect to 2-KG, with $K_i = 1.3 \pm 0.1$ μM, comparable to the K_i value determined from the ISC-utilizing reaction.

As discussed above, (+)-CHCD is accepted as an alternative substrate by MenD and the apparent Michaelis constant is 12.0 ± 0.6 μM. Moreover, the potent inhibitor MMSP exhibited reversible, competitive inhibition with respect to 2-KG in the MenD-catalyzed reaction of CHCD (Figure 3.24). These findings enable the use of MMSP as a mechanistic probe to investigate the kinetic mechanism of the reaction (refer to Table 1.1). Plausibly, the MenD-catalyzed reaction of CHCD should share the exact reaction

mechanism as the ISC-utilizing reaction. Thus, the results of kinetic mechanism probed by MMSP for CHCD-utilizing reaction can be assumed to represent the naturally occurring MenD reaction.

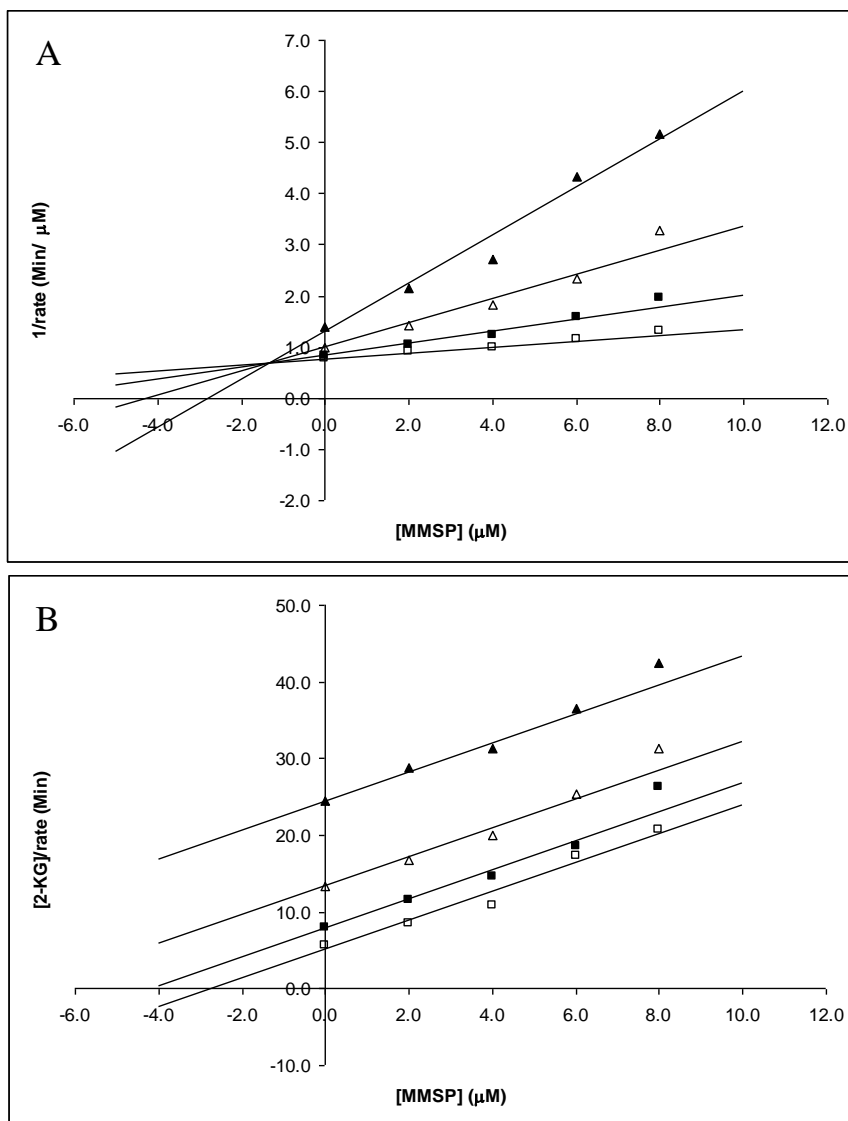


Figure 3.24: Graphic determination of MMSP inhibition with respect to 2-KG in the MenD-catalyzed reaction of CHCD. (A) Dixon plot (1/rate vs. [MMSP]); (B) Cornish-Bowden plot ([2-KG]/rate vs. [MMSP]). The reaction rate was determined with 60 nM MenD, 100 mM Tris (pH 7.4), 5 mM MgCl₂, 50 μM ThDP and 50 μM (+)-CHCD (100μM (±)-CHCD). [2-KG] was at 4 μM (▲), 8 μM (△), 16 μM (■), 32 μM (□).

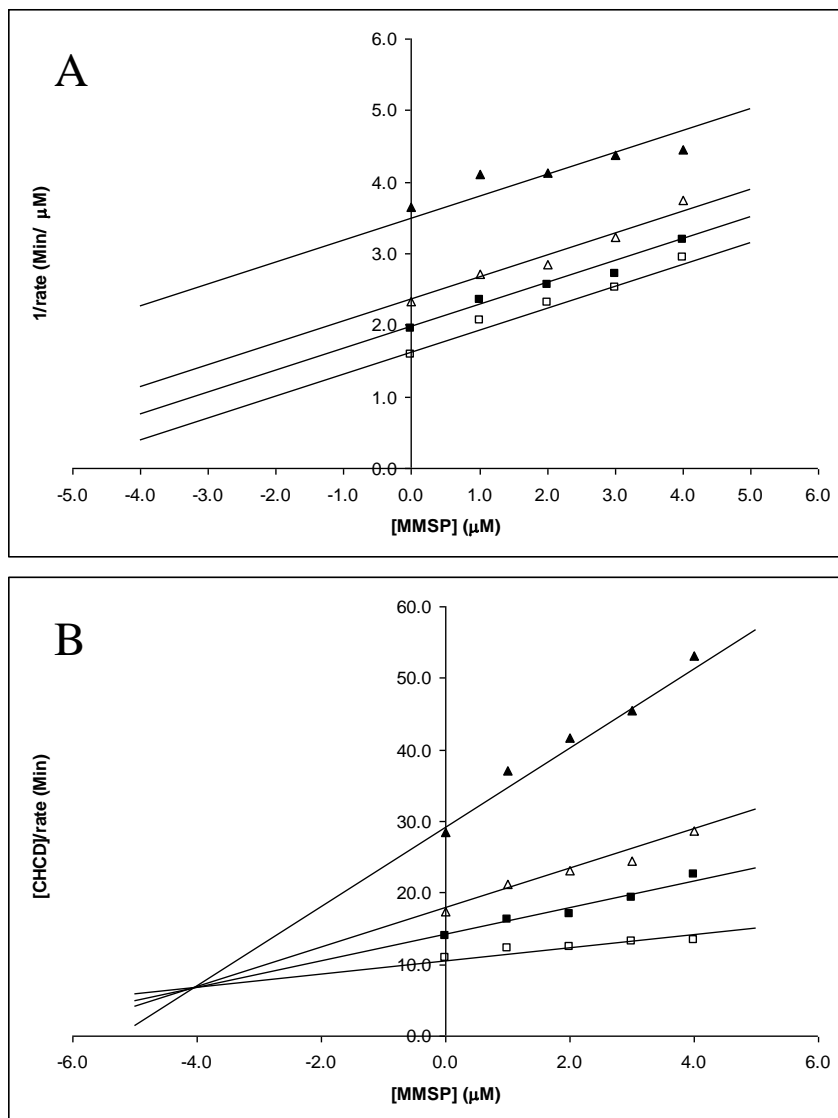


Figure 3.25: Graphic determination of MMSP inhibition with respect to CHCD in the MenD-catalyzed reaction of CHCD. Reaction conditions refer to **2.2.12**. (A) Dixon plot (1/rate vs. [MMSP]); (B) Cornish-Bowden plot ([CHCD]/rate vs. [MMSP]) for MenD reaction with CHCD as substrate. [2-KG] was fixed at 6 μM and [CHCD] was at 3 μM (\blacktriangle), 6 μM (\triangle), 9 μM (\blacksquare), 18 μM (\square).

Following this idea, [2-KG] was fixed at 6 μM and [(+)-CHCD] was varied around its Michaelis constant, and the MenD reaction was determined kinetically in the presence of MMSP. As indicated in Figure 3.24, MMSP was determined graphically as a

reversible, competitive inhibitor with respect to 2-KG, while the pattern of Dixon plot and Cornish-Bowden plot in Figure 3.25 showed that MMSP is an uncompetitive inhibitor ($K_{iu} = 4.1 \pm 0.3 \mu\text{M}$) with respect to CHCD (refer to section 1.8). Given that 2-KG was proposed bind first, the results agree with the pattern for ping-pong bi bi reaction, as suggested by Segel (Table 1.1)⁶⁷.

Encouraged from the application of MMSP in probing the kinetic mechanism of MenD, it was certainly expected that this compound will gain great attention in studies of 2-KG-utilizing enzymes, especially ThDP-dependent ones, as widely used as methyl acetylphosphonate (MAP).

In summary, for the first time, the kinetic mechanism of the MenD reaction was demonstrated to be ping-pong bi bi, by two different approaches. This conclusion is an important step towards elucidation of the MenD reaction mechanism.

3.12 Kinetic analysis of MenD and mutants

In order to investigate catalytically important residues in the active site of MenD, 14 mutants (S32A, S32D, R33K, R33Q, E55D, R107K, Q118E, K292Q, R293K, S391A, R395A, R395K, R413K, and I418L) were designed based on sequence alignment and structural analogy between MenD and homologous enzymes. The potential functions of these mutants were already briefly reviewed and predicted in section 1.5. Activity assays of these mutants and comparison of their kinetic parameters with that of the wild type MenD were expected to be informative for elucidation of the interaction between substrate, cofactors and active site.

At first, the MenD-catalyzed reaction was assayed using ISC as substrate (Table 3.3). The K_m^a of ISC was so small that the measurement of UV absorbance at [ISC] varied around K_m^a became effectively impossible due to the low signal noise ratio, i.e. the saturation curve of ISC could not be obtained. Therefore, K_m^a of ISC was denoted as < 2 μM in Table 3.3. For the same reason, k_{cat}^a of ISC was not determined and k_{cat}^a / K_m^a was denoted as $> 9 \text{ min}^{-1} \cdot \mu\text{M}^{-1}$.

Table 3.3: Kinetic constants of wt-MenD. ND: not determined.

Enzymes	Substrate	K_m^a (μM)	k_{cat}^a (Min^{-1})	k_{cat}^a / K_m^a ($\text{Min}^{-1} \cdot \mu\text{M}^{-1}$)
Wt-MenD	2-KG	9.9 ± 0.6	17 ± 2	1.7 ± 0.1
	ThDP	8 ± 1		2.13 ± 0.02
	MgCl_2	44.4 ± 0.3		0.38 ± 0.04
	ISC	< 2	ND	> 9
	(+)-CHCD	12.0 ± 0.6	25 ± 1	2.08 ± 0.02

When (+)-CHCD was used as an alternative substrate for the MenD-catalyzed reaction instead of ISC, steady-state kinetics can be readily determined using a continuous assay. It was found that the k_{cat}^a of the MenD-catalyzed reaction of CHCD is higher than that of the ISC-utilizing reaction, but the catalytic specificity k_{cat}^a / K_m^a is appreciably lower.

All the mutants (S32A, S32D, R33K, R33Q, E55D, R107K, Q118E, K292Q, R293K, S391A, R395A, R395K, R413K, and I418L) were assayed using ISC and CHCD as wild type MenD. The results and discussion of the kinetics are as follows.

3.12.1 Residues interacting with ThDP

Table 3.4: Kinetic constants of I418L, E55D and S391A. ND: not determined.

Enzymes	Substrate	K_m^a (μM)	k_{cat}^a (Min^{-1})	k_{cat}^a / K_m^a ($\text{Min}^{-1} \cdot \mu\text{M}^{-1}$)
I418L	2-KG	200 ± 30	12.5 ± 0.7	0.063 ± 0.006
	ThDP	600 ± 100		0.021 ± 0.002
	MgCl ₂	400 ± 80		0.031 ± 0.005
	ISC	< 2	ND	> 6
	(+)-CHCD	27 ± 3	23 ± 1	0.85 ± 0.06
E55D	2-KG	12 ± 2	12.8 ± 0.7	1.1 ± 0.1
	ThDP	24 ± 4		0.53 ± 0.06
	MgCl ₂	8 ± 2		1.6 ± 0.3
	ISC	< 2	ND	> 6
	(+)-CHCD	2.5 ± 0.5	22 ± 1	9 ± 1
S391A	2-KG	13 ± 1	17.6 ± 0.5	1.35 ± 0.07
	ThDP	17 ± 1		1.04 ± 0.03
	MgCl ₂	13 ± 2		1.4 ± 0.2
	ISC	< 2	ND	> 9
	(+)-CHCD	36 ± 3	12.5 ± 0.5	0.35 ± 0.02

As is well known for ThDP-dependent enzymes, tautomerization and ionization of ThDP occurs by a conserved mechanism^{18,21}. Enzyme-bound ThDP is commonly oriented to the unfavored V-shape conformation with the aid of active site residues so as to facilitate proximity of 4'-NH₂ and C2-H (Figure 1.12). Frank *et al.*³⁶ reported that residue I415 in PDC from *S. cerevisiae* located under ThDP and substitutions to methionine or leucine caused a great reduction in the k_{cat}^a value. Computational studies further indicated the large side chain of I415 reduces the flexibility of ThDP. For this purpose, methionine is used in ThDP-dependent POX and leucine is used in transketolase.

As shown in Figure 1.11, residue I418 in MenD is located near ThDP with its uncharged side chain inserting between the aminopyrimidine ring and the thiazolium ring. It was therefore predicted that I418 in MenD plays the same role as I415 in PDC. Therefore, mutant I418L was prepared and assayed (Table 3.4). Changing this isoleucine to leucine caused a 20-fold decrease in K_m^a of 2-KG, a 10-fold in K_m^a of Mg^{2+} and a 75-fold in K_m^a of ThDP. Unlike the only ca. 3% residual activity observed for PDC I415L³⁶, MenD I418L exhibited very close activity in both cases of the ISC-utilizing and CHCD-utilizing MenD reactions when compared to wild type. The observation that catalytic specificity of ThDP was lowered up to 100-fold strongly supports that this highly conserved residue is important for cofactor binding and activation in MenD, as expected. Since I418 was considered an important residue assisting V-conformation of ThDP in facilitation of C2-H proton abstraction, kinetic results that K_m^a of CHCD was almost unchanged and mutant activity was only slightly reduced imply that ThDP activation or aminopyridine proton relay should not be rate-limiting and is independent of binding and turnover of the second substrate. In the future, systematic substitution of I418 in MenD, for instance, to valine, alanine and glycine, may provide more information to understand its role in catalysis.

Before the solved MenD structure was reported, the glutamate residue (E55) was predicted to be important for highly conserved glutamate-aided tautomerization in ThDP-dependent enzymes¹⁴. In our lab, E55Q was found to be essentially inactive as assayed by SHCHC formation. In the widely accepted mechanism for ThDP activation, it is the glutamic acid that interacts with N1' of aminopyrimidine giving rise to abstraction of the C2-H proton³⁷. Herein, MenD E55D was designed to investigate the function of this

residue (Table 3.4). The conservative exchange of glutamate to aspartate that has been used for several different ThDP-dependent enzymes is advantageous over activity-abolishing mutation, as indicated by Tittmann *et al.*, by which the differences of pK_a and distance may shed light on individual catalytic steps⁸⁹. Unlike the significant reduction of catalytic activity observed for IPDC E52D mutant⁸⁹, mutant E55D showed only slightly reduced activity, but the catalytic specificity of ThDP is 4-fold smaller. This result supports the proposed role of E55 in the activation with ThDP. However, the catalytic specificity of Mg^{2+} is also 4-fold smaller, implying that the disturbance of the interaction with ThDP also affects the binding of Mg^{2+} . Furthermore, it appears that the role of residue E55 solely focuses on ThDP binding, since the kinetic constants with respect to 2-KG, ISC or CHCD are virtually unchanged.

Although a structural comparison indicated that S391 of MenD is analogous to H260 of homologous ThDP-dependent 2-KG dehydrogenase E1 subunit from *E. coli* (KGDH E1)⁸⁸, quite different functions were proposed for the two residues. H260 in KGDH E1 has potential recognition with the distal carboxylate (i.e. 4-carboxylate of 2-KG). In contrast, the hydroxyl of S391 in MenD is within hydrogen bonding distance of the diphosphate and sulfur atom of ThDP. MenD mutant S391A has activity comparable to wild type and the mutation exhibits little influence on kinetic constants (Table 3.4). Similar to S32A (discussed below), mutant S391A may also play a structural role dependent on the backbone amide, or a water molecule may act to rescue the function of the deleted hydroxyl group⁸⁸.

3.12.2 Residues interacting with 2-KG-ThDP adduct

Table 3.5: Kinetic constants of S32A, S32D and Q118E. ND: not determined; a, the kinetic parameters were derived from Hanes-Woolf equation plot.

Enzymes	Substrate	K_m^a (μM)	k_{cat}^a (Min^{-1})	k_{cat}^a / K_m^a ($\text{Min}^{-1} \cdot \mu\text{M}^{-1}$)
S32A	2-KG	9.92 ± 0.08	13.6 ± 0.3	1.37 ± 0.02
	ThDP	4.3 ± 0.3		3.2 ± 0.2
	MgCl_2	80 ± 10		0.17 ± 0.02
	ISC	< 2	ND	> 7
	(+)-CHCD	42 ± 2	14.5 ± 0.5	0.35 ± 0.01
S32D	2-KG	ND	ND	ND
	ThDP	ND	ND	ND
	MgCl_2	ND	ND	ND
	ISC ^a	263	2.5	0.0095
	(+)-CHCD	No (or trace) activity		
Q118E	No activity			

In analogy to S26 in BFDC, S32 in MenD was in our lab predicted as catalytically important residue by sequence alignment⁴¹. Later, the solved structures of BFDC with (R)-mandelate and methyl benzoylphosphonate (MBP) were published^{42,52,53}. Commonly, S26 in BFDC was found to form potential hydrogen bonds to the carboxylate anion of mandelate and the phosphonate moiety of the ThDP-MBP adduct with its main chain and side chains. Notably, benzoylphosphonic acid was proved to covalently modify S26 by phosphorylation in BFDC⁴³. These studies indicated clearly that S26 is found near the 1-carboxylate of benzoylformate (the leaving group⁸⁷) in BFDC. The X-ray structure of MenD with a 2-KG-ThDP adduct has not been published yet, but S32 in MenD seems to occupy a similar position to S26 in BFDC. Therefore, MenD S32A and S32D were designed to test the importance of this residue (Table 3.5).

S32A showed slightly reduced catalytic activity with almost unchanged catalytic specificity with respect to 2-KG, ThDP and Mg^{2+} , whereas the catalytic specificity towards (+)-CHCD was lowered ca. 6-fold with the Michaelis constant increasing approximately 4-fold. The results suggest that the removal of S32 hydroxyl is tolerated in MenD, although it affects CHCD binding. The tolerance of a hydrophobic amino acid at the S26 position in BFDC was also observed, but to a lesser extent, in extensive mutagenesis experiments⁹⁰. Maybe ISC binding is also compromised although steady-state kinetics failed to demonstrate it due to the extremely small Michaelis constant of ISC.

However, MenD S32D showed significant alteration of kinetic constants when compared to wild type MenD. The Michaelis constant of ISC drastically increased to 263 μ M from less than 2 μ M for the wild type MenD so that catalytic specificity towards ISC decreased at least 10^4 times; catalytic activity of this mutant decreased to ca. 15% of wild type, while no activity was detected when CHCD was used. For this mutant, because the extremely high saturating values of ISC have an absorbance beyond the limit of the spectrophotometer, a kinetic assay determining UV absorbance at full range of concentrations of ISC could not be conducted experimentally. Therefore, the kinetic constants of 2-KG, ThDP and Mg^{2+} were not determined, and the Michaelis constant of ISC was estimated by Hanes-Woolf plot (refer to section **1.8**). As a result, substitution of the neutral hydroxyl group to a carboxylic acid substantially impaired enzymatic turnover of MenD, maybe by sharply weakening the binding affinity of ISC and CHCD.

The steady-state kinetic analysis of both mutants S32A and S32D showed effects on the interaction with ISC or CHCD. This appears very different from the well-accepted

assignments of the role of S26 in BFDC, where S26 was found to use its side chain hydroxyl and backbone to interact with 1-carboxylate anion of ThDP-substrate adduct^{42,43,52,53}. A plausible explanation is that in MenD, S32 plays a role mainly using the backbone amide. Due to its proximity to the catalytic center, substitution of hydroxyl with carboxylate essentially interferes with subsequent carbonylation between the incipient enamine/carbanion and ISC, or carboxylate anion of mutant S32D is structurally incompatible with ISC which bears negative charges.

Q118 in MenD was speculated as the counterpart to H70 in BFDC and Q113 in BAL^{30,52}. Those two residues were both revealed in X-ray structures to interact with C2 α -OH of ThDP adduct intermediate. In addition, Q113 in BAL participates in stabilization of 1-carboxylate of ThDP adduct via a water molecule. Furthermore, Q112 in POX and H473 in TK are analogous to the residues of BFDC and BAL⁸⁷. The side chain of glutamine can be either a hydrogen bond acceptor or donor. It was pointed out that the exchangeable properties of thiazolium-proximal glutamine and histidine in the context suggest that they are hydrogen bond acceptors rather than acid-base residues^{30,91}. In the family of 2-keto acid-utilizing ThDP-dependent enzymes, addition of the ThDP nucleophilic carbene to the 2-keto group and formation of an enamine/carbanion intermediate is the universally conserved mechanism. Therefore, stabilizing the incipient addition product is supposed to be critical to subsequent catalytic steps. Unlike residues for substrate or cofactor binding as discussed above, Q118 in MenD, similar to its counterparts such as histidine in BFDC or TK and glutamine in BAL or POX, is predicted to have a large impact on enzymatic activity. It was found that substitution of Q118 to glutamate was catastrophic for MenD activity. This supports the proposal that

Q118 may play multifaceted roles such as orientation of 2-KG, the tetrahedral 2-KG-ThDP adduct intermediate and even post-decarboxylation enamine/carbanion. In the future, systematic mutagenesis study of this residue, e.g. Q118A and Q118N etc, would certainly provide more information for elucidation of this critically important residue.

3.12.3 Residues interacting with ISC

According to the model proposed by Hunter *et al.* of MenD with bound substrates (2-KG and ISC) (Figure 1.13), several basic residues (Arg33, Arg107, Lys292, Arg293, Arg395 and Arg413) surround the acidic side of ISC, consisting of two carboxylate anions and a hydroxyl, while the hydrophobic side of ISC is accommodated by a hydrophobic patch created by Ile474, Phe475 and Leu478 (Figure 1.13)³¹. These basic residues may also interact with other acidic species such as 2-KG or ThDP. Therefore, in order to confirm the model and provide insight into the roles these residues play in active site of MenD, mutants R33K, R33Q, R107K, K293Q, R293K, R395A, R395K and R413K were prepared and assayed kinetically. In summary, conservative exchanges as R33K, R107K and R395K result in significantly larger Michaelis constants of ISC up to measurable values (Table 3.6), while K292Q, R293K and R413K show little effect on that of ISC and CHCD. Commonly, these mutants exhibit unchanged or slightly reduced activity.

R33 of MenD seems to be a more important residue for binding preference of ISC in that mutant R33K and R33Q show trace activity and ca. 10% residual activity by CHCD assays, respectively (Table 3.6). In Hunter's model, R33 is predicted to interact with the enolpyruvyl chain of ISC, where CHCD possesses a more flexible carboxymethyl

moiety lacking planar conjugation. Presumably R33 participates in orienting the enolpyruvyl chain of ISC to facilitate enamine/carbanion's attack to ISC.

Table 3.6: Kinetic constants of R33K, R33Q, R107K, R395A and R395K. ND: not determined; a, the kinetic parameters were derived from Hanes-Woolf equation plot; b, EDTA abolished the activity.

Enzymes	Substrate	K_m^a (μM)	k_{cat}^a (Min^{-1})	k_{cat}^a / K_m^a ($\text{Min}^{-1} \cdot \mu\text{M}^{-1}$)
R33K	2-KG	ND	ND	ND
	ThDP	ND	ND	ND
	MgCl ₂	ND	ND	ND
	ISC ^a	135	6.3	0.047
	(+)-CHCD	No (or trace) activity		
R33Q	2-KG	ND	ND	ND
	ThDP	ND	ND	ND
	MgCl ₂	ND	ND	ND
	ISC ^a	54	7.3	0.14
	(+)-CHCD ^a	434	2.4	0.0055
R107K	2-KG	5.3 ± 0.9	10.4 ± 0.4	2.0 ± 0.3
	ThDP	4.8 ± 0.7		2.2 ± 0.2
	MgCl ₂	49 ± 8		0.21 ± 0.03
	ISC	7.5 ± 0.5		1.39 ± 0.04
	(+)-CHCD ^a	91	7.1	0.078
R395A	2-KG	ND	ND	ND
	ThDP	ND	ND	ND
	MgCl ₂	ND	ND	ND
	ISC ^a	36	2.55	0.07
	(+)-CHCD ^a	393	2.4	0.006
R395K	2-KG	45 ± 3	7.9 ± 0.3	0.18 ± 0.01
	ThDP	2.2 ± 0.2		3.6 ± 0.2
	MgCl ₂ ^b	< 2		> 4
	ISC ^a	5.3 ± 0.9	ND	1.5 ± 0.2
	(+)-CHCD ^a	109	10.9	0.10

According to Hunter's model, R395 is in proximity to unsaturated carboxylate and hydroxyl of bound ISC. Mutagenesis study of R395 for MenD is similar to that of R33 (Table 3.6). Nonconservative mutant R395A has relatively lower activity than mutant R395K, suggesting that residue R395 has acid-base interaction with ISC. The two mutants exhibit greatly increased Michaelis constant with respect to ISC, reminding us the potential role that R395 may play in active site of MenD as a residue responsible for recognition of ISC, in addition to R33.

Table 3.7: Kinetic constants of K292Q, R293K. ND: not determined; a, the kinetic parameters were derived from Hanes-Woolf equation plot; b, EDTA abolished the activity.

Enzymes	Substrate	K_m^a (μM)	k_{cat}^a (Min^{-1})	k_{cat}^a / K_m^a ($\text{Min}^{-1} \cdot \mu\text{M}^{-1}$)
K292Q	2-KG	2.6 ± 0.3	11.9 ± 0.3	4.6 ± 0.4
	ThDP	2.0 ± 0.2		6.0 ± 0.4
	MgCl_2^b	2.6 ± 0.7		5 ± 1
	ISC	< 2	ND	> 6
	(+)-CHCD	50 ± 1	17.2 ± 0.2	0.34 ± 0.01
R293K	2-KG	9.1 ± 0.8	18 ± 1	1.98 ± 0.06
	ThDP	4.7 ± 0.3		3.83 ± 0.03
	MgCl_2	200 ± 100		0.09 ± 0.04
	ISC	< 2	ND	> 9
	(+)-CHCD	4.2 ± 0.7	24 ± 1	5.7 ± 0.7

Relatively, mutant R107K shows only moderate K_m^a increase for ISC and CHCD (Table 3.6). Maybe this is because R107 is not positioned properly to interact with the acidic moieties of ISC as R33 and R395 in MenD active site.

K292 and R293 are more distant from C2 of ThDP (Figure 1.11), so maybe less relevant in substrate binding and catalysis. MenD mutant K292Q and R293K show little

effect on activity, but puzzlingly alter Michaelis constants towards Mg^{2+} significantly (Table 3.7). In the case of K292Q, an extremely low Michaelis constant of Mg^{2+} was observed even with dialyzed mutant enzyme, whereas the Mg^{2+} -dependent activity was abolished by EDTA. The same phenomenon was also found in the assay of mutant R395K.

3.12.4 Residues interacting with 2-KG

Table 3.8: Kinetic constants of R413K. ND: not determined.

Enzymes	Substrate	K_m^a (μM)	k_{cat}^a (Min^{-1})	k_{cat}^a / K_m^a ($Min^{-1} \cdot \mu M^{-1}$)
R413K	2-KG	220 ± 40	6.1 ± 0.3	0.028 ± 0.004
	ThDP	5 ± 1		1.2 ± 0.2
	$MgCl_2$	10 ± 2		0.61 ± 0.09
	ISC	< 2	ND	> 3
	(+)-CHCD	10 ± 1	10.0 ± 0.2	1.0 ± 0.1

Interestingly, MenD mutant R413K exhibits an apparent change of the kinetic constant of 2-KG exclusively among the basic mutants discussed (Table 3.8). Compared with wild type MenD, the Michaelis constant with respect to 2-KG increases 20-fold, accompanying a ca. 60-fold reduction of catalytic specificity. This result supports that R413 is responsible for binding to 2-KG or a 2-KG derived intermediate. In Hunter's model, R413 seems to be oriented to such a conformation by which its guanidine group is able to potentially interact with either 2-KG or ISC. However, binding affinity of CHCD (K_m^a) is same as for wild type MenD, and the K_m^a of ISC remains very small. Therefore, R413 is identified as a residue interacting specifically with 2-KG, and is distinguished from other arginines discussed above.

Overall, the kinetic study of 14 mutants revealed constructive information for assignments of the roles of active site residues. Undoubtedly, X-ray structures of MenD with a trapped 2-KG-ThDP adduct intermediate or phosphonate analogue will clarify these hypotheses and delineate a more accurate map of active site residues in catalytic process. Based on combined knowledge learned from other extensive studies of ThDP-dependent enzymes and kinetic analysis of MenD mutants herein, a diagram of binding mode for bound tetrahedral adduct intermediate and binding pocket of ISC can be putatively described as Figure 3.26.

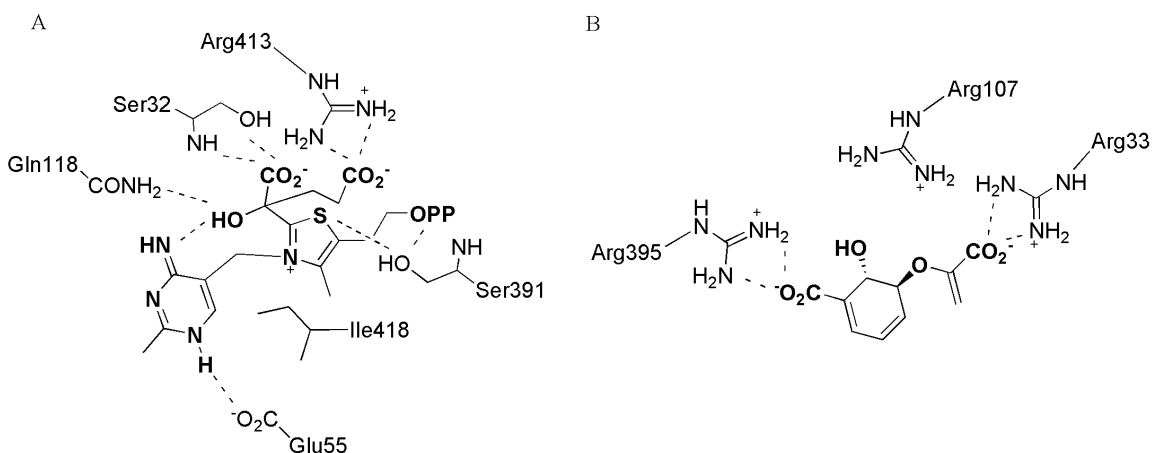


Figure 3.26: Proposed diagram of active site of MenD. (A) Binding mode for bound tetrahedral ThDP intermediate; (B) binding pocket of ISC.

3.13 A recent report of a mutagenesis study of *B. subtilis* MenD

On June 18, 2010, an online report (doi:10.1016/j.jmb.2010.06.025) about *B. subtilis* MenD (*BsMenD*) in the Journal of Molecular Biology appeared. In the paper, the medium-resolution X-ray structure of *B. subtilis* MenD with ThDP and Mn²⁺ was

reported, and a mutagenesis study of eight active site residues, such as R32, R106, K299, R409, R428, I489, F490 and L493, was performed.

The sequence alignment of *EcMenD* and *BsMenD* demonstrates that, in *EcMenD*, the arginine residues such as R33, R107, R395, R413 are corresponding to R32, R106, R409, R428 respectively. It was indicated that, in *BsMenD*, R409 plays a significant role in binding with 2-KG and ISC, and R428 interacts with 2-KG while R32 and R106 are critical for the recognition of ISC. This is consistent with our findings for the assignment of roles for the four arginine residues in *EcMenD*. As the K292 in *EcMenD*, K299 in *BsMenD* showed little influence on the reaction. R293 in *EcMenD* is not conserved in *BsMenD* and our mutagenesis study showed that this residue has little influence too.

In our project, the roles of the residues in *EcMenD*, which are corresponding to I489, F490 and L493 in *BsMenD*, were not explored by mutagenesis study, but it is predicted that the conserved I474, F475 and L478 in *EcMenD* may play the same roles in the binding of ISC and the stabilization of ThDP.

4. CONCLUSIONS

The main goal of this thesis was to elucidate the mechanism of the MenD-catalyzed reaction. MenD, a member of the ThDP-dependent enzyme superfamily, catalyzes the formation of SEPHCHC from ISC and 2-KG. MenD is currently annotated as SEPHCHC synthase after being called SHCHC synthase for many years.

At first, the steady-state assay method was evaluated by spectrophotometric measurement and HPLC analysis. It was proved that the rate isochorismate consumption in the MenD-catalyzed reaction can be determined by measuring the UV absorbance change at 278 nm or 300 nm.

Once the assay method was validated, the steady-state kinetic parameters of the MenD-catalyzed reaction were determined and other kinetic studies on this enzyme became possible. In order to find mechanistic probes to investigate MenD catalysis, phosphonate analogues of 2-KG were synthesized. It was found that the succinyl phosphonate analogues are potent competitive inhibitors against MenD with varied inhibition constants, but 2-hydroxyphosphonate analogues failed to inhibit MenD.

Racemic CHCD and CHCDMe, the structural analogues of ISC, were synthesized and tested for the MenD reaction. (+)-CHCD was found to be the alternative substrate, whereas (-)-CHCD is not accepted by MenD and does not inhibit MenD; CCHC was isolated and the structure was determined, supporting that the compound is derived from CHCD turnover product. CHCDMe was not accepted by MenD.

The kinetic mechanism of the MenD-catalyzed reaction was explored by two different approaches. The double reciprocal plot of the CHCD-utilizing MenD reaction appeared as a parallel set of lines, suggesting a ping pong bi bi mechanism. Alternatively, the CHCD-utilizing MenD reaction was probed by phosphonate analogue MMSP. MMSP exhibited competitive inhibition with respect to 2-KG ($K_{ic} = 1.3 \pm 0.1 \mu\text{M}$) and uncompetitive inhibition with respect to CHCD ($K_{iu} = 4.1 \pm 0.3 \mu\text{M}$). These inhibition patterns against 2-KG and CHCD also support the conclusion of ping pong bi bi mechanism for the MenD-catalyzed reaction.

Kinetic parameters of mutants S32A, S32D, R33K, R33Q, E55D, R107K, Q118E, K292Q, R293K, S391A, R395A, R395K, R413K, and I418L were determined and compared with that of wild type MenD. Ser32 shows influence on the interaction with ISC or CHCD, except for the predicted role of interacting with 1-carboxylate of ThDP-2-KG adduct. Ile418 is apparently involved in assisting formation of V conformation of ThDP and Glu55 demonstrates the highly conserved role in the activation of ThDP. Ser391 may interact with ThDP via the backbone or a water molecule. Among the basic residues such as Arg33, Arg107, Lys292, Arg293, Arg395 and Arg413, Arg33 seems to interact with the enolpyruvyl side chain of ISC or CHCD and Arg107 is also relevant in the acid-base interaction with ISC or CHCD; Arg395 may mainly interact with the 1-carboxylate anion of ISC or CHCD, whereas Arg413 is likely to recognize 2-KG. As in homologous ThDP-dependent enzymes, the thiazolium-proximal Gln118 plays a very important role in stabilizing ThDP-2-KG adduct by interacting with C2 α -OH. Moreover, this catalytically important residue may have other functions in MenD catalysis.

Relatively, Lys292 and Arg293 show less influence on ISC binding according to the kinetic results.

5. FUTURE WORK

The steady-state kinetic assay of the MenD-catalyzed reaction has been established and several effective mechanistic probes are available, the future work of this project will certainly benefit from these progresses.

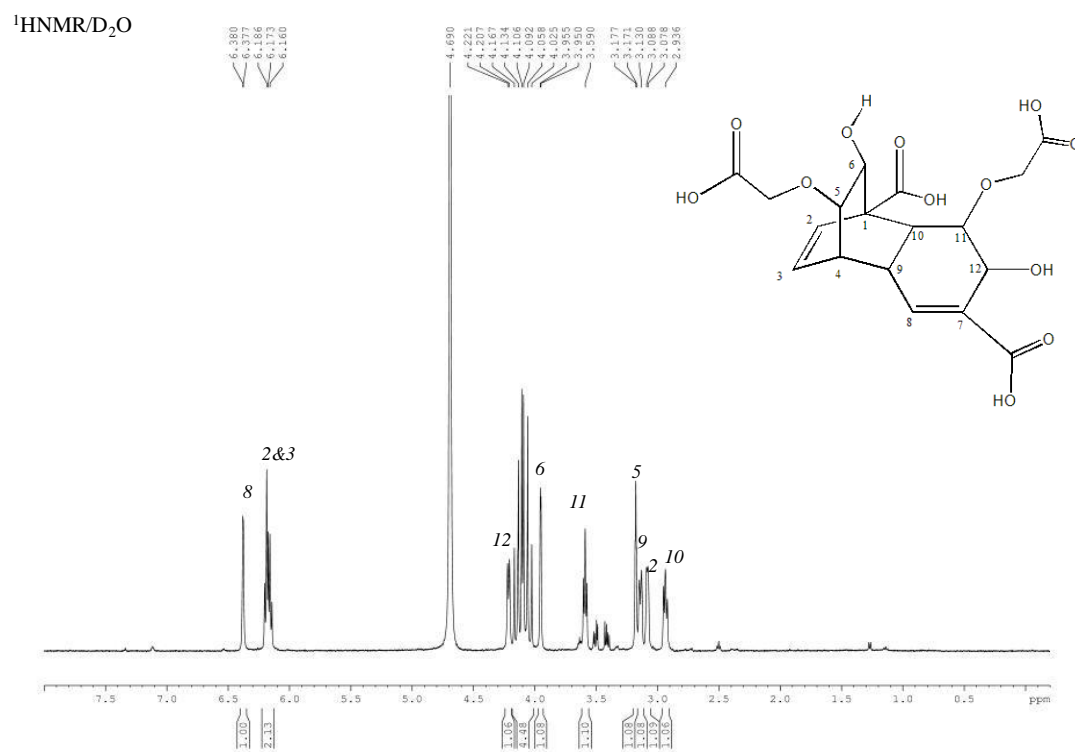
At first, solving X-ray structures of MenD with 2-keto phosphonate analogues or ThDP-phosphonate covalent adducts will certainly provide rich information about the active site and further help the understanding of structure-function relationship in the MenD catalysis. Secondly, the spectroscopic study of ThDP-phosphonate covalent adduct, such as by circular dichroism, will enable the investigation of ThDP activation and probably all ThDP-related intermediates in the catalytic steps.

The syntheses of novel substrate analogues and ThDP covalent complexes with substrates or analogues may develop useful probes for the MenD-catalyzed reaction. The pre-steady-state kinetics and ^1H NMR detection of active intermediates have not been explored and need to be paid attention to. ThDP analogues have been proven to be effective mechanistic probe in the studies of the structures and mechanisms for many ThDP-dependent enzymes, thus the application of ThDP analogues in the MenD reaction will be promising to complement the exploitation of the substrate analogues.

The results of mutations of some active site residues provide useful guidance for a systematic research on the residues of interest or other catalytically important residues in

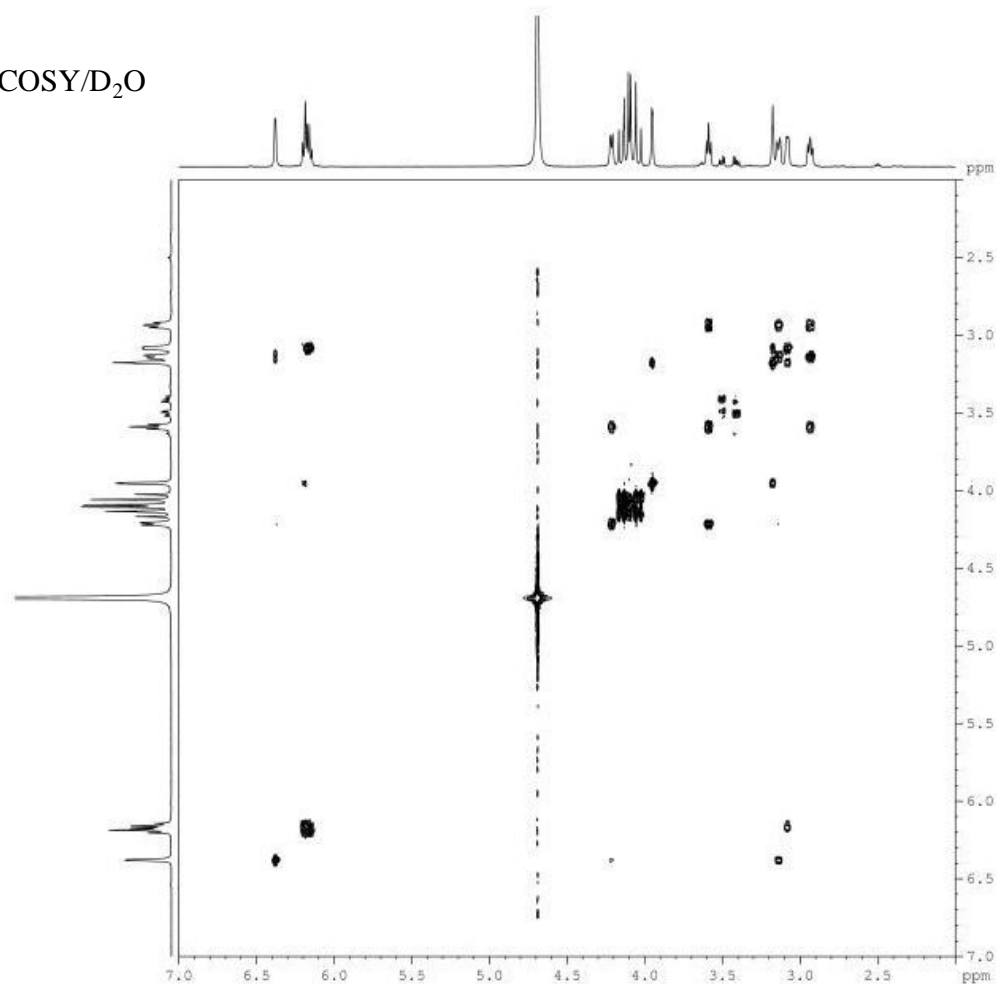
MenD. Moreover, the inhibition studies of 2-KG phosphonate analogues against the mutants likely help identify the catalytic roles of certain residues.

6. APPENDIX



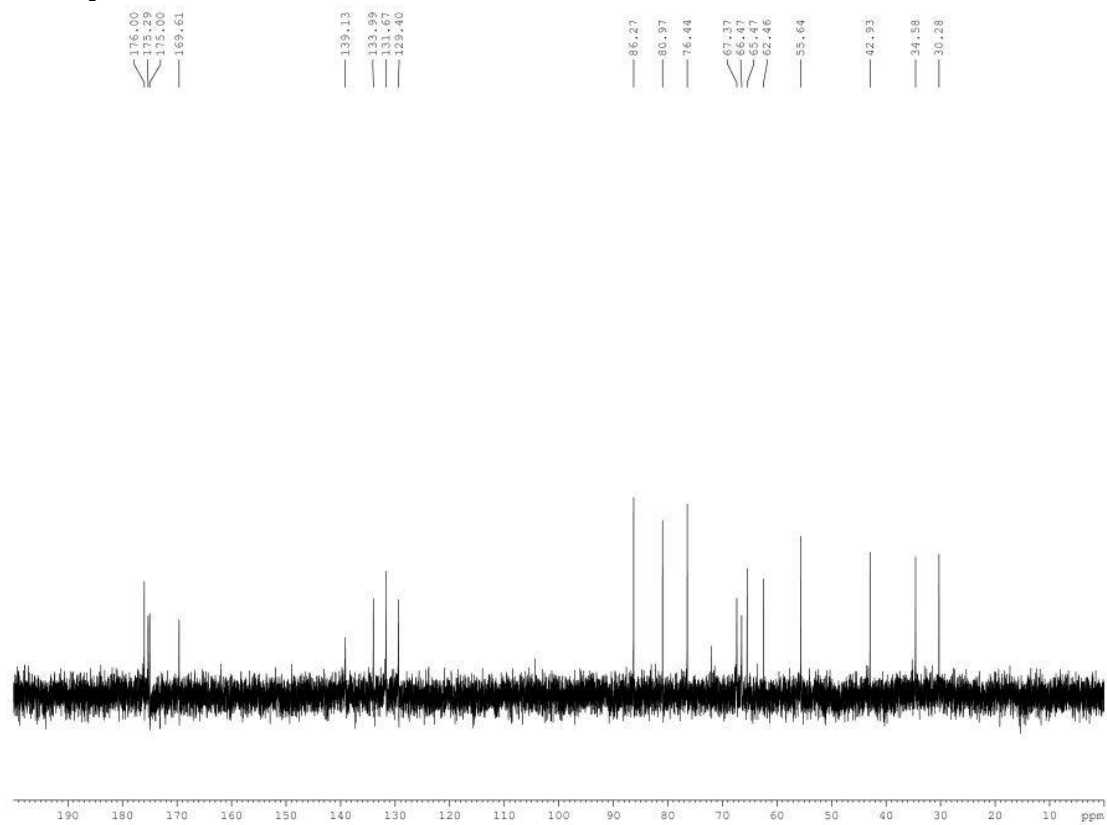
Appendix 1: ¹HNMR of the isolated Diels-Alder product of CHCD (refer to Figure 3.3, fraction at 42.2 min).

H-H COSY/D₂O



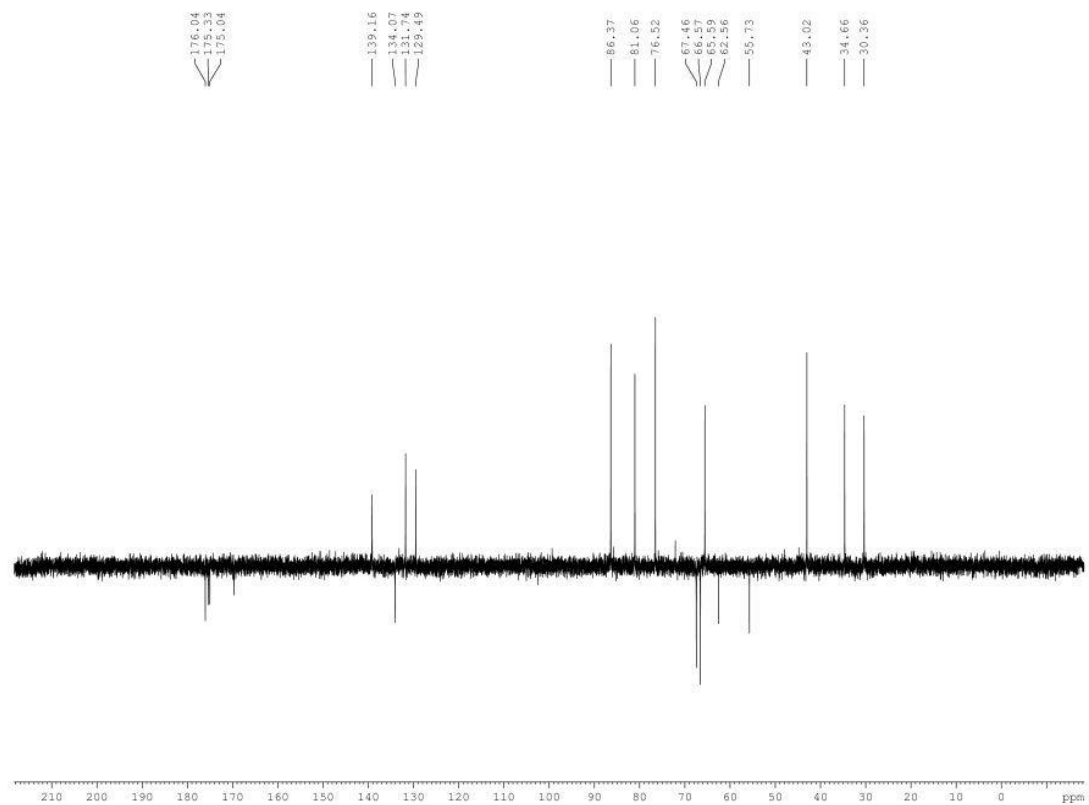
Appendix 2: H-H COSY of the isolated Diels-Alder product of CHCD (refer to Figure 3.3, fraction at 42.2 min).

^{13}C NMR/ D_2O



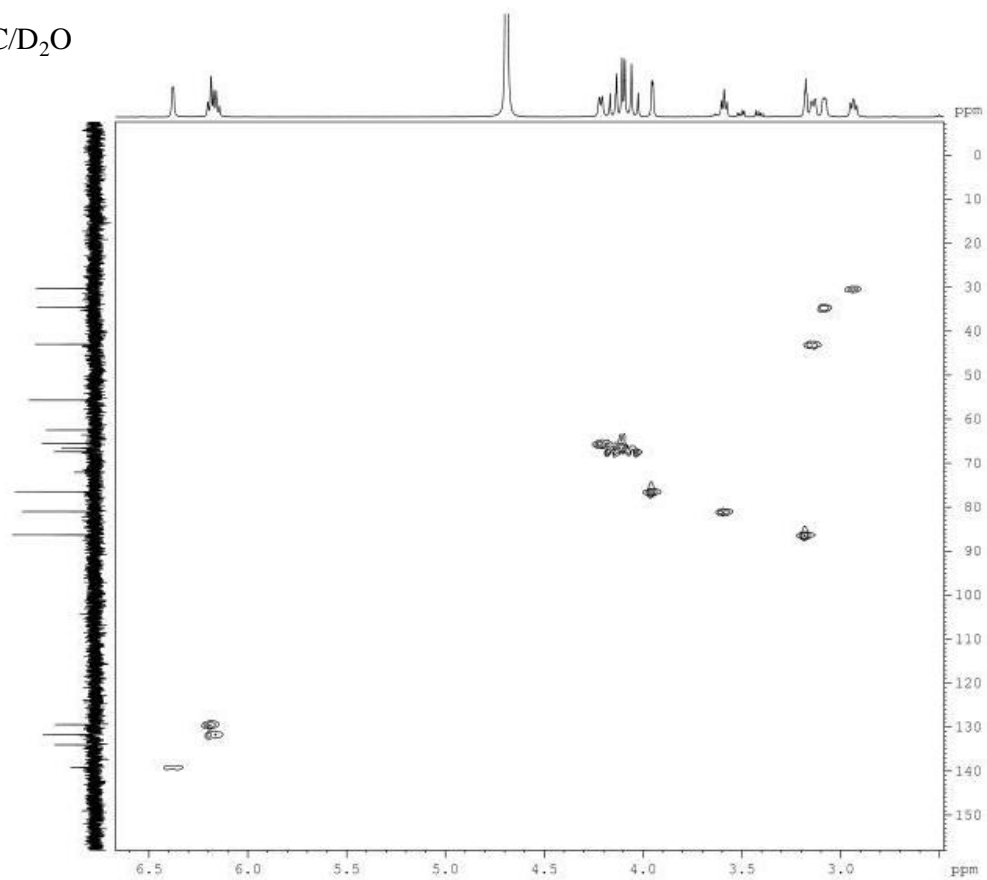
Appendix 3: ^{13}C NMR of the isolated Diels-Alder product of CHCD (refer to Figure 3.3, fraction at 42.2 min).

JMOD-¹³CNMR/D₂O

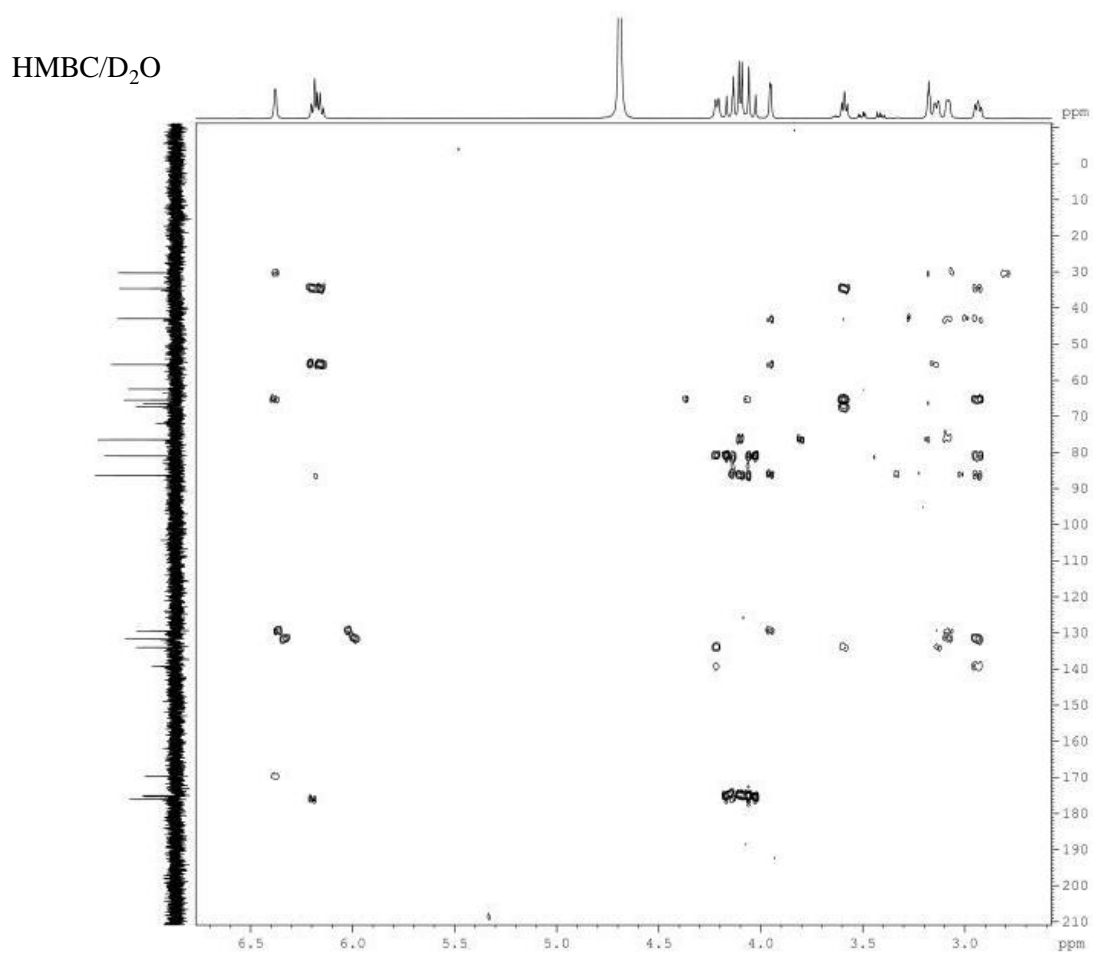


Appendix 4: JMOD-¹³CNMR of the isolated Diels-Alder product of CHCD (refer to Figure 3.3, fraction at 42.2 min).

HMQC/D₂O



Appendix 5: HMQC of of the isolated Diels-Alder product of CHCD (refer to Figure 3.3, fraction at 42.2 min).



Appendix 6: HMBC of of the isolated Diels-Alder product of CHCD (refer to Figure 3.3, fraction at 42.2 min).

7. REFERENCES

- 1 Oldenburg, J., Marinova, M., Müller-Reible, C. and Watzka, M., *Vitam. Horm.* **2008**, 78, 35-62.
- 2 Bentley, R., Meganathan R., *Microbiol. Rev.* **1982**, 46, 241-280.
- 3 Meganathan, R., *Vitam. Horm.* **2001**, 61, 173-218.
- 4 Truglio, J. J., Theis, K., Feng, Y., Gajda, R., Machutta, C., Tonge, P. J. and Kisker, C., *J. Biol. Chem.* **2003**, 278, 42352-42360.
- 5 Jiang, M., Chen, X., Guo, Z., Cao, Y., Chen, M. and Guo, Z., *Biochemistry* **2008**, 47, 3426-3434.
- 6 Jiang, M., Cao, Y., Guo, Z., Chen, M., Chen, X. and Guo, Z., *Biochemistry* **2007**, 46, 10979-10989.
- 7 Seto, H., Jinnai, Y., Hiratruka, T., Fukawa, M., Furihata, K., Itoh, N. and Dairi, T., *J. Am. Chem. Soc.* **2008**, 130, 5614-5615.
- 8 Hiratsuka, T., Furihata, K., Ishikawa, J., Yamashita, H., Itoh, N., Seto H. and Dairi, T., *Science* **2008**, 321, 1670-1673.
- 9 Hiratsuka, T., Itoh, N., Seto H. and Dairi, T., *Biosci. Biotechnol. Biochem.* **2009**, 73, 1137-1141.
- 10 Kurosu, M., Narayanasamy, P., Biswas, K., Dhiman, R. and Crick, D. C., *J. Med. Chem.* **2007**, 50, 3973-3975.
- 11 Lu, X., Zhang, H., Tonge, P. J. and Tan, D., *Bioorg. Med. Chem. Lett.* **2008**, 18, 5936-5966.

- 12 Tian, Y., Suk, D., Cai, F., Crich, D. and Mesecar, A. D., *Biochemistry* **2008**, 47, 12434-12447.
- 13 Emmons, G. T., Campbell, I. M. and Bentley, R., *Biochem. Biophys. Res. Commun.* **1985**, 131, 956-960.
- 14 Bhasin, M., Billinsky, J. L. and Palmer, D. R. J., *Biochemistry* **2003**, 42, 13496-13504.
- 15 Jiang, M., Chen, M., Cao, Y., Yang, Y., Sze, K. Chen, X. and Guo, Z., *Org. Lett.* **2007**, 9, 4765-4767.
- 16 Marley, M. G., Meganathan, R. and Bentley, R., *Biochemistry* **1986**, 25, 1304-1307.
- 17 Meganathan, R., *J. Biol. Chem.* **1981**, 256, 9386-9388.
- 18 Jordan, F., *Nat. Prod. Rep.* **2003**, 20, 184-201.
- 19 Ugai, T., Tanaka, S. and Dokawa, S., *J. Pharm. Soc. Jpn.* **1943**, 63, 269.
- 20 Breslow, R., *J. Am. Chem. Soc.* **1958**, 80, 3719-3726.
- 21 Kluger, R., and Tittmann, K., *Chem. Rev.* **2008**, 108, 1797-1833.
- 22 Tittmann, K., *FEBS J.* **2009**, 276, 2431.
- 23 Jordan, F., Nemeria, N. S., Zhang, S., Yan, Y., Arjunan, P. and Furey, W., *J. Am. Chem. Soc.* **2003**, 125, 12732-12738.
- 24 Nemeria N., Baykal, A., Josheph, E., Zhang, S., Yan, Y., Furey, W. and Jordan, F., *Biochemistry* **2004**, 43, 6565-6575.
- 25 Nemeria, N., Chakraborty, S., Baykal, A., Korotchkina, L. G., Patel, M. S. and Jordan, F., *Proc. Natl. Acad. Sci. USA.* **2007**, 104, 78-82.
- 26 Stetter, H., *Angew. Chem., Int. Ed. Engl.* **1976**, 15, 639.
- 27 Stetter, H., *Synthesis* **1977**, 1977, 403.

- 28 Myers, M. C., Bharadwaj, A. R., Milgram, B. C. and Scheidt, K. A., *J. Am. Chem. Soc.* **2005**, 127, 14675-14680.
- 29 Nemeria N. S., Chakraborty, S., Balakrishnan, A. and Jordan, F., *FEBS J* **2009**, 276, 2432-2446.
- 30 Frank, R. A. W., Leeper, F. L. and Luisi, B. F., *Cell. Mol. Life Sci.* **2007**, 64, 892-905.
- 31 Dawson, A., Fyfe, P. K. and Hunter, W. N., *J. Mol. Biol.* **2008**, 384, 1353-68.
- 32 Duggleby, R. G., *Acc. Chem. Res.* **2006**, 39, 550-557.
- 33 Priyadarshi, A., Saleem Y., Nam, K., Kim, K., Park, S., Kim, E. and Hwang, K., *Biochem. Biophys. Res. Commun.* **2009**, 380, 797-801.
- 34 Bhasin, M. A kinetic study of the reaction catalyzed by 2-succinyl-6-hydroxyl-2,4-cyclohexadiene-1-carboxylate synthase from *Escherichia coli.*, University of Saskatchewan, 2005.
- 35 Hawkins, C. F., Borges, A., Perham, R. N., *FEBS Lett.* **1989**, 255, 77-82.
- 36 Guo, F., Zhang, D., Kahyaoglu, A., Farid, R. S. and Frank, J., *Biochemistry* **1998**, 37, 13379-13391.
- 37 Shaanan, B., and Chipman, D. M., *FEBS J.* **2009**, 276, 2447-2453.
- 38 Kaplun, A., Binshtein, E., Vyazmensky, M., Steinmetz, A., Barak, Z., Chipman, D. M., Tittmann, K. and Shaanan, B., *Nat. Chem. Biol.* **2008**, 4, 113-118.
- 39 Brandt, G. S., Nemeria, N., Chakraborty, S., McLeish, M. J., Yep, A., Kenyon, G. L., Petsko, G. A., Jordan, F. and Ringe, D., *Biochemistry* **2008**, 47, 7734-7743.
- 40 Caines, M. E., Elkins, J. M., Hewitson, K. S. and Schofield, C. J., *J. Biol. Chem.* **279**, 7, 5685-5692.

- 41 Macova, A. Structure-function relationship of the enzyme MenD ((1R,6R)-2-succinyl-6-hydroxy-2,4-cyclohexadiene-1-carboxylate (SHCHC) synthase) from *Escherichia coli*, University of Saskatchewan, 2005.
- 42 Polovnikova, E. S., McLeish, M. J., Sergienko, E. A., Burgner, J. T., Anderson, N. L., Bera, A. K., Jordan, F., Kenyon, G. L. and Hasson, M. S., *Biochemistry* **2003**, 42, 1820-1830.
- 43 Bera, A. K., Polovnikova, L. S., Roestamadji, J., Widlanski, T. S., Kenyon, G. L., McLeish, M. J. and Hasson, M. S., *J. Am. Chem. Soc.* **2007**, 129, 4120-4121.
- 44 Reprinted from Dawson, A., Fyfe, P. K. and Hunter, W. N., *J. Mol. Biol.* **2008**, 384, 1353-68, with permission from Elsevier.
- 45 Agyei-Owusu, K., and Leeper, F. J., *FEBS J.* **2009**, 276, 2905-2916.
- 46 Golbik, R., Neef, H., Hübner, G., König, S., Seliger, B., Meshalkina, L., Kochetov, G. A. and Schellenberger, A., *Bioorg. Chem.* **1991**, 19, 10-17.
- 47 Hawksley, D., Griffin, D. A. and Leeper, F. J., *J. Chem. Soc., Perkin Trans. 1* **2001**, 144-148.
- 48 Mann, S., Melero, C. P., Hawksley, D. and Leeper, F. J., *Org. Biomol. Chem.* **2004**, 2, 1732-1741.
- 49 Berthold, C. L., Toyota, C. G., Moussatche, P., Wood, M. D., Leeper, F. L., Richard, N. G. J. and Lindqvist, Y., *Structure* **2007**, 15, 853-861.
- 50 Xu, H., Graham, M., Karelis, J., Walker, S. and Tonge, P. J. In Abstracts of papers, 237th ACS National Meeting, Salt Lake City, UT, United States, May 22-26, 2009.
- 51 Kluger, R., and Pike, D. C., *J. Am. Chem. Soc.* **1977**, 99, 4504-4506.

- 52 Brandt, G. S., Kneen, M. M., Chakraborty, S., Baykal, A. T., Nemeria, N., Yep, A., Ruby, D. I., Petsko, G. A., Kenyon, G. L., McLeish, M. J., Jordan, F. and Ringe, D., *Biochemistry* **2009**, 48, 3247-3257.
- 53 Bruning, M., Berheide, M., Meyer, D., Golbik, R., Bartunik, H., Liese, A. and Tittman, K., *Biochemistry* **2009**, 48, 3258-3268.
- 54 Kluger, R., and Pike, D. C., *J. Am. Chem. Soc.* **1979**, 101, 6425-6428.
- 55 Arjunan, P., Sax, M., Brunskill, A., Chandrasekhar, K., Nemeria, N., Zhang, S., Jordan, F., Furey, W., *J. Biol. Chem.* **2006**, 281, 15296-15303.
- 56 Wille, G., Meyer, D., Steinmetz, A., Hinze, E., Golbik, R. and Tittmann, K, *Nat. Chem. Biol.* **2006**, 2, 324-328.
- 57 Chakraborty, S., Nemeria, N., Yep, A., McLeish, M. J., Kenyon, G. L. and Jordan, F., *Biochemistry* **2008**, 47, 3800-3809.
- 58 Biryukov, A. I., Bunik, V. I., Zhukov, Y. N., Khurs, E. N. and Khomutov, R. M., *FEBS Lett.* **1996**, 382, 167-170.
- 59 Bunik, V. I., Denton, T. T., Xu, H., Thompson, C. M., Cooper, A. J. L. and Gibson, G. E., *Biochemistry* **2005**, 44, 10552-10561.
- 60 Kabysheva, M. S., Storozhevykh, T. P., Pinelis, V. G. and Bunik, V. I., *Biochem. Pharmacol.* **2009**, 77, 1531-1540.
- 61 DeClue, M. S., Baldrige, K. K., Kast, P. and Hilvert, D., *J. Am. Chem. Soc.* **2006**, 128, 2043-2051.
- 62 Busch, F. R., and Berchtold, G. A. , *J. Am. Chem. Soc.* **1983**, 105, 3346-3347.
- 63 Young, I. G., Batterham, T. J. and Gibson, F., *Biochim. Biophys. Acta* **1969**, 177, 389.
- 64 Walsh, C. T., Liu, J., Rusnak, F. and Sakaitani, M., *Chem. Rev.* **1990**, 90, 1105-1129.

- 65 Kurutscha, A., Richtera, M., Brechta, V., Sprengerb, G. A., Müller, M., *J. Mol. Catal. B: Enzym.* **2009**, 61, 56-66.
- 66 Payne, R. J., Kerbarh, O., Minguel, R. N., Abell, A. D. and Abell, C., *Org. Biomol. Chem.* **2005**, 3, 1825-1827.
- 67 Segel, I. H., *Enzyme kinetics*. Wiley: New York, 1975.
- 68 Dixon, M., *Biochem. J.* **1953**, 55, 170-171.
- 69 Cornish-Bowden, A., *Biochem. J.* **1974**, 137, 143-144.
- 70 Cornish-Bowden, A., *Analysis of enzyme kinetic data*. Oxford University Press: New York, **1995**.
- 71 Cornish-Bowden, A., *Fundamentals of enzyme kinetics*. Portland Press Ltd: London, 1995.
- 72 Copeland, R. A., *Evaluation of enzyme inhibitors in drug discovery: a guide for medicinal chemists and pharmacologists*. John Wiley & Sons, Inc.: Hoboken, New Jersey, **2005**.
- 73 Sharma, S. K., Miller, M. J., Payne, S. M., *J. Med. Chem.* **1989**, 32, 357-367.
- 74 Karaman, R., Goldblum, A., Breuer, E., Leader, H., *J. Chem. Soc., Perkin Trans. 1* **1989**, 4, 765-774.
- 75 Riegel, B., Lilienfeld, W. , *J. Am. Chem. Soc.* **1954**, 67, 1273-1275.
- 76 Somerville, L. F., and Allen, C. F. H., *Org. Synth.* **1933**, 2, 81.
- 77 Srinivas, C., Raju, C. M. H. and Acharyulu, P. V. R., *Org. Process Res. Dev.* **2004**, 8, 291-292.
- 78 Mullah, K. B., and Bentrude, W. G., *J. Org. Chem.* **1991**, 56, 7218-7224.

- 79 Conole, G., Mears, R. J., Silva, H. D. and Whiting, A., *J. Chem. Soc., Perkin Trans. 1* **1995**, 1995, 1825-1836.
- 80 Pàmies, O., and Bäckvall, J., *J. Org. Chem.* **2003**, 68, 4815-4818.
- 81 Elisabeth, O., and Silvia, K., *Synthesis* **1993**, 5, 497-502.
- 82 Defoin, A., Pires, J. and Streith, J. , *Helv. Chim. Acta* **1991**, 74, 1653-1670.
- 83 Kozlowski, M. C., and Bartlett, P. A. , *J. Am. Chem. Soc.* **1991**, 113, 5897-5898.
- 84 Coleman, R. S., and Grant, E. B. , *J. Am. Chem. Soc.* **1995**, 117, 10889-10904.
- 85 Toogood, D. Structural studies of MenD-A crystallographic endeavor, University of Saskatchewan, 2008.
- 86 Rusnak, F., Liu, Jun., Quinn, N., Berchtold, G. A. and Walsh, C. T., *Biochemistry* **1990**, 29, 1425-1435.
- 87 Tittmann, K. and Wille, G., *J. Mol. Catal. B: Enzym.* **2009**, 61, 93-99.
- 88 Fang, M., Toogood, R. D., Macova, A., Ho, K., Franzblau, S. G., McNeil, M. R., Sander, D. A. R. and Palmer, D. R. J., *Biochemistry* **2010**, 49, 2672-2679.
- 89 Schütz, A., Golbik, R., König, S., Hübner, G., and Tittmann, K., *Biochemistry* **2010**, 44, 6164-6179.
- 90 Yep, A., Kenyon, G. L. and Mcleish, M. J. *Proc. Natl. Acad. Sci. U. S. A.* **2008**, 105, 5733-5738.
- 91 Pei, X., Titman, C.M., Frank, R. A. W., Leeper, F. J. and Luisi, B. F. *Structure* **2008**, 16, 1860-1872.